STUDIES OF RADIO FREQUENCY RADIATIONS FROM THE PLANETS

By

THOMAS DEADERICK CARR

A DISSERTATION PRESENTED TO THE GRADUATE COUNCIL OF
THE UNIVERSITY OF FLORIDA
IN PARTIAL FULFILLMENT OF THE REQUIREMENTS FOR THE
DEGREE OF DOCTOR OF PHILOSOPHY

UNIVERSITY OF FLORIDA

June, 1958

ACKNOWLEDGEMENTS

The writer expresses his most sincere gratitude to the Chairman of his Graduate Committee, Dr. A. G. Smith, whose assistance, advice, and encouragement throughout the course of the project played a very large part in its success. He also wishes to express his appreciation to Dr. R. C. Williamson, Chairman of the Physics Department, whose initial support and continued interest made the work possible and permitted the establishment of radio astronomy as an active field of research at the University of Florida.

The writer wishes to thank Dr. J. W. Flowers, Dr. G. C. Omer, and Dr. D. C. Swanson of the Physics Department faculty for their advice and encouragement. He is greatly indebted to his colleagues, Mr. R. J. Pepple and Mr. C. H. Barrow, for their assistance in most of the phases of the research and also in the preparation of the illustrations for this dissertation. He also wishes to express his appreciation to Mr. George Harris of the Physics Department Shop for his assistance in the construction of antennas, to Mr. J. K. Jackson, Mr. H. L. Register, and Mr. W. H. Perkins for their assistance in the maintenance of nightly watches and in the construction of equipment, to Mr. H. W. Schrader, Mr. C. C. Pennell, Mr. A. L. Garris, and Mr. R. Warren of the Physics Department Shop for the construction of antenna components and for other aid, to Mr. M. L. Vatsia and Mr. A. R. Phillips for photographic assistance, and to Mrs. Barbara Jones

for typing this manuscript.

Finally, acknowledgement is due Dr. Roger M. Gallet of the National Bureau of Standards, whose suggestion it was that the inaugural project in radio astronomy at the University of Florida consist of a study of the newly-discovered radio frequency radiation from Jupiter.

The writer wishes to express his appreciation for the financial support of the National Science Foundation, which made much of the work possible.

TABLE OF CONTENTS

		Page
ACKNOWLEDGEMENTS		ii
LIST OF TABLES		vi
LIST OF ILLUSTRATIONS		vii
Chapter I.	HISTORICAL BACKGROUND	1
	The Beginnings of Radio Astronomy	1
	Previous Investigations of Radio Radiation from the Planets	5
II.	PLANETARY ATMOSPHERES	18
	Jupiter	18
	Saturn	21
	Uranus and Neptune	22
	Venus	23
	Mars	24
	Mercury	25
	Pluto	26
	Earth	26
III.	THEORY OF THE PROPAGATION OF RADIO WAVES IN IONIZED GASES	30
	Propagation in the Absence of a Magnetic Field	31
	Polarization in the Presence of a Magnetic Field	32
	Polarization in the Longitudinal Case	33
	Polarization in the Transverse Case	33
	Polarization in the General Case	33
	Determination of Magnetic Field Intensity by Means of Polarization Measurements	34
	Simplified Appleton Polarization Formula	35
	Conditions for Reflection of Ordinary and Extraordinary Components	36
	Effects of Collisions	37
	Behavior of Transients Originating within an Ionosphere	38

Page

IV. RECEIVING APPARATUS OF THE UNIVERSITY OF FLORIDA OBSERVATORY. 40

Project Chronology and Participants. 40
The 18 Mc/s Broadside Array. 42
Receiving, Recording, and Calibration Equipment used During the First Apparition. 49
Calculation of Broadside Array Pattern and Gain. . 54
The 22.2 Mc/s Corner Reflector Array 69
A Method for the Measurement of the Pattern and Gain of Large Antennas. 79
The 18 Mc/s Yagi Array 84
The 27.6 Mc/s Yagi Array 87
The 22.2 Mc/s Polarimeter. 89
Receiving and Recording Equipment used During the Second Apparition 100

V. OBSERVATIONAL PROCEDURES. 109

VI. JUPITER DURING THE FIRST APPARITION 114

Observational Data 114
Rotational Periods 118
The Jovian Ionosphere. 127
The 8-Day Cycle. 130
Radiation Intensity Distribution 133
Waveform Studies 133

VII. JUPITER DURING THE SECOND APPARITION. 135

Flux Intensity Distributions 135
Correlation with System III Longitude. 137
Polarimeter Measurements 138
The Sunrise Effect 145

VIII. SATURN, URANUS, AND VENUS 149

Saturn During the First Apparition 149
Uranus During the Second Apparition. 151
Saturn During the Second Apparition. 152
Venus During the Second Apparition 152

IX. SUMMARY. 154

LIST OF REFERENCES 158

BIOGRAPHICAL SKETCH 161

LIST OF TABLES

Table		Page
1	LENGTHS OF PHASING CABLES.	76
2	SYSTEM II LONGITUDES OF RADIO SOURCES.	120
3	COMPARISON OF RADIO PEAK WIDTHS WITH SUNSPOT NUMBERS .	129
4	POLARIMETER DATA	141
5	OCCURRENCES OF THE SUNRISE EFFECT.	146
6	OCCURRENCES OF SATURN NOISE (SECOND APPARITION). . . .	152

LIST OF ILLUSTRATIONS

Figure		Page
1.	Periods of occurrence of 18.3 Mc/s radiation from Jupiter plotted against longitude of the central meridian at the time of observation. . . .	9
2.	Periods of occurrence of 22.2 Mc/s radiation from Jupiter plotted against System II longitude; data of Burke and Franklin	12
3.	Configuration of the 18 Mc/s broadside array.	43
4.	View of the broadside array from the southwest. . . .	45
5.	Block diagram of system used during first apparition.	50
6.	Essentials of calibration circuit	52
7.	Electronic and recording equipment, first apparition.	55
8.	Factors making up the pattern of the 18 Mc/s broadside array in the east-west vertical plane. .	57
9.	Factors making up the pattern of the 18 Mc/s broadside array in the north-south vertical plane.	58
10.	Diagram for $F_b(\theta)$ derivation.	59
11.	Diagram for $F_c(\theta)$ derivation.	61
12.	Diagram for $F_d(\theta)$ derivation.	62
13.	East-west pattern of 18 Mc/s broadside array, calculated from Eq. (15)	64
14.	North-south pattern of 18 Mc/s broadside array, calculated from Eq. (17)	65
15.	Configuration of the corner reflector array	70
16.	The 22.2 Mc/s corner reflector array as seen from the east	72

Figure		Page
17.	Junction box for the 22.2 Mc/s corner reflector array	74
18.	Measured east-west pattern of the 22.2 Mc/s corner reflector array	77
19.	Measured north-south pattern of the 22.2 Mc/s corner reflector array	78
20.	Commutated record comparing a single-dipole corner reflector array with a standard array	81
21.	Sighting structure for determining direction of the airplane	82
22.	The antenna field	85
23.	The 27.6 Mc/s Yagi array and the polarimeter array	88
24.	Polarization diagram	95
25.	Block diagram of receiving and recording equipment used during the second apparition	101
26.	Antenna matching and calibration input circuit	103
27.	Electronic equipment used during the second apparition	108
28.	Typical recordings of Jupiter noise made at 18 Mc/s	115
29.	Periods of occurrence of 18 Mc/s radiation from Jupiter (first apparition) plotted against System II longitude of the central meridian at the time of observation	117
30.	Probability of occurrence of 18 Mc/s radiation from Jupiter (first apparition) plotted for 5° intervals of System II longitude	119
31.	Long-term drift lines for radio and visual features of Jupiter	121
32.	System III histogram of observations of Jupiter made between December 31, 1956 and March 6, 1957	125
33.	Histogram of the observations of Shain and of Burke and Franklin plotted in System III longitudes	126

Figure Page

34. Jupiter activity (in arbitrary units) plotted as a function of date, showing 8-day cyclic behavior. 131

35. System III histogram of observations of Jupiter radiation on 18 and 22.2 Mc/s between December 19, 1957 and March 31, 1958 139

36. Polarimeter record of a Jupiter burst on 22.2 Mc/s . . 140

CHAPTER I

HISTORICAL BACKGROUND

The Beginnings of Radio Astronomy

Man has always wondered at the stars. Probably since the very days when the spark of human intelligence first began to glow, he has yearned for knowledge about them. The planets caught his attention early. Thousands of years before the dawn of recorded history the ancients recognized these wanderers in the sky, which slowly change position with respect to the rest of the firmament. After the invention of the Arabic number system, the wanderings of the planets began to be systematized. This marked the beginning of the science of astronomy, although it was to be a very long time before the disentanglement of astronomy from astrology was achieved.

About three hundred years before Christ, Aristarchus of Samos advanced the theory that, contrary to the prevailing idea of a geocentric universe, the earth actually revolves about the sun in a circular orbit. This notion seemed so preposterous, however, that it was disregarded until nearly 2,000 years later. About 1540 the Polish monk Copernicus, reviving and extending the theory of Aristarchus, presented a qualitatively correct picture of the solar system in which the planets and the earth, itself a planet, revolve in orbits about the sun.

Proof of the Copernican theory was provided in the early seventeenth century by Tycho and Kepler, and by Galileo. The theoretician Kepler, using the remarkably precise planetary observations made earlier by the experimentalist Tycho without the aid of a telescope, deduced his celebrated three laws describing the elliptical motion of the planets around the sun. Galileo, who shares with Newton the honor of being the founder of the classical physics of today, heard about the accidental discovery of the principle of the telescope by the Dutch optician Lipperhey, and promptly built himself one at Venice. Using an improved model of his telescope in 1610, Galileo observed that the planets appear as luminous discs while the stars remain points of light. He discovered the more prominent moons of Jupiter, the rings of Saturn, the crescent phases of Venus, sunspots, and the rotation of the sun. After the discovery by Newton toward the end of the seventeenth century of the law of gravitation, the formulation of his three laws of motion, and his advances in optics, steady progress in astronomy and physics was assured.

So began astronomy. In 1888, at about the start of the epoch of the great modern American observatories, Heinrich Hertz in Germany proved experimentally the existence of electromagnetic radiation. The characteristics of this radiation had previously been worked out mathematically in great detail by Maxwell. Using microwaves produced by spark discharges, Hertz demonstrated the rectilinearity of propagation, shadow production, reflection, refraction, interference,

and polarization. He further showed that the radiation propagates with the velocity of light and is indeed a manifestation of the same phenomenon as light, differing only in wavelength and frequency. Long distance propagation of electromagnetic radiation was first accomplished by Marconi in 1901, marking the birth of radio. After the invention of the electron tube by Fleming and de Forest, the development of radio technology was rapid. An ionized layer in the high atmosphere capable of reflecting radio waves was postulated by Kennelly and Heaviside in 1902, but its existence was not proven experimentally until 1925. By means of the pulse echo method devised in 1926 by Breit and Tuve (a technique which was the forerunner of radar), it was demonstrated that waves of frequencies below a critical value are reflected by the ionosphere, while those above this value penetrate it.

In 1931 an electrical engineer working at the Bell Telephone Laboratories, Karl Jansky (1), using a steerable multi-dipole antenna array on a frequency of about 20 Mc/s, identified a persistent hissing noise emanating from his radio receiver as of extraterrestrial origin. Jansky, after having taught himself the fundamentals of astronomy, determined beyond doubt that the radio noise was arriving from a widely-dispersed source centered approximately at declination -10°, right ascension 18^{h}, corresponding to the approximate direction of the center of our galaxy, the Milky Way. Thus did a perceptive engineer with no previous astronomical training become the father of radio astronomy.

Subsequent to the pioneer work of Jansky, Reber further investigated the distribution of the galactic noise in direction and frequency in considerable detail. Southworth and Reber independently found that the sun itself emits radio noise, which at times fluctuates radically in intensity. The intensity was found always to be in excess of that expected from a black body radiator at the temperature of the surface of the sun.

Following the rapid advance made in radio and radar during World War II, radio astronomy came of age, with great parabolic reflectors and multielement antenna arrays springing up in various parts of the globe. A large number of radio stars were found, only a few of them coinciding with visible objects detectable with even the largest optical telescopes. A single radio spectral line was found, that at a wavelength of 21 centimeters, resulting from the emission or absorption of the neutral hydrogen gas thinly dispersed throughout space.

Although most of the post-war activity has been at the higher radio frequencies where the resolution necessary to separate radio stars is more easily achieved, some work has continued at frequencies in the vicinity of 20 Mc/s, which approaches the lowest frequency capable of penetrating the terrestrial ionosphere. The radio interferometer, consisting of two widely-separated antennas connected to produce an interference pattern made up of a set of fan-shaped lobes, has been widely used to achieve resolution at these lower frequencies. The radio interferometer is an outgrowth of the radio direction-finder, and is analogous with the optical

interferometer. It was first applied to radio astronomy by Ryle. Although the interferometer has the disadvantage that its multilobed pattern is highly ambiguous in the determination of direction, it remained for some time the only feasible method for obtaining apertures of several wavelengths when the wavelength is as long as 50 feet. However, Mills of Australia developed an ingenious type of antenna array which achieved with a reasonable number of dipoles the same resolution as a rectangular dipole array so large that it would be impracticable, and which possessed the advantage over the interferometer of being unambiguous. This array is called the Mills Cross.

Previous Investigations of Radio Radiation from the Planets

A Mills Cross antenna was constructed at the Carnegie Institution at Washington in 1954 for the frequency 22.2 Mc/s. Burke and Franklin (2), while studying the radiation from the Crab Nebula with this array, frequently noticed a burst of interference which always occurred at approximately the same sidereal time, and always lasted about the length of time required for a point source to pass through the antenna beam. The interference appeared to be coming from the direction of Jupiter. This was verified when the plot of the right ascension of the interference over a period of two months showed the same drift as that of Jupiter. The radiation was extremely sporadic. Out of a total of 31 records of the passage of Jupiter through the beam, only 9 showed the bursts of noise, the intensity of the bursts varying over a wide range. The flux per

unit bandwidth of this radiation often reached 5.2×10^{-23} watts m^{-2} $(c/s)^{-1}$, and occasionally was several times greater. Calculations by Burke and Franklin indicated that the peak power radiated by the source was at least 300 watts per c/s of bandwidth. On one occasion when measurements were made simultaneously on 22.2 Mc/s and on 38.7 Mc/s with an interferometer of higher gain, the radiation from Jupiter was strong at the lower frequency but was completely absent at the higher. The conclusion of Burke and Franklin was that the radio noise is concentrated below 38 Mc/s.

The discovery by Burke and Franklin was also reported in an editorial note in Nature (3). This brief report suggested that Jupiter signals might be caused by distrubances in the planetary atmosphere similar to terrestrial thunderstorms, but on a much larger scale. The radiation field produced by a single terrestrial lightning flash, as determined by E. T. Pierce, was given as 15 volts/m at a distance of 20 km on a frequency of 1 Mc/s and bandwidth of 1 Mc/s. Making reasonable assumptions about the frequency spectrum, and making use of the fact that there are on the average about 100 lightning flashes per second in the terrestrial atmosphere, it was calculated that the terrestrial thunderstorm static would produce at the distance of Jupiter a power flux of about 5×10^{-21} watts m^{-2} $(c/s)^{-1}$. This is 100 times greater than the value for the Jupiter radiation given by Burke and Franklin; it was thus concluded that discharges akin to terrestrial lightning are a possible cause of the noise from Jupiter. However, it was pointed out that the resultant

signal from the many lightning flashes occurring each second on earth would appear at the distance of Jupiter as a steady noise rather than the irregular bursts actually observed from Jupiter.

Upon learning of the discovery of Burke and Franklin, Shain (4,5) in Australia made a search of old records, taken in 1950-1951 at a frequency of 18.3 Mc/s, for possible occurrences of noise from Jupiter. Many such occurrences which had previously been mistaken for terrestrial interference were indeed found, confirming the work of Burke and Franklin, and leading to the further conclusion that in 1951 the radiation came from a localized region of the planet.

Two series of records were studied. The first series was obtained using an antenna array having the relatively narrow beam-width 17°. Radiation from Jupiter appeared on about half of these records. The radiation appeared as violent fluctuations, often going off-scale at an intensity greater than 5×10^{-21} watts m^{-2} $(c/s)^{-1}$. Fairly accurate direction-finding was possible from some of the records which were obtained with the use of a split-beam technique, indicating that the direction of the noise source was the same as that of Jupiter to within $\pm 1^{\circ}$. Over the six-month period during which this series of records was made, the right ascension of the noise source changed in the same manner as did that of Jupiter, substantiating the indentification.

The other series of records was made using an antenna beam which was narrow in declination, but which was eight hours wide in hour angle, almost the length of time required for a full rotation

of Jupiter. This series revealed Jupiter radiation on 27 out of the 30 days on which there were suitable records, although in every case the bursts of radiation come in groups of only an hour or two in duration. A close correlation was found to exist between the times of occurrence of the bursts and the rotation of Jupiter. Figure 1 shows the longitudes of the central meridian of the luminous disc of Jupiter during the times when bursts were received. A steady drift is apparent in the plot using System I longitude, which is based on a rotation period of $9^h\ 50^m\ 30^s$. However, in the plot using System II longitude, based on a rotational period of $9^h\ 55^m\ 40.^s6$, the lines indicating times of occurrence are almost directly under one another. Most of the occurrences lie between 0^o and 135^o longitude (System II), indicating that the major source of radiation is centered at about 67^o longitude (System II). Actually a slight negative drift can be detected in the System II diagram of Figure 1. Shain took this as an indication that the period of rotation of the source was slightly less than that of the System II longitude coordinates. From the slope of this slight drift, he calculated the rotation period of the noise source to be $9^h\ 55^m\ 13^s$ ($\pm 5^s$). Shain briefly mentioned that he used this rotation period to extrapolate backward in time from his second series of records to the first, six months earlier, to ascertain at what System II longitude the noise center should have been when the first series was made. It turned out that the occurrence bands for the first series were centered at a longitude about 80^o smaller than that indicated by the extrapolation. Shain gave no explanation for this disparity.

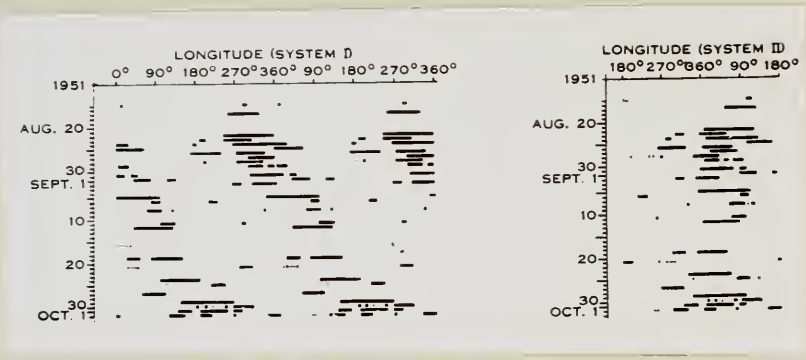

Fig. 1.—Periods of occurrence of 18.3 Mc/s radiation from Jupiter plotted against longitude of the central meridian at the time of observation. [After Shain, Australian Journal of Physics 9, 67 (1956).]

It had been brought to Shain's attention by Fox of the British Astronomical Association that a small white spot at the boundary between the South Temperate Zone and the South Temperate Belt, which had been studied by Reese, possessed a rotational period of $9^h\ 55^m\ 13^s$, the same as that attributed to the noise center. Shain thus concluded (erroneously, as will be shown later) that the Reese white spot was probably the source of the radio noise.

In speculating on possible explanations of the observed fact that the radiation occurrences are concentrated within a well-defined band of longitude of the central meridian, Shain suggested that an ionosphere on Jupiter may be the cause. Such an ionosphere would restrict the Jupiter rotation angle during which radiation could be received at the earth. That is, the ionosphere would cut off the outgoing radiation when the earth is at low altitudes as seen from the source below the ionosphere. Shain suggested that the radiation from Jupiter could be used in studying radio propagation in the space between Jupiter and the earth, particularly through the corona of the sun. In fact, by comparing some of his records taken at midday when Jupiter and the sun were near conjunction with other records taken at night when Jupiter was at opposition, he thought that he could detect a difference in the average intensity of the signals, caused by partial absorption of those which had passed through the corona. He also pointed out that measurement of the refraction of Jupiter radiation passing through the corona would provide information of great interest. Finally, Shain stated that observations of radiation

from Jupiter were being made at the time the report was written in 1955, but that the occurrences were less frequent than in 1951.

Shortly after publication of the reports by Burke and Franklin and by Shain, Smith (6) in England, using antenna arrays of relatively high gain, attempted unsuccessfully to receive radiation from Jupiter at 38 Mc/s and at 81 Mc/s. He could have detected 10^{-24} watts m^{-2} $(c/s)^{-1}$ on 38 Mc/s, and 3×10^{-26} watts m^{-2} $(c/s)^{-1}$ on 81.5 Mc/s, the recorder response time being 6 seconds in both cases. The significance of these observations would seem to be somewhat doubtful, since the integrating time exceeded the expected burst duration. He estimated on the basis of his negative results and the positive results of his predecessors at lower frequencies that the spectrum of the Jupiter radiation must vary at least as rapidly as the 5.5 power of the wavelength.

The report of Burke and Franklin did not contain enough detailed data for a study of the correlation of noise occurrences at 22.2 Mc/s with Jupiter longitudes. However, Burke and Franklin sent some of their later data to Brookes (7), who published it in the form shown in Figure 2. As in the case of Shain's data obtained at 18.3 Mc/s, the 22.2 Mc/s noise occurrences were grouped in a particular band of System II longitudes, although the groups in the two cases were centered at different places. Brookes pointed out that the 22.2 Mc/s noise center, the Red Spot, and certain bright areas in the South Temperate Zone were all at approximately the same System II longitude. He suggested that the radio source and these visual features were closely associated. (It will be shown later that this apparent

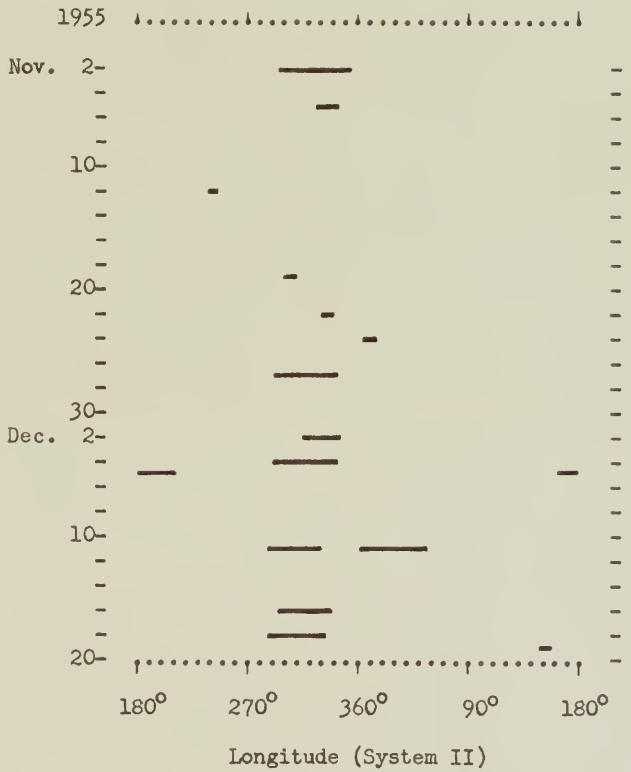

Fig. 2.—Periods of occurrence of 22.2 Mc/s radiation from Jupiter plotted against System II longitude; data of Burke and Franklin. [After Brookes. Journal of the Association of Lunar and Planetary Observers 10, 15 (1956).]

association at the time the data of Burke and Franklin were obtained was a coincidence.)

In a paper presented at the March, 1956 meeting of the American Astronomical Society, Franklin and Burke (8) reported further progress in their study of radio radiation from Jupiter. They mentioned the observed correlation of the radio source at 22 Mc/s with System II longitude, the possible correlation between the Red Spot and the radio source, and the fact that the white region suggested by Shain as the source could no longer be so considered. They suggested the possible significance of the fact that Shain received radiation in 1950-1951 during approximately 135° of rotation of Jupiter, while their data in 1955-1956 show a characteristic rotation angle of the order of 50°. They reported further that data have been obtained by their colleague, H. W. Wells, at two other frequencies, 18 Mc/s and 27 Mc/s. These data indicated that the Jupiter radiation is not part of a continuum. There was no correlation between the occurrence of bursts on the three frequencies, and only a general agreement between the times of prolonged disturbances. It appeared, however, that the sources at all three frequencies were located predominantly between System II longitudes 280° and 60°. An interferometer was constructed for the purpose of determining if the Jupiter radiation is circularly polarized. Many records were obtained indicating a high degree of right-hand circular polarization, nearly 100 percent in some cases. One event exhibited successively right-hand and left-hand circular polarization.

In another paper presented at the March, 1956 meeting of the

American Astronomical Society, Kraus (9) of Ohio State University described some observations of the waveform of the Jupiter disturbances at 26.6 Mc/s. He reported that although many of the signals consist of single pulses, a considerable number occur in pairs or triplets of pulses. These seemed to fall into two groups, adjacent pulses in the groups being separated by about $\frac{1}{4}$ second and 1/40 second, respectively. The individual pulses were of the order of 10 milliseconds duration or less. Kraus suggested two possible mechanisms for these multiple pulses, namely, that they are multiple electrical discharges on Jupiter, or that they are an echo phenomenon in which the second and third pulses are echoes of the first. Kraus estimated the peak radiated power of the Jupiter signals to be of the order of 10 kilowatts per c/s bandwidth.

At the same meeting, Gallet (10) of the National Bureau of Standards at Boulder, Colorado, described his simultaneous observations of the radiation from Jupiter on 18 Mc/s and 20 Mc/s. There was usually more radiation at 18 Mc/s than at 20. Individual signals observed at one of these frequencies were absent on the other, indicating that single pulses contain only a narrow range of frequencies. The signals appeared to be of two types, slow bursts lasting two or three seconds and sharp clicks, some of which were as short as 0.001 second, like those caused by terrestrial lightning. Gallet stressed the possibility of a detailed study of the ionosphere of Jupiter by radio methods. He pointed out that a study of the polarization of the radiation might indicate whether or not Jupiter

has a magnetic field, and the angle at which the radiation is cut off as the planet rotates whould give information on the properties of its ionosphere. (Kraus also suggested that the fact that the radiation is apparently cut off before the source reaches the limb of the planet is due to total internal reflection from its ionosphere, as had Shain earlier.) Gallet expressed the belief that the Red Spot is one of the sources of the radiation. Finally, he suggested that the mechanism producing the radiation lies in the agitation of an ionized atmosphere by shock waves originating at the surface of the planet.

Kraus (11, 12, 13) in 1956 reported in a series of three articles in Nature the discovery of impulsive radio signals from the planet Venus at a frequency of 26.7 Mc/s. He classified the signals into two types, one appearing as sharp spikes of duration less than 1 second, and the other more sustained and apparently modulated at an audio-frequency rate. The peak power flux density of the bursts from Venus was given as 8.9×10^{-22} watts m^{-2} $(c/s)^{-1}$. The signals were observed many times, always when Venus was within the antenna beam. The antenna used was actually an interferometer, and the presence of nulls in the observed data coinciding with expected interferometer nulls from a source in the direction of Venus was given as the main evidence that the source was indeed Venus. These nulls were illustrated in a sample record in one of the reports; however, it must be said that the nulls in this record are not very well-defined, nor is the agreement with the expected positions particularly striking. Kraus reported finding several characteristic periodicities in the data, as well as

echoes from the moon of pulses originating on Venus, but none of the evidence appears conclusive. All of the observations were made during daytime or early evening, when the terrestrial ionosphere is sufficiently dense to permit sky-wave propagation at this frequency, with the result that terrestrial interference was heavy.

At the spring, 1957 joint meeting of the International Scientific Radio Union and the Institute for Radio Engineers in Washington, Gallet (14) presented some conclusions from his investigations of Jupiter radiation at 18 and 20 Mc/s over a two year period. The antennas used permitted continuous observation of the planet for longer than the 10-hour rotation period. Several sources spaced in longitude were resolved by the method originated by Shain. From a comparison of the data recorded by Shain in 1951 with his own data recorded in 1956 and 1957, Gallet concluded that the sources do not move relative to each other and must therefore be fixed to the solid body of Jupiter. He established the rotation period as about 10 seconds less than that of System II. He stated that the ionosphere of Jupiter is an important controlling factor in the reception of radiation from Jupiter, and that he has observed a correlation between the occurrence of the radiation and the solar activity. He further stated that the total activity at 20 Mc/s is only 0.6 that at 18 Mc/s. In a private communication received later from Franklin, Gallet's value of the rotational period of the radio sources (and of the solid core of Jupiter) was given as $9^h\ 55^m\ 29^s.4$ ($\pm 0^s.1$).

In 1957, Smith and Douglas (15) at Yale University made a

search for radiation from Jupiter and Saturn at the frequency 21.1 Mc/s, using a pair of four-element Yagi arrays 2.3 wavelengths apart connected as a phase-switching interferometer. Nine probable Jupiter events were recorded during March, 1957. Saturn was observed during April and May, with the result that on a total of 13 nights radiation was presumably received from this planet. These 13 events all satisfied several criteria for Saturnian origin, including fit to the interferometer pattern and to a possible rotation period of $10^h\ 22^m$. It was stated, however, that these preliminary results must be considered inconclusive pending more data, better discrimination against terrestrial atmospherics and galactic background, and comparison with work of others.

CHAPTER II

PLANETARY ATMOSPHERES

Well-established or at least highly plausible information on planetary atmospheres, which has been gained largely by telescopic and spectroscopic observations and by theoretical considerations, will be summarized in this chapter. Major emphasis will be placed on those planets known or suspected to be sporadic radio emitters. The principal sources of this information are Jones (16) and Kuiper (17).

Jupiter

The four major planets, Jupiter, Saturn, Uranus, and Neptune, possess many similarities to each other and many dissimilarities to the lesser planets. This is due largely to the fact that, unlike the earth and its smaller neighbors, the major planets are massive enough so that they have been able to retain vast quantities of the light gases hydrogen and helium in their atmospheres. They also have in common relative remotensess from the sun, resulting in low atmospheric temperatures. The largest of these giant planets is Jupiter.

When observed through a telescope, Jupiter appears as a bright disk, slightly flattened at the poles, and possessing a number of dark belts parallel to the equator. The flattening at the poles and corresponding equatorial bulge probably result from the relatively high rotational velocity, the rotational period being less than ten hours.

The dark belts are probably clouds formed of droplets of condensed vapors floating in the atmosphere. The belts may show considerable internal structure, such detail as light or dark spots, bulges, and curling wisps being common. Some of the markings last only a few hours, others weeks or months, and a few, notably the great Red Spot, for years. The periods of rotation of the various belts differ slightly. The belts are often colored, with red, brown, and orange predominating.

The existence of a number of permanent currents in the visible material on Jupiter has been established; these currents are parallel to the equator, and account for differences in rotational periods of the belts. Velocity differences in adjacent currents may be sufficient to produce differential speeds of up to two hundred miles per hour. The atmosphere is in a perpetual state of meterological turmoil. Although the currents are permanent, their positions and rotational rates may vary from year to year. The broadest is the equatorial current, which covers a zone 10,000 to 15,000 miles wide and has an average period of about $9^h\ 50^m\ 30^s$. This is the rotational period upon which the central meridian longitude coordinates designated "System I" are based. These are the coordinates which are usually employed for specifying positions of equatorial markings. The periods of rotation of the other currents lie between $9^h\ 55^m$ and $9^h\ 56^m$, but bear no apparent relation to the latitude. The central meridian longitude coordinates designated "System II", corresponding to a rotational period of $9^h\ 55^m\ 40^s.6$, are usually the ones in which

positions of markings occurring in the non-equatorial currents are expressed.

The great Red Spot was observed as far back as 1857, and may be identical with a marking observed by Hooke in 1664. Its appearance changes considerably. At times it is very conspicuous and of a brick red color; at other times it loses its color and disappears. It is about 30,000 miles long and 7,000 miles wide, the long axis being parallel to the equator. Its rotational period is subject to large and irregular variations; it obviously cannot be attached to the solid surface of the planet. Wildt has suggested that the Red Spot may be a vast solid body, possibly solid hydrogen, floating in an ocean of highly compressed atmospheric gases. The observed behavior of the Red Spot is not inconsistent with such a hypothesis.

Another long-enduring marking is the South Tropical Disturbance, an elongated dark region lying in the belt just south of the Red Spot. It was first seen in 1901, was lost in 1940, and reappeared in 1955.

The mean density of Jupiter is 1.34 times that of water. According to one theory the planet possesses a rocky core of about 22,000 miles radius. Above it is postulated a layer of ice about 16,000 miles thick, and an atmosphere about 6,000 miles thick. However, only the outer hundred miles (or less) of the atmosphere is in the gaseous state, that below having been compressed to a liquid or solid.

Jupiter's atmosphere is believed to consist mainly of hydrogen and helium. However, spectroscopically observable quantities of methane and ammonia are also present. Gaseous methane and ammonia are estimated

to be present in the amounts 150 and 7 meter-atmospheres, respectively. There is no free oxygen nor carbon dioxide, and probably no free nitrogen. Clouds consisting of droplets of liquid ammonia or small crystals of frozen ammonia are undoubtedly present.

Jupiter is about 5.2 times farther from the sun than is the earth, so it receives only 0.037 as much solar radiation. As a consequence, surface temperatures are much lower than on earth. The measured temperature of the visible part of Jupiter is -140° C. Jupiter's orbital period is 11.9 years. Seasonal effects are probably insignificant, since the inclination of the axis of rotation is only about 3°.

Jupiter has twelve known satellites. The largest, designated J III, posseses sufficient mass to retain an atmosphere, as do some of the others. However, no atmosphere has yet been detected.

Saturn

Saturn, the second largest of the planets, is noted for its unique rings. They are composed of myriads of granules of solid matter, either ice or some other material coated with frost. The surface of Saturn is marked by light and dark belts parallel to the equator, as in the case of Jupiter. Saturn's belts, however, are sparser and contain less detail than those of Jupiter. Occasionally, white spots appear. Those occurring near the equator have a rotational period of about $10^h\ 16^m$; a spot observed at latitude 36° north had a period of $10^h\ 38^m$. The rotation of the atmosphere thus appears more rapid at the equator

than elsewhere, the effect being even more pronounced than in the case of Jupiter. Saturn also shows more flattening at the poles and bulging at the equator than does Jupiter, an indication of an even more extensive atmosphere. Saturn is about 9.5 times as far from the sun as is the earth; it receives only 0.011 the terrestrial intensity of solar radiation. Its temperature is -155° C, 15° lower than that of Jupiter.

Saturn is believed to consist of a rocky core about 14,000 miles in radius, above which is a layer of ice some 6,000 miles thick, and on top of this an atmosphere 16,000 miles thick. However, the atmosphere is gaseous only within the outer few hundred miles. The atmosphere probably consists largely of hydrogen and helium. Observable quantities of methane and ammonia are also present. The amount of methane is 350 meter-atmospheres, while that of ammonia is about 2 meter-atmospheres. Condensed ammonia droplets or crystals are probably present in the form of clouds.

Saturn's orbital period is 29.5 years.

Saturn's largest satellite, Titan, has an atmosphere of its own. Spectroscopic observations of it indicate the presence of methane, in the amount of 200 meter-atmospheres.

Uranus and Neptune

Due to their remoteness, less information is available on Uranus and Neptune. They both appear sea-green in the telescope. Extremely faint belts have been seen on Uranus. Spectroscopic and

photoelectric observations give a value of about $10^h\ 40^m$ for the rotational period of Uranus (which shows a decided oblateness), and $15^h\ 40^m$ for Neptune. Uranus is about 20.0 times as far from the sun as is the earth, and Neptune about 30.0 times; Uranus receives only 0.0025 the terrestrial intensity of solar radiation, and Neptune only 0.0011. Temperature measurements indicate that Uranus is colder than -180° C; Neptune's temperature cannot be measured, but must be lower than this.

It is postulated that both planets have an ice coating 6,000 miles thick, while the depths of the atmosphere are 3,000 miles for Uranus and 2,000 miles for Neptune, only the outer portions of which are gaseous. The atmospheres are largely hydrogen and helium, but methane is observable spectroscopically; indeed, it is the absorption due to methane which gives the planets their characteristic green color. The amount of methane on Uranus is 1,500 meter-atmospheres and on Neptune 2,500 meter-atmospheres. All the gaseous ammonia has apparently been frozen out.

The orbital period of Uranus is 84 years; that of Neptune is 165 years.

Venus

Venus is the brightest object in the sky, other than the sun and moon. Since its orbit is inside that of the earth, the illuminated face of Venus goes through phases similar to those of the moon. The mass of Venus is 0.82 that of the earth. Its orbital period is 225

days, and the synodic period is about a year and seven months. Since its surface cannot be observed because of perpetual clouds, its rotational period is not known. Being about 0.72 times as far from the sun as is the earth, it receives 1.9 times the solar radiation. The measured temperature of the bright side is 55° C; that of the dark side is -20° C. The temperature at the surface of the planet, beneath the cloud cover, is believed to be well above 100° C.

The only gas which has been detected with certainty in the atmosphere of Venus[1] is carbon dioxide, but this is present in abundance. The amount is about 1,000 meter-atmospheres. Oxygen and water vapor, if present at all, are very scarce.

According to Jones (16) the entire surface of Venus is desert (although according to another common theory it is covered by ocean!). Jones states that never-ending storms, much more violent than any on earth, continually stir up yellow dust from the surface and blow it high into the atmosphere. The whole atmosphere is hazy from dust. It is this which makes Venus so bright in reflected sunlight, and also prevents us from seeing its surface. If this picture is correct, one would surmise that it might be possible to detect radio radiation from discharges of static electricity occurring in the violent dust storms.

Mars

Mars is considerably smaller than the earth. Its orbit being just outside that of the earth, Mars under favorable conditions

---

[1]It has just been learned from Professor Harlow Shapley that an aurora on Venus showing the presence of nitrogen gas has recently been detected spectroscopically.

approaches the earth more closely than any other planet except Venus. Unlike the other planets, the surface of Mars can be seen in some detail. Visible features are snowcaps near the poles, a white strip presumably of frost seen along the east side just after sunrise, occasional cloudiness and dust storms, the famed and controversial "canals", and large greenish areas believed to be vegetation. Its temperature is 20° C in the hottest portions and about -85° C in the coldest.

Carbon dioxide has been detected in the atmosphere of Mars, in the amount of 4.4 meter-atmospheres. Water vapor is undoubtedly also present in a very small amount. There is probably little free oxygen. Other possible atmospheric components are unknown, although the presence of nitrogen is highly probable. The atmosphere is very thin, rarer apparently than on the highest mountains on earth. Clouds are seldom seen. There is apparently little meteorological activity on Mars of the type expected to result in large electrical discharges, although there is the possibility of lightning in the occasional dust storms.

The rotational period of Mars is about that of the earth; its orbital period is 1.9 years.

Mercury

Mercury, the planet with the innermost orbit, is difficult to observe because of its proximity to the sun. It is so hot and so small that it has no atmosphere, and is therefore of little interest in the present study.

Pluto

Pluto, the most remote of the known planets, is probably smaller than the earth. Virtually nothing is known about its atmosphere. Pluto is not considered likely to be an observable radio emitter.

Earth

The atmosphere of the earth near the surface is composed of 78% nitrogen (by volume), 21% oxygen, 0.9% argon, 0.03% carbon dioxide, 0.01% hydrogen, traces of the other noble gases, and variable amounts of water vapor. Its major divisions are the troposphere, the stratosphere, and the ionosphere. The troposphere, the layer nearest the surface, is characterized by the presence of great clouds of water droplets, other manifestations of weather, and a decrease of temperature with height. In the stratosphere the temperature is essentially constant and there are few clouds. The ionosphere is made up of sparsely distributed atmospheric molecules, atoms, and ions. If the temperature of the earth were measured in the same way as that for the other planets, a value of about 14° C would be obtained.

The tropospheric phenomenon of greatest interest in the present study is the thunderstorm. The thunderstorm is of concern for two reasons. Lightning discharges are the source of atmospheric radio noise, which is the most serious form of interference to be combatted in the observation of planetary radio radiation. Further, the mechanism by means of which lightning is produced may provide a clue to the origin of the planetary radio radiation. A typical

thunderstorm originates when a small area of land becomes heated by the sun more than its surroundings. The heated, moisture-laden air in the vicinity rises into levels of lower pressure and temperature. Adiabatic expansion and cooling cause condensation of a part of the moisture; the condensation liberates heat. The rising air, warmer now than its ever-cooler surroundings by virtue of the condensing moisture, continues its buoyant ascent. In this way a violent updraft is formed and maintained. The resulting cumulus cloud will billow a mile upward, stopping only when it runs out of moisture. Water drops continually forming inside are lifted by the updraft to higher altitudes, where they freeze to form hail or snow. The hail and snow may alternately rise and fall within the cloud many times before it finally reaches the ground as rain. Somehow in this process positive charge accumulates in the top of the cloud and negative charge in the bottom. A tremendous potential difference between top and bottom is thus built up, finally resulting in a lightning discharge. The discharge may occur between the top and bottom of the cloud, between the cloud and ground, or between oppositely charged portions of adjacent clouds.

The mechanism causing the separation of charge within the cloud is not known, although there are several theories (18). One of the more plausible is the ice-friction theory. It has been shown that when two insulators of the same material are rubbed together they become charged, usually negatively, while the air becomes positively charged. High fields have been observed in Antarctic

blizzards and in dust storms. According to the ice-friction theory, ice particles forming and being blown violently about in the upper part of the thundercloud become charged negatively by friction, leaving the air positively charged. As they grow heavier they settle to the base of the cloud, where they hang suspended for a time by the electrostatic attraction between the negative charges they carry and the positively charged air they left behind in the top of the cloud. Finally, when the lightning discharge occurs, the potential difference is neutralized, and the hail and raindrops held in the ominously dark base of the great cloud fall to the ground in a deluge.

Lightning discharges radiate a large amount of energy in the radio spectrum. Although the maximum energy occurs at a frequency of about 15 Kc/s, there is enough in the spectral region 15 to 30 Mc/s to interfere seriously at times with planetary reception.

There are on earth about 100 lightning discharges every second, on the average. Some of the radio radiation from this continual activity, at frequencies high enough to penetrate the ionosphere, will pass out into space. The terrestrial radiation in the 15-30 Mc/s band, as observed with a radio receiver at a distant point in the solar system, would appear as a steady noise of random (gaussian) amplitude distribution, since it is composed of randomly-occurring, overlapping pulses. It would seem to be of about the same character as the galactic noise.

The ionosphere of the earth occurs in the outer fringe of the atmosphere, where the mean free path of the rarified gaseous components

is very long and the rate of collision is relatively low. The principal daytime ionospheric layers are the D layer at about 35 miles altitude, the E layer at about 60 miles, the F_1 layer at about 120 miles, and the F_2 layer at about 180 miles. Generally at night only the F layer (no longer divided into sub-layers) is present.

These ionized layers are due to the action of ultraviolet radiation from the sun, the different layers resulting from photo-dissociation of different atmospheric constituents. In the lower layers recombination by collision is rapid, and the layer disappears with the setting of the sun. However, in the F layer collisions are so infrequent that some ionization persists throughout the night, although the ion density usually drops until sunrise. The behavior of the night-time F layer ion density is subject to snomalies resulting from magnetic disturbances and atmospheric tides. The average maximum electron number density for the F layer at midnight is $2.5 \times 10^5/cm^3$. The electron number density is about four times greater during a sunspot maximum than during a sunspot minimum. The number density of neutral particles in the F layer is $2 \times 10^{10}/cm^3$. The F layer collision frequency is of the order of $10^3/s$.

The earth is the only planet known to have a magnetic field (prior to the studies of Jupiter's radio radiation), although it is possible that every planet has one. The magnetic axis of the earth is inclined at about 12° to the rotational axis. At Gainesville, the resultant magnetic field intensity is 0.51 gauss, the dip is 58°, and the magnetic declination is 1° E.

CHAPTER III

THEORY OF THE PROPAGATION OF RADIO WAVES IN IONIZED GASES

Much can be learned about the variable radio radiation from Jupiter (or other planets) and about environmental conditions at the source by the application of certain results of the well-established theory of propagation of radio waves through ionized gases. The elementary theory for propagation in the absence of a static magnetic field was provided by Eccles and Larmor. Later, Lorentz laid the foundations for a theory including the effects of a steady externally applied magnetic field, known as magneto-ionic theory, by considering the special cases of propagation directly along the magnetic field and also at right angles to it. Following this, Appleton in about 1927 generalized the Lorentz theory to include propagation in any direction with respect to the static magnetic field, and applied it to explain the observed phenomena related to propagation of radio waves in the terrestrial ionosphere. Hartree and also Goldstein independently arrived at the Appleton formula at about the same time.

The general theory is extremely complicated. The discussion which follows is based largely on material which is found in textbooks by Mitra (19) and by Pawsey and Bracewell (20). This information will later be used in attempts to prove from the experimental data that Jupiter indeed has an ionosphere, and to deduce from the observed

polarization of the received signals as much as possible about the magnetic field on Jupiter, if any. A theory due to Jaeger and Westfold (21) concerning the propagation of transient electromagnetic phenomena originating within an ionized medium will also be summarized briefly, since it may shed some light on the nature of the source of the radiation from Jupiter.

Propagation in the Absence of a Magnetic Field

Considering first the relatively simple case of propagation in a horizontally stratified ionosphere without a static magnetic field (19), let a radio wave be incident on the boundary at an angle i. The wave will be refracted at the boundary, and also within the medium if the electron density varies with height. If the electron density gradually increases with height, a refracted ray which entered the ionosphere from below will be bent more and more away from the normal until it finally becomes horizontal. After having become horizontal, the ray will continue bending downward and will eventually emerge from the lower ionospheric boundary. This constitutes total internal reflection. The refractive index in any layer is

$$n^2 = 1 - Ne^2/(\pi m f^2) \qquad (1)$$

and from Snell's Law the condition for reflection from a particular layer is

$$\sin^2 i = n^2 = 1 - Ne^2/(\pi m f^2) \qquad (2)$$

where i = angle of incidence with respect to the normal;

n = refractive index in the layer;

N = number of electrons per unit volume in the layer;

f = wave frequency;

e, m are the electronic charge and mass.

If the incidence is vertical, n = 0 at the height of reflection, in which case

$$f_o^2 = Ne^2/(\pi m) \qquad (3)$$

where f_o is the critical frequency (also called the plasma frequency) for the layer having electron density N; i.e., it is the highest frequency which will be reflected at normal incidence.

Eq. (1) can be rewritten,

$$n^2 = 1 - f_o^2/f^2 \qquad (4)$$

So long as there is no externally applied static magnetic field, the ionized medium has no effect on the polarization of the wave.

Polarization in the Presence of a Magnetic Field

If a static magnetic field is present the analysis is greatly complicated (19). However, in general a single incident wave will split into two components due to the fact that the medium is now anisotropic. These two components, or propagation modes, will be polarized differently and will usually follow different paths in the medium; they will travel at different velocities, will be reflected at different layers (if at all), and will experience different amounts of absorption. In analogy with optical birefringence, the two modes are referred to as the "ordinary" and "extraordinary" modes.

Polarization in the Longitudinal Case

For the special case of propagation in the same direction as that of the static magnetic field, i.e., the longitudinal case, the ordinary mode is circularly polarized in the left-handed sense and the extraordinary mode is circularly polarized in the right-handed sense, provided $f > f_o$ (implying relatively high frequency or low electron density). On the other hand, if $f < f_o$ (implying relatively low frequency or high electron density), the polarization senses are the converse. For propagation in the opposite direction to that of the static magnetic field, the senses of polarization are converse to those for propagation in the same direction as the magnetic field.

Polarization in the Transverse Case

For the special case of propagation at right angles to the direction of the static magnetic field, i.e., the transverse case, the two modes are both plane polarized, at right angles to each other. In this case the electric vector is parallel (or antiparallel) to the magnetic field for the ordinary mode, and perpendicular to the magnetic for the extraordinary mode. In this particular instance the magnetic field has no effect on the ordinary ray, since the electric vector and static magnetic field vector lie along the same line.

Polarization in the General Case

For the general case of propagation at any angle with respect to the static magnetic field (other than 0^o or 90^o) the two modes are elliptically polarized (19). The polarization ellipses for the

individual modes have the same ratio of major to minor axis. The major axis orientations for the two are perpendicular, and the senses of polarization are opposite to each other. The rules for determining the sense of elliptical polarization are similar to those for circular polarization in the longitudinal case. If there is a component of the static magnetic field in the same direction as that of propagation, then for $f > f_o$, the elliptical polarization is left-handed for the ordinary mode and right-handed for the extraordinary mode; but for $f < f_o$, the converse is true. If there is a component of the static magnetic field in the opposite direction to that of propagation, all the polarization senses are just the converse of corresponding ones in the previous statement. The major to minor axis ratio of the polarization ellipses is a function of the direction of the magnetic field with respect to that of propagation, the magnetic field intensity, and the ratio f_o/f. Transitions from ellipses which become circles at one extreme to ellipses which become straight lines at the other are continuous with variations in the above parameters.

Determination of Magnetic Field Intensity by Means of Polarization Measurement

If in the outer reaches of a planetary ionosphere the electron density (and hence f_o) decreases gradually to zero with increasing height while an appreciable magnetic field still remains, then the axial ratio of the ordinary and extraordinary polarization ellipses is a function only of the direction and magnitude of the magnetic field at the height at which the electron density became essentially zero (20).

Subsequent travel of rays through a vacuum after exit from the top of the ionosphere will not alter the polarization existing at emergence.

If both the ordinary and extraordinary components penetrate the ionosphere from below and arrive at a point outside with approximately equal intensities, the resultant polarization at any instant due to the superposition of the two components (which are individually elliptical) could be elliptical in either sense, depending upon the phase relationship of the two. The sense of the resultant polarization would be expected to vary erratically due to the effect of fluctuations in the polarizing ionosphere. On the other hand, if the polarization is actually observed to be predominantly of one particular sense, then it can be assumed that only one of the components is escaping from the ionosphere, the other having been reflected internally or absorbed. In such a case, measurement of the elliptical axial ratio provides a means of determining the static magnetic field intensity if the angle between the field and the propagation direction is known.

Simplified Appleton Polarization Formula

If the effect of collisions of electrons and other ions with neutral molecules and atoms is neglected, the formula derived by Appleton expressing quantitatively the state of polarization can be greatly simplified (19), probably without causing too much error for the cases of interest. The simplified polarization formula is

$$R = -j\left[\frac{f_H}{2f}\frac{\sin^2\theta}{\cos\theta}\frac{1}{1-\frac{f_o^2}{f^2}} \pm \left[1+\left(\frac{f_H}{2f}\frac{\sin^2\theta}{\cos\theta}\frac{1}{1-\frac{f_o^2}{f^2}}\right)^2\right]^{\frac{1}{2}}\right] \qquad (5)$$

where $R = E_z/E_y$, E_z and E_y being the complex vector representations of the electric field components along the z and y axes, respectively, when the x axis is in the direction of propagation (imaginary terms signify phase quadrature with real terms);

$f_o^2 = Ne^2/(\pi m)$, N, e, and m having the same interpretations as before;

$f_H = He/(2\pi mc)$, H being the intensity of the static magnetic field (the quantity f_H is called the gyrofrequency of the electron);

f = wave frequency, as before;

θ = angle between the direction of propagation and the static magnetic field.

For $f \gtrless f_o$, the extraordinary ray is given by the upper (positive) sign before the radical in Eq. (5), and the ordinary ray is given by the lower (negative) sign. For $f < f_o$, the converse is true.

When R is a real number, 0, or ∞, the wave is plane polarized. When R = -j or +j, the polarization is circular in the right-handed or left-handed sense, respectively. When R is any other negative or positive imaginary number, the polarization is elliptical in the right-handed or left-handed sense, respectively. All the rules previously given for determining the state of polarization can be deduced from Eq. (5).

Conditions for Reflection of Ordinary and Extraordinary Components

There are two different sets of reflection conditions for the ordinary and extraordinary components (19). The gyrofrequency of the electron, $He/(2\pi mc)$, determines which of the sets of conditions prevails. The two situations are as follows:

a) Wave frequency greater than gyrofrequency. If $f > He/(2\pi mc)$, the ordinary ray will be reflected when $Ne^2/(\pi mf^2) = 1$; and the extraordinary ray will be reflected when

$$Ne^2/(\pi mf^2) = 1 + He/(2\pi mcf) \text{ or } 1-He/(2\pi mcf)$$

(whichever sign is encountered first).

b) Wave frequency less than gyrofrequency. If $f < He/(2\pi mc)$, the ordinary ray will be reflected when $Ne^2/(\pi mf^2) = 1$; and the extraordinary ray will be reflected when

$$Ne^2/(\pi mf^2) = 1 + He/(2\pi mcf).$$

Effects of Collisions

Since the effects of collisions of electrons and other ions with neutral atoms and molecules have thus far been neglected, it is now necessary to consider them (19). In general, collisions will cause absorption. Absorption tends toward a maximum as the refractive index approaches a minimum. Either the ordinary ray or the extraordinary ray may suffer the greater absorption, depending upon other parameters. Collisions can also give rise to a state of polarization different from that indicated by Eq. (5) if the collision frequency approaches a certain critical value given by

$$\nu_c = (He \cos \theta)/(2mc \tan \theta).$$

Near the top of a planetary atmosphere, where the polarization of an escaping ray attains its final state, the collision frequency is zero and Eq. (5) can obviously be used. However, for a ray traversing the terrestrial ionosphere from the direction of Jupiter the collision frequency is not zero, but is of the order of 10^3/second (i.e., the value for the F layer just after midnight). The minimum value of ν_c during the period of the polarimeter measurements was about

2.8×10^7, occurring when Jupiter was on the meridian (at which time $\theta = 9^\circ$). Since this value is several orders of magnitude higher than the collision frequency, Eq. (5) is valid for this case also.

Behavior of Transients Originating within an Ionosphere

Jaeger and Westfold (21) have studied the mathematical problem of propagation of transient phenomena originating within an ionized medium, with a view to accounting for certain observed features of the solar radio radiation. The assumption was made that a localized region of the medium is disturbed very suddenly and briefly by an external force; the theory deals with the resulting transient electromagnetic wave. Exact solutions of a number of transient problems of linear propagation in a homogeneous ionized medium without a static magnetic field were first obtained, utilizing the Fourier transform. This was followed by examinations of the effects of a magnetic field, the possibilities of extension to two- or three-dimensional systems, and the effects of inhomogeneity in the medium.

Although the theory is exact only for greatly oversimplified cases, a number of conclusions can be drawn regarding the propagation of a disturbance originating within the corona of the sun (and, it is hoped, within the ionosphere of Jupiter). The more interesting of these conclusions are as follows (21):

a) Radiation will be emitted at all frequencies greater than the plasma frequency, f_o, and there will be no radiation at frequencies less than f_o (neglecting any static magnetic field).

b) The intensity of the radiation at any frequency f which is greater than f_o will normally decrease with frequency; this decrease will be according to a law such as f^{-2} or f^{-4}.

c) The intensity of a pulse of radiation sent out will decay with time, possibly with the time factor $e^{-\nu t}$, where ν is the collision frequency at the point of origin.

d) There will be a time difference in the arrival of direct waves of various frequencies, higher frequencies arriving first and the frequency f_o last.

e) If the source is above the level of maximum electron density, then the radiation propagated inward will be reflected at the level for which f_o equals f; thus for all frequencies greater than f_o, pulses leaving the ionosphere will be double, the second peak being smaller than the first.

There is considerable experimental support for these conclusions in the case of solar radiation. However, it must be emphasized that the effects can be expected only if the source lies within the ionosphere, and only then in case the original disturbing force is in the form of a brief but intense pulse, for otherwise a persisting originating disturbance will mask the transient reaction produced by the medium.

It should be possible to test some of the above predictions experimentally in the case of radiation from Jupiter.

CHAPTER IV

RECEIVING APPARATUS OF THE UNIVERSITY OF FLORIDA OBSERVATORY

Project Chronology and Participants

A broadside antenna array for operation at 18.0 Mc/s was designed by the writer in February, 1956. It was constructed by Mr. C. H. Barrow, Mr. George Harris, and the writer, between March and September, 1956. The array was used for Jupiter observations between December, 1956 and April, 1957, being the only antenna in operation during this period. Observers participating were Prof. A. G. Smith, Mr. Barrow, the writer and beginning about midway in the season, Mr. R. J. Pepple.

Observations of Saturn were made with the 18 Mc/s array between February and April, 1957.

During the period of the Jupiter observations, preliminary experiments were also performed on the detection of possible fluctuations of light arriving from the planet coincidentally with the radio bursts.

In order to increase the probability of detecting radiation from Saturn, a 22.2 Mc/s corner reflector array was designed, largely by the writer (but with substantial contributions by Prof. Smith, as was usual). It was constructed by Prof. Smith, personnel from the

Physics Department Shop, and the writer in April, 1957. Observations of Saturn made in May with this array were not valid, since it was later discovered that the array was not functioning properly at the time. The defect was located and corrected in August, 1957.

Up to this point the work of the Radio Observatory had been financed entirely from Physics Department funds, made available through the support of Prof. R. C. Williamson, departmental chairman. In August of 1957, however, a grant of $20,000 was made to the Observatory by the National Science Foundation. This generous assistance made possible a great expansion of the program.

A method for the measurement of directional patterns and gains of large antenna arrays was developed largely by the writer and applied between July and November, 1957.

A great deal of effort was also expended throughout this period on improvements in the corner reflector array, and on innovations aimed at improving performance, which were not always successful.

A polarimeter for operation at 22.2 Mc/s was designed by Mr. Pepple and the writer, and was constructed by Mr. Pepple between November, 1957 and January, 1958.

Two Yagi arrays, for operation at 22.2 Mc/s and 27.6 Mc/s respectively, were purchased during 1957. Steerable masts to support them were constructed and the arrays were erected. The Yagi arrays were operational in January, 1958.

Following the construction or installation of each array, considerable work was required in the preparation of associated

impedance matching, phasing, receiving, switching, recording, and calibration equipment inside the observatory.

Five channels were in operation during most of the second apparitions[1] of the planets of interest, from December, 1957 to May, 1958, one of the channels being the polarimeter. The frequencies employed were 18.0, 22.2, and 27.6 Mc/s. Observers participating during this season were Prof. Smith, Mr. Barrow, Mr. Pepple, Mr. J. K. Jackson, Mr. W. H. Perkins, Mr. H. I. Register, and the writer. Extensive observations were made of Jupiter, Saturn, Uranus, and Venus.

In March, 1958, results of the studies of Jupiter during the first apparition were published in the Astrophysical Journal (22).

The 18 Mc/s Broadside Array

The 18 Mc/s broadside array consists of eight half-wave dipoles suspended a quarter wavelength above a reflecting plane, as shown schematically in Figure 3. The dipoles arranged in two east-west lines of four each, with a spacing of one-half wavelength between the lines. The reflecting screen is 133 feet long in the east-west direction, and 82 feet wide in the north-south direction. It consists of 28 tautly stretched No. 6 aluminum wires, spaced 3 feet apart. This spacing is close enough so that the system of wires

---

[1] The term "first apparition" will be used henceforth to designate observations made during the period December, 1956 to May, 1957, and "second apparition" to designate observations made between December, 1957 and May, 1958.

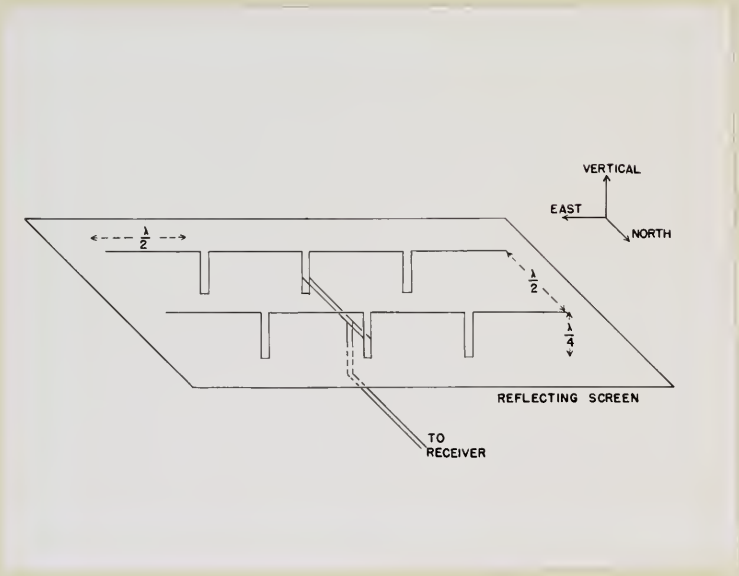

Fig. 3.--Configuration of the 18 Mc/s broadside array.

is almost as efficient a reflector for 18 Mc/s waves of east-west polarization as a continuous sheet of metal. Each line of four dipoles is itself a center-fed collinear sub-array, the individual dipoles in it being end fed. Quarter-wavelength shorted phasing stubs between the adjacent dipoles in each half of the collinear sub-array provide the 180° phase shift necessary to maintain the four dipoles in phase coincidence for a source lying on the main lobe axis. The feed points of the two collinear sub-arrays are joined by a length of line passing between them, and the main transmission line is connected to an intermediate point on this bridging line. The position of the junction point determines the relative phasing of the two collinear sub-arrays, which in turn determines the declination (i.e., the position in the north-south vertical plane) of the axis of the main lobe of the antenna pattern. No east-west directional control of the main lobe axis was provided; the axis is confined to the meridian plane. A portion of the array is shown in Figure 4.

The dipole lengths (23), l, were determined from the formula,

$$l = 468/f, \qquad (6)$$

where l is in feet and the frequency, f, is in Mc/sec. The value of l in this case is 26.0 feet. The height of the dipoles above the reflecting plane, $\lambda/4$, and the spacing between collinear sub-arrays, $\lambda/2$, were determined from the free space wavelength (23) calculated by the formula

$$\lambda = 984/f, \qquad (7)$$

λ being in feet and f in Mc/sec. The value of λ in this case is

Fig. 4.--View of the broadside array from the southwest.

54.7 feet. The lengths of the phasing stubs could be determined either by calculation (i.e., 0.975 $\lambda/4$, where 0.975 is the propagation velocity factor for the line used), or as was actually done, by direct measurement with the standing wave indicator.

The dipoles were made of No. 14 copper-clad steel wire. The phasing stubs between dipoles, the bridging line between collinear sub-arrays, and the main transmission line are all of commercially available 300-ohm open wire line. The collinear sub-arrays are supported between 2" x 4" wooden masts (which were coated with preservative where in contact with soil) and are guyed with galvanized iron wire broken up into non-resonant lengths by small insulators.

For use in matching impedances in the array, an 18 Mc/s Hartley oscillator, of a few watts power, and a simple standing wave indicator were built in accordance with instructions given in references (23) and (24). The standing wave indicator consists essentially of a pickup coil which could be clamped to the open wire transmission line, a resonant coil and condenser, a crystal diode detector, and a 0-100 microampere meter. By obtaining meter readings at various points along a line in which the current distribution was known, the standing wave indicator was found to be linear within the required limits.

As the first step in matching impedances in the array, a 300-ohm feed point at the center of each of the collinear sub-arrays was provided. This was accomplished by means of a strategically placed matching stub. The required length and position of the matching

stub were determined with the aid of the standing wave indicator in the following manner. A temporary transmission line was connected at the center of one of the sub-arrays (i.e., directly to the adjacent ends of the two entral dipoles). The oscillator was coupled to the temporary transmission line. The standing wave ratio in this line and the distance of the first null from the antenna were determined with the aid of the indicator. Using these two parameters and a graph given in reference (24), the proper length and position along the line for a matching stub (a shorted stub in this case) were determined. Such a matching stub was connected, and the portion of the temporary transmission line beyond it was clipped off. The remaining terminals, across which the impedance is 300-ohms pure resistance, are the feed point for the collinear sub-array. In the same manner a 300-ohm feed point was provided for the other collinear sub-array.

After connecting the 300-ohm bridging line between the feed points of the two collinear sub-arrays, and the main transmission line to the proper point along the bridging line, one more matching stub was necessary before the array was completely matched to the line. Since at the junction the 300-ohm transmission line is connected in effect to the two portions of the 300-ohm bridging line in parallel, there is a 300-ohm to 150-ohm mismatch. The length and position along the main line for a matching stub which would eliminate the mismatch (an open one in this case) was found in the same manner as before, and the stub was connected.

After the matching was completed, the voltage standing wave

ratio in the main transmission line was determined to be less than 1.4. This was considered satisfactory.

The main transmission line is routed beneath the wires of the reflecting plane (maintaining at least 6" clearance) to the edge of the array, and then via poles to the observatory building. Just outside the building the transmission line is connected to a J-type, or half wave, balun (balance to unbalance transformer) made of RG-11/U 75-ohm coaxial cable. This was necessary because one side of the receiver input is grounded, whereas the open wire line is balanced with respect to ground (also, it is much more convenient to bring coaxial cable into a building than open wire line). The J-type balun provides a 4 to 1 impedance transformation, which in this case was desired. Another type of balun made of coaxial cable, the π-type, or quarter wave, balun (also called the "bazooka"), does not alter the impedance. Both types are described in references (23) and (24).

An L-section matching network (i.e., a series inductance and a shunt capacitance) was used to match the 75-ohm cable to the receiver, the input impedance of which was about 200 ohms. Approximate values for L and C in the matching network were calculated from formulas in reference (25), but the final adjustment was made with the aid of an antenna bridge.

The antenna bridge, an extremely useful and relatively inexpensive instrument, is essentially a Wheatstone bridge operating at radio frequencies. A grid-dip meter tuned to 18 Mc/s is used as the voltage source. The bridge indicates the value of the resistance

when there is no reactance. Resonant antennas and matched transmission lines always appear to be pure resistances. When an impedance is not pure resistance, the bridge reading has no significance; however, the non-zero null in such a case is a useful indication of the fact that reactance is present.

The 18 Mc/s array has also been described by Barrow (26,27).

Receiving, Recording, and Calibration Equipment used During the First Apparition

A block diagram of the entire system used during the first apparition of the planets of interest, in the winter and spring of 1956-1957, is shown in Figure 5.

The receiver was a Hallicrafters SX-62, a commercial communications receiver. The bandwidth at the selectivity setting used ("sharp-normal") was estimated to be 3 to 5 Kc/s between half voltage points. The audio output was rectified by means of a crystal diode and was used to deflect an Esterline-Angus pen recorder. The recorder time constant is about 1 second. A standard paper speed of 6 inches per hour was employed for the daily records made with this recorder. A Brush pen recorder having paper speeds up to 125 mm/s was operated in addition, at the discretion of the observer, in order to obtain higher resolution during periods of Jupiter activity. The amplifier of the Brush recorder was also driven from the audio output of the receiver, the audio frequency signal being rectified by means of a crystal diode and smoothed somewhat with a resistance-capacitance filter having a time constant of about 0.05 second. A loudspeaker

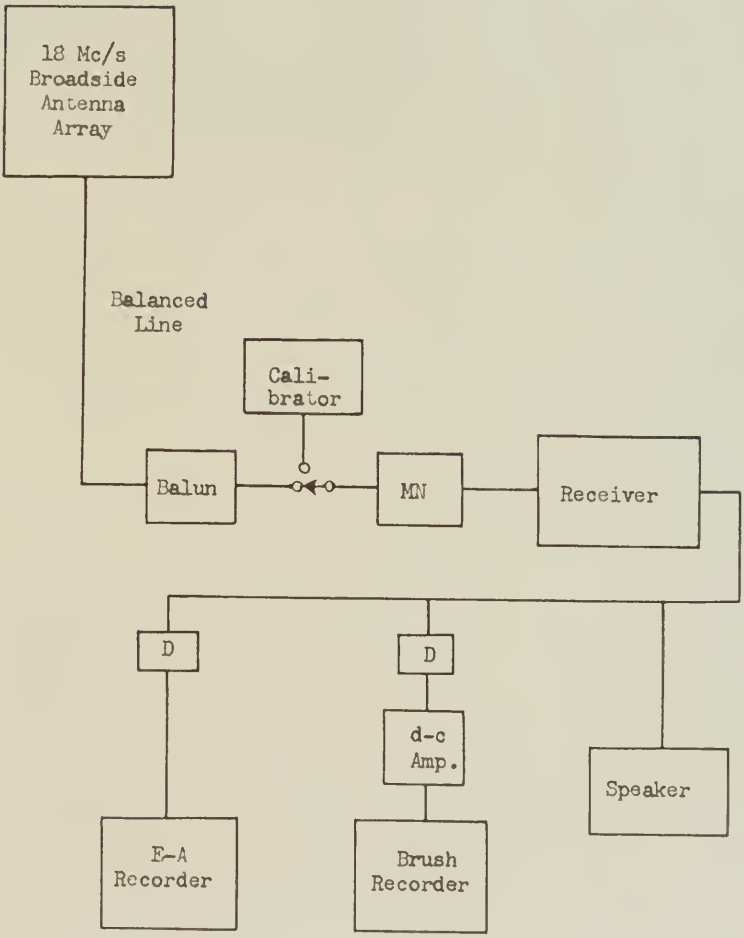

Fig. 5.—Block diagram of system used during first apparition (MN = matching network; D = diode rectifier).

was connected to the same receiver for aural monitoring.

In order that calibration steps could be added at the end of each record on which there had been any Jupiter activity, a temperature-limited noise diode calibration circuit was constructed. The circuit is shown in Figure 6.

The shot-effect noise in the diode current can be determined accurately when the current flow is limited by the filament temperature --i.e., when all the emitted electrons are attracted to the plate. In such a case, the noise component of the diode current is given by

$$\bar{i}^2 = 2eI\Delta f, \qquad (8)$$

where $\bar{i}$ = rms value of noise current, in amperes, having frequency components in the band Δf (Δf being measured in c/s);

e = electronic charge (i.e., 1.59×10^{-19} coulombs);

I = d-c diode current in amperes.

If the receiver input is connected in parallel with R, the two having the same impedance, half the noise current will flow through R and half through the receiver input resistance. The power delivered to the receiver input will be $(\frac{1}{2}\bar{i})^2R$, from which

$$p = eIR\Delta f/2, \qquad (9)$$

where p = noise power delivered to the receiver input, in watts.

The noise power delivered from the antenna to the receiver input as a result of a Jupiter disturbance is (assuming the noise spectrum to be essentially flat over the receiver bandwidth),

$$p = p_1 A\Delta f/2, \qquad (10)$$

where p_1 = power flux from Jupiter per unit bandwidth, measured in watts m^{-2} $(c/s)^{-1}$;

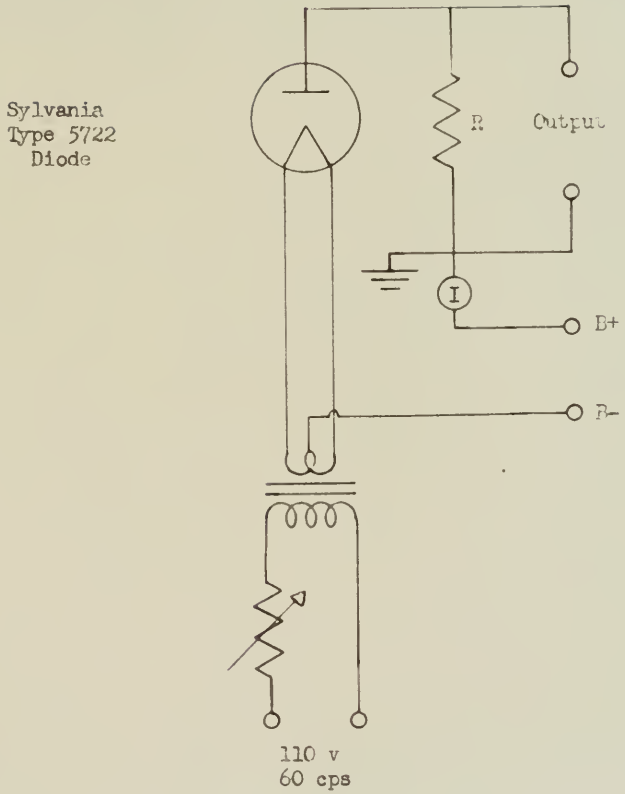

Fig. 6.--Essentials of calibration circuit (various by-pass condensers and RF chokes have been omitted). R was 75 ohms during the first apparition; afterward it was changed to 300 ohms.

A = effective area of the antenna array normal to the direction of Jupiter, in meters^2.

The reason for the division by 2 in Eq. (10) is that only half the power incident on any antenna is delivered to the receiver input (assumed to be matched), the other half being re-radiated. If after noise from Jupiter is recorded, the antenna is replaced by the calibrator at the receiver input, and I is varied until the same deflection is obtained as in the case of the Jupiter noise, then the values of p from the two sources, as given by Eqs. (9) and (10), are equal. It follows that

$$p_1 = eIR/A. \qquad (11)$$

If high accuracy in the determination of p_1 is required, it is then necessary to account for transmission line losses, and to deduct for the contribution of galactic noise to the resultant deflection (remembering that the square root of the sum of the squares of the Jupiter and galactic deflection components gives the resultant deflection). Eq. (11) then becomes

$$p_1 = e(I_{JG} - I_G)\, R/AT, \qquad (11a)$$

where I_{JG} = noise diode current giving the same deflection as the planetary noise and the galactic noise combined;

I_G = noise diode current giving the same deflection as the galactic noise alone;

T = power transmission coefficient for the transmission line.

Eqs. (11) and (11a) are correct if the radiation and the antenna are both plane polarized, in the same plane. However, if the radiation is circularly polarized and the antenna is plane polarized, only half of the available power is received. In this case, the right

hand sides of Eqs. (11) and (11a) must be multiplied by the factor 2.

Figure 7 shows the electronic and recording equipment used during the winter and spring of 1956-1957.

Calculation of Broadside Array Pattern and Gain

Although a method for the measurement of the directional pattern and power gain of an antenna array was later developed for testing the corner reflector array, it was considered adequate to calculate these parameters for the broadside array. The pattern calculation can be performed either graphically by means of vectors, or analytically. The graphical method is very instructive, helping one to appreciate just how the various lobes and nulls in the pattern come about; however, the analytical development will be presented here because it can be done more compactly.

The calculation of the 18 Mc/s broadside array pattern is begun by invoking two simplifying principles of antenna analysis. The first has to do with image antennas. If an antenna is suspended with its center a distance h above a perfectly conducting plane of infinite extent, then for either transmitting or receiving, the relative field intensity pattern above the plane is the same as that which would be obtained if a mirror image of the antenna were located a distance h below the plane, and the plane were removed. Current components in the image antenna which are parallel to the plane must be equal, but oppositely directed, to corresponding components in the real antenna; image components perpendicular to the plane must be equal to and in the same direction as those of the real antenna. This

Fig. 7.--Electronic and recording equipment, first apparition.

follows as a direct consequence of Maxwell's Equations. Although in practice the reflecting plane is neither infinite nor a perfect conductor, the method of images can often give a close approximation to the correct result.

The second simplifying principle has to do with the method of treatment of arrays of arrays. If an array is composed of regularly spaced and identical sub-arrays (or dipoles), the pattern of the array is equal to that of a single sub-array (or dipole) multiplied by that which would be obtained if each sub-array (or dipole) were replaced at its center of symmetry by an isotropic antenna, the phase relationships between the isotropic antennas being the same as those of the feed points of the sub-arrays.

The pattern of the 18 Mc/s broadside array in the east-west vertical plane passing through the array center is thus proportional to the product $F_a(\theta)\ F_b(\theta)\ F_c(\theta)$, where the functions represent the respective patterns of the elementary configurations shown in Figure 8.

Similarly, the pattern of the 18 Mc/s broadside array in the north-south vertical plane passing through the array center is proportional to the product $F_d(\theta)\ F_c(\theta)$, where the symbols represent the respective patterns of the elementary configurations shown in Figure 9.

It is here assumed that the two collinear sub-arrays of the broadside array (giving rise to F_d in Figure 9) are connected in phase, which was true for Jupiter observations during the first season. The reason there is no dipole factor in this case is that the equatorial pattern of a dipole is constant with respect to the angle.

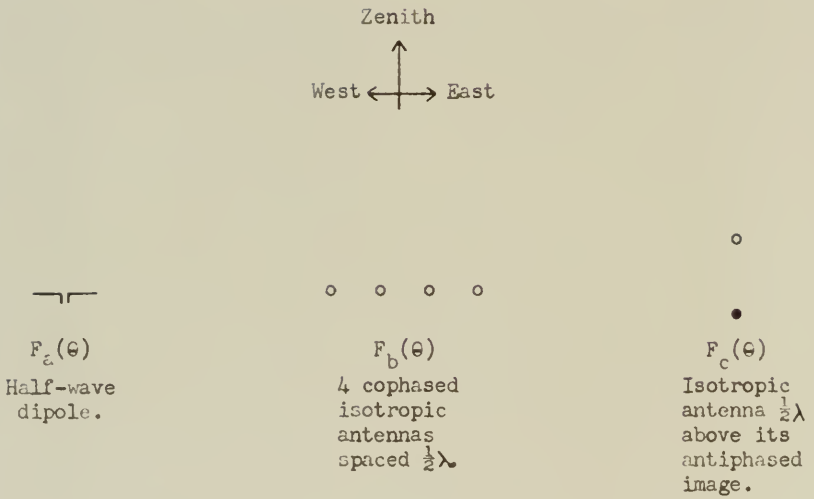

Fig. 8.--Factors making up the Pattern of the 18 Mc/s Broadside Array in the East-West Vertical Plane.

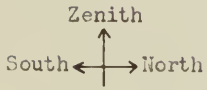

$F_d(\theta)$

Cophased pair of isotropic antennas spaced $\frac{1}{2}\lambda$.

$F_c(\theta)$

Isotropic antenna $\frac{1}{2}\lambda$ above antiphased image.

Fig. 9.--Factors making up the Pattern of the 18 Mc/s Broadside Array in the North-South Vertical Plane.

As the first step in deriving the complete expression for the east-west pattern, the factor $F_a(\theta)$, the pattern of a half-wave dipole within a plane passing through the dipole, must be evaluated. This is done for a transmitting dipole by integrating the radiation from current elements along the entire dipole length, for the angle (θ) with respect to the normal. The pattern for a receiving dipole is the same, by virtue of the principle of reciprocity. The derivation is rather lengthy and can be found in standard references (28), so that it will not be given here. The result is

$$F_a(\theta) = \cos\left(\tfrac{1}{2}\pi \sin\theta\right)/\cos\theta. \qquad (12)$$

It is necessary next to derive an expression for $F_b(\theta)$, the pattern for an east-west row of cophased isotropic antennas, expressed as a function of the angle from the zenith in the east-west plane (28). (By "cophased" is meant that the antennas are assumed to be connected to a receiver by equal lengths of transmission line.) Let WW' be a wave front striking the row of antennas at angle θ, as in Figure 10.

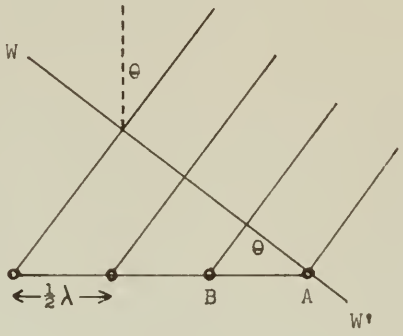

Fig. 10.--Diagram for $F_b(\theta)$ derivation.

The path length to antenna B is longer than that to A by the distance $\frac{1}{2}\lambda \sin\theta$. Similarly, the length of path to each following antenna increases by this same amount. Thus the phases of the sucessive antennas are delayed by $2\pi(\frac{1}{2}\lambda \sin\theta)/\lambda = \pi \sin\theta = \Psi$. In complex vector notation, the resultant a-c voltage at the receiver is proportional to

$$\begin{aligned} & 1 + e^{j\Psi} + e^{2j\Psi} + e^{3j\Psi} \\ &= (e^{4j\Psi} - 1)/(e^{j\Psi} - 1) \\ &= \frac{e^{2j\Psi}(e^{2j\Psi} - e^{-2j\Psi})}{e^{\frac{1}{2}j\Psi}(e^{\frac{1}{2}j\Psi} - e^{-\frac{1}{2}j\Psi})} \\ &= \sin(2\Psi)/\sin(\tfrac{1}{2}\Psi)\ e^{\frac{3}{2}j\Psi}. \end{aligned}$$

Inserting the factor $\frac{1}{4}$ to make the maximum value equal to unity, the amplitude of the complex voltage at the receiver input for the simple case considered is thus proportional to

$$F_b(\theta) = \tfrac{1}{4} \sin(2\pi \sin\theta)/\sin(\tfrac{1}{2}\pi \sin\theta). \qquad (13)$$

We must finally evaluate the factor $F_c(\theta)$, the pattern of an isotropic antenna and its antiphased image located a half wavelength below it. (By "antiphased" it is meant that the respective transmission lines from the isotropic antenna and the image antenna to the receiver are assumed to differ in length by a half wavelength.) In Figure 11, WW' represents a wave front striking two such antiphased antennas, the incident rays making an angle θ with respect to the vertical. The wave front must travel an additional distance $\frac{1}{2}\lambda \cos\theta$ to reach the lower antenna after striking the upper one, corresponding to a phase delay of $2\pi(\frac{1}{2}\lambda \cos\theta)/\lambda$, or $\pi \cos\theta$. There is an additional phase delay

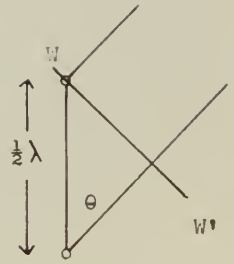

Fig. 11.--Diagram for $F_c(\theta)$ derivation.

of π due to the assumed half wavelength greater length of the transmission line from the lower antenna to the receiver. Thus the resultant voltage at the receiver input is proportional to

$$1 + e^{j(\pi + \pi \cos \theta)}.$$

The real component of this is

$$1 + \cos(\pi + \pi \cos \theta) = 1 - \cos(\pi \cos \theta).$$

The imaginary component is

$$\sin(\pi + \pi \cos \theta) = -\sin(\pi \cos \theta).$$

The amplitude is the square root of the sum of the squares of these two components, or

$$\left[2 - 2 \cos(\pi \cos \theta)\right]^{\frac{1}{2}} = (2)^{\frac{1}{2}} \left[1 - \cos(\pi \cos \theta)\right]^{\frac{1}{2}}$$

$$= 2 \sin(\tfrac{1}{2} \pi \cos \theta).$$

Thus

$$F_c(\theta) = \sin(\tfrac{1}{2} \pi \cos \theta), \qquad (14)$$

the factor 2 having been dropped to make the maximum value of the function unity.

The complete expression for the pattern of the 18 Mc/s broad-array in the east-west vertical plane is thus

$$F_{ew}(\theta) = F_a(\theta)\, F_b(\theta)\, F_c(\theta)$$

$$= \frac{\cos\left(\frac{1}{2}\pi \sin\theta\right) \sin\left(2\pi \sin\theta\right) \sin\left(\frac{1}{2}\pi \cos\theta\right)}{4 \cos\theta \sin\left(\frac{1}{2}\pi \sin\theta\right)} \qquad (15)$$

The factor $F_d(\theta)$ contained in the expression for the north-south pattern must be evaluated next. This is the pattern of a pair of isotropic antennas spaced a half wavelength apart, connected to a receiver by equal lengths of transmission line. In Figure 12, let WW' be a wavefront striking the two antennas, represented by circles,

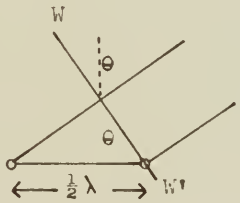

Fig. 12.—Diagram for $F_d(\theta)$ derivation.

at the angle θ with respect to the line joining them. The wavefront must travel an additional distance $\frac{1}{2}\lambda \sin\theta$ to reach the left-hand antenna after striking the right-hand one, corresponding to a phase delay of $2\pi(\frac{1}{2}\lambda \sin\theta)/\lambda$, or $\pi \sin\theta$. Thus the resultant voltage at the receiver input is proportional to

$$1 + e^{j\pi \sin\theta}.$$

The real component of this is $1 + \cos(\pi \sin\theta)$, and the imaginary component is $\sin(\pi \sin\theta)$. The amplitude is the square root of the sum of the squares of the two components, or

$$\left[2 + 2\cos(\pi \sin\theta)\right]^{\frac{1}{2}}$$

$$= (2)^{\frac{1}{2}} \left[2 - 2\sin^2\left(\tfrac{1}{2}\pi \sin\theta\right)\right]^{\frac{1}{2}}$$

$$= 2\cos\left(\tfrac{1}{2}\pi \sin\theta\right).$$

Thus

$$F_d(\theta) = \cos\left(\tfrac{1}{2}\pi \sin\theta\right). \qquad (16)$$

The complete expression for the pattern of the 18 Mc/s array in the north-south vertical plane is

$$F_{ns}(\theta) = F_d(\theta)\, F_c(\theta) = \cos\left(\tfrac{1}{2}\pi \sin\theta\right) \sin\left(\tfrac{1}{2}\pi \cos\theta\right). \qquad (17)$$

The point by point computation of $F_{ew}(\theta)$ and $F_{ns}(\theta)$ for plotting is greatly simplified by the use of tables of the functions $\sin\left(\frac{1}{2} S \sin\theta\right)$, $\sin\left(\frac{1}{2} S \cos\theta\right)$, and $\cos\left(\frac{1}{2} S \sin\theta\right)$ for appropriate values of S. Such tables can be found in reference (29).

Figure 13 is a plot of $F_{ew}(\theta)$. It is seen that there is a null in the pattern 30° to each side of the main lobe axis; there are small secondary lobes centered about 42° to each side. The ratio in decibels of $F_{ew}(\theta)$ at a secondary lobe maximum to that at the main lobe maximum is 20 log 0.15, or -16.5 db. The east-west half power beamwidth (i.e., the angle between the 0.707 values of $F_{ew}(\theta)$) is 25°.

Figure 14 is the plot of $F_{ns}(\theta)$. There are no side lobes in this case. The north-south half power beamwidth is 58°.

The power gain of an array is the ratio of the power which would be delivered into a matched receiver input by the array, to that which would be delivered into a matched receiver by a free space dipole. It is assumed that the same intensity of radiation is incident on the array and on the dipole, and that the source is in the direction of the main lobe maximum of each. The ratio is usually expressed in decibels, one advantage of this being that it is then unnecessary to specify whether power gain or voltage gain is meant. The gain of an

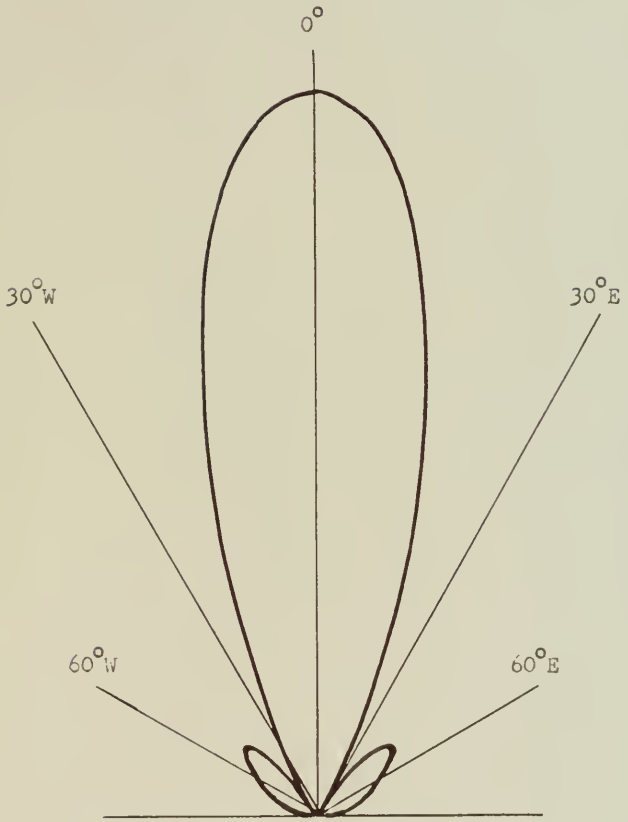

Fig. 13.--East-west pattern of 18 Mc/s broadside array, calculated from Eq. (15).

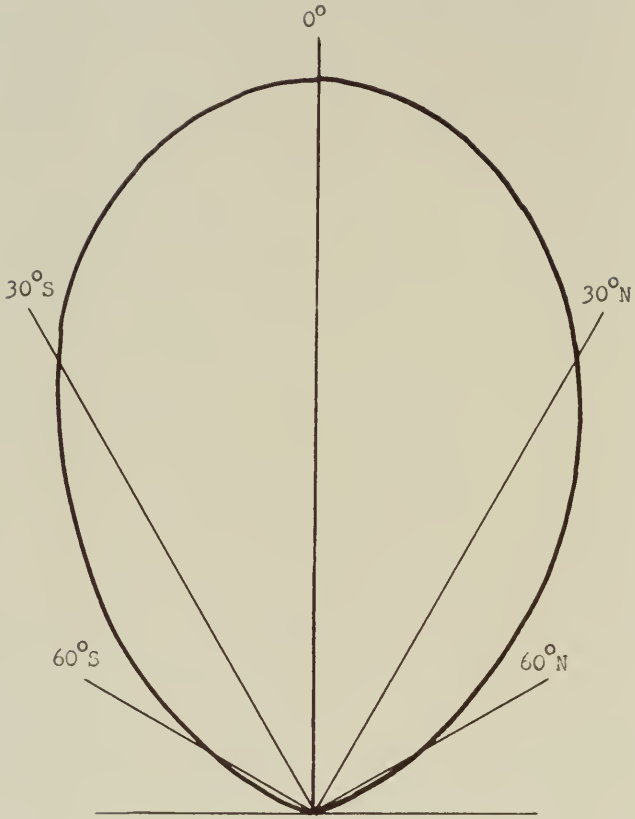

Fig. 14.--North-south pattern of 18 Mc/s broadside array, calculated from Eq. (17).

array can be calculated by either of two methods; one involves the integration of the square of the pattern in three dimensions, and the other involves determining mutual impedances between all possible dipole pair combinations in the array. Both methods can be very complicated. In the present case the gain of the broadside array will be estimated from empirical data, as is most often done.

The resultant gain of an array can be expressed as the product (or sum, if decibels are used) of component gains. In the case of the 18 Mc/s broadside array the component gains are those of (a) a four element collinear array in free space, (b) a cophased pair of parallel eipoles spaced a half wavelength apart, and (c) a single dipole a quarter wavelength above a large plane reflector. All three component gains can be found in reference (24) and are used to obtain the resultant gain as follows:

a)	4 collinear elements,	4.3 db
b)	Parallel dipole pair, spaced $\frac{1}{2}\lambda$,	4.0
c)	Dipole above reflector, Ht. $\frac{1}{4}\lambda$,	6.0 (or a bit less)
	Total	about 14 db.

Thus, the gain of the 18 Mc/s broadside array is about 14 db (with respect to a free space dipole) when the main lobe is perpendicular to the reflecting plane.

During the first apparition, the array was operated with the main lobe vertical during Jupiter watches. However, when Jupiter reached the meridian it was still south of the main lobe axis by about 30°. It is thus necessary to calculate the effective gain

corresponding to this off-axis direction. From Figure 14 it is seen that $F_{ns}(\theta)$ drops to 0.707 (i.e., 3 db below the maximum) at about 29°. The effective gain in the direction of Jupiter at meridian transit was therefore about 14 - 3 = 11 db.

Eq. (11) for the flux per unit bandwidth contains the effective area of the array in the direction of the source. Gain and effective area are proportional, the relation between them being

$$A = 1.64\ G\lambda^2/(4\pi) = 0.130\ G\lambda^2. \qquad (18)$$

(The factor 1.64 is the gain of a free space dipole relative to an isotropic antenna.) In this formula G must be expressed as the power ratio (relative to a free space dipole) rather than in decibels. If $G_{db} = 11$ db $= 10 \log G_p$, then $G_p = 12.6$. For $\lambda = 54.7$ feet $= 16.7$ meters, the corresponding value of A is 459 meters^2. This is the effective area of the array for Jupiter radiation (near meridian transit) during the first observing season.

For Saturn observations during the first season, and Jupiter and Saturn observations during the second season, the main lobe of the 18 Mc/s broadside array was not perpendicular to the reflecting plane, but was tilted southward. This was accomplished by connecting the main transmission line to a point north of the midpoint of the bridging line between the two collinear sub-arrays, causing a phase difference to exist between them. If a wave arrives from a direction φ south of the vertical, it must travel an additional distance $\frac{1}{2}\lambda \sin\varphi$ after reaching the south sub-array before reaching the north one, corresponding to a time difference $(\frac{1}{2}\lambda \sin\varphi)/c$, where c is the propagation

velocity in free space. If it is desired that φ be the direction of the main lobe axis, the length of line from the south sub-array to the junction with the main transmission line must be made just enough longer than that from the north sub-array to compensate for this time difference. Then the two signals will add in phase at the junction. Thus,

$$(\tfrac{1}{2}\lambda \sin\varphi)/c = (2s)/(0.975\ c),$$

where (2s) is the difference in lengths of the two lines and (0.975 c) is the propagation velocity on the lines. The propagation velocity on transmission lines is less than c; the actual values for common types of lines can be found in references (23) and (24). The difference in the lengths of the two parts of the bridging line is 2s when the junction is a distance s north of center. Therefore,

$$s = \tfrac{1}{4}\ 0.975\ \lambda \sin\varphi \qquad (19)$$

is the required distance of the junction north of center to tilt the beam an angle φ south of the vertical.

The north-south pattern of the array after the beam is tilted could, of course, be calculated. However, this is not considered necessary. The beam no doubt becomes a bit broader in the north-south plane, as well as having its maximum displaced, but the east-west pattern is relatively unaffected (except, of course, that $F_{ew}(\theta)$ is now the pattern in the east-west plane inclined southward at the angle φ, rather than in the east-west vertical plane). When the beam is displaced 45° southward, the main lobe gain is probably 1 or 2 db less than when it is vertical. In this case the main lobe gain would be about 12 db instead of 14 db.

The 22.2 Mc/s Corner Reflector Array

The corner reflector antenna, apparently originated by Kraus (30), utilizes the familiar principle in optics by which multiple images are produced from a single light source placed between two intersecting plane mirrors. It can readily be shown geometrically that three virtual images are formed if the mirrors intersect at 90°, or five images if the intersection is at 60°. In the case of the radio analogue, the light source is replaced by a dipole (or a series of dipoles) and the mirrors by metallic reflecting planes. The dipole and its virtual images can be considered a multi-element antenna array, maximum directivity occurring along a line which is perpendicular to the dipole and which bisects the reflector intersection angle.

The corner reflector array which was constructed here for operation at 22.2 Mc/s consists of a collinear group of four dipoles suspended between two plane reflectors intersecting at an angle of 60°. The main features are shown in Figure 15.

The string of dipoles is parallel to the east-west line formed by the intersection of the planes. The entire structure can be rotated about this line, permitting the axis of the array beam to be swung to any angle within an arc passing through the zenith and extending to 30° above the horizon in the north and to 30° above the horizon in the south. By adjusting the relative phasing of the four dipoles, the beam can also be swung eastward or westward in the plane bisecting the angle between the reflectors. The half power beamwidth, as determined by a method to be described later, is about 22° east and west, and about 45°

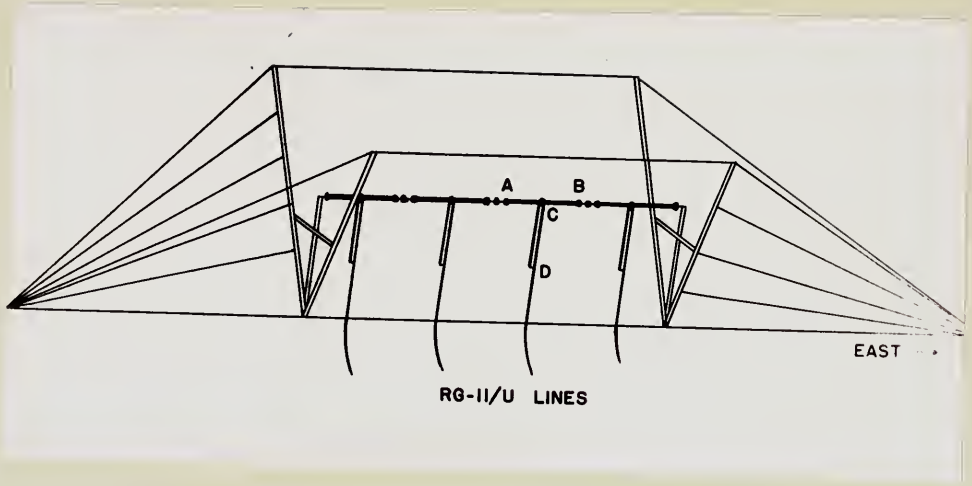

Fig. 15.--Configuration of the corner reflector array. AB is one of the dipoles; CD is a balun. (The wires constituting the reflecting planes and most of the guys have been omitted from the diagram.)

north and south. In operation, the array is tilted to the approximate declination of the planet under observation and is locked at this angle. Then the beam is phased as far eastward as is feasible without excessive loss of gain, actually about 45°. As the planet progresses across the sky, the beam is shifted westward in 15° steps at the proper times by plugging appropriate additional cable lengths into the transmission lines from the four dipoles. This operation is performed at the receiver, the observer's presence not being required at the antenna once it has been set to the proper declination. A photograph of the antenna is shown in Figure 16.

Each of the two reflecting planes is 108 feet long (east to west) and 48 feet from the vertex to the outer edge. Each reflector consists of 30 parallel copper-clad steel wires (No. 18) stretched east and west between large V-shaped supports made of aluminum television tower sections. Each of the four dipoles is 20 feet long, the ends of adjacent dipoles being separated by 3-foot lengths of wire interspersed with insulators. The dipoles are made of No. 14 copper-clad steel wire. The string of dipoles is suspended within the angle formed by the intersecting reflectors at a distance of about one-half wavelength (22 feet) from the vertex. The mast at each end of the string of dipoles is rigidly attached within the V-member at that end. The vertex of each V-member is pivoted on a steel base set on a concrete foundation. At each end of the reflectors, a system of guys from attachment points located every 6 feet along each leg of the V-support converges to a pivoted guy anchor. The axles at the bases of

Fig. 16.--The 22.2 Mc/s corner reflector array as seen from the east.

the two V-supports and the axles of the two guy anchors all lie in the same straight line, so that as the structure is tilted the tension in the guys cannot change. The tilt is controlled by means of a pair of windlasses, one to the north and the other to the south. Flexible steel cables passing around pulleys connect each windlass to the nearer legs of the V-supports. As cable is taken up on one windlass, tilting the structure toward it, cable must be allowed to pay out from the other. When the desired declination is reached, as read from a graduated scale at one end of the pivoted bases, the structure is held securely by locking both windlasses.

Each dipole is connected at its center to a separate 75-ohm coaxial cable (RG-11/U). The radiation resistance of the dipoles can be made very nearly 75 ohms by slight adjustment of the dipole height above the reflector vertex. Transformation from the balanced dipole feed points to the unbalanced coaxial line is accomplished without change in impedance by means of a π-type balun at each dipole, as at CD in Figure 15. The four coaxial lines lead into the observatory building to a junction box; these lines are all the same length. The junction box is shown schematically in Figure 17. It is provided with pairs of sockets for inserting additional lengths of cable into the four transmission lines in order to achieve the desired phase relationship between the dipoles. The transmission lines and phasing cables are made of RG-11/U 75-ohm cable. After passing through the phasing cables, signals from the four lines are brought to a common point in the junction box. The impedance at this point is one-fourth that of

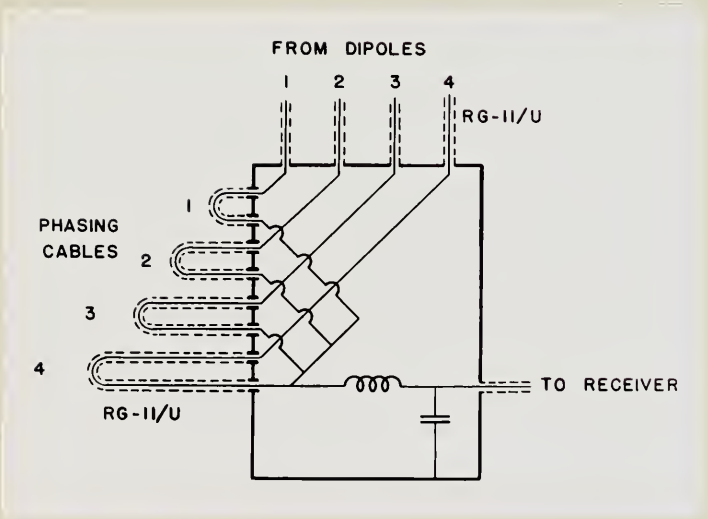

Fig. 17.--Junction box for the 22.2 Mc/s corner reflector array.

the individual lines, or about 19 ohms. An L-section network in the junction box is used to match this low impedance to that of the cable leading to the receiver. The voltage standing wave ratio in each of the four transmission lines was found by measurement to be less than 1.10 at the design frequency, 22.2 Mc/s.

The lengths of the phasing cables to be inserted into the four lines for directing the beam axis to various angles θ east or west of the normal to the dipoles are given in Table 1. The line numbers correspond to those of the dipoles, which are numbered from east to west. Each quantity in parentheses represents a separate cable length. L is the length of the shortest cables, which can be any convenient length. ΔL_θ for each value of θ is given by the formula

$$\Delta L_\theta = (v/c)\, S \sin \theta, \qquad (20)$$

where v = velocity of propagation in the cable,

c = velocity of propagation in free space,

and S = distance between centers of adjacent dipoles (23 feet).

It is seen that if the phasing cables are equipped with plugs, permitting them to be joined to each other as well as to the sockets in the junction box, then any of the seven angles listed in Table 1 can be obtained by choosing the appropriate cables from a stock of ten.

The pattern of the 22.2 Mc/s array was measured by an especially developed method, to be described later in this chapter. The pattern in the east-west and north-south planes of symmetry of the array are shown in Figures 18 and 19, respectively. As was stated earlier, the measured beamwidth between half power points is about 22° east-west and about 45° north-south.

TABLE 1

LENGTHS OF PHASING CABLES

θ	Line No. 1	Line No. 2	Line No. 3	Line No. 4
49°E	$(L-3\Delta L_{15})+(L+3\Delta L_{30})$	$(L+2\Delta L_{15})+(L+2\Delta L_{30})$	$(L+\Delta L_{15})+(L+\Delta L_{30})$	(L)+(L)
30°E	$(L+3\Delta L_{30})$	$(L+2\Delta L_{30})$	$(L+\Delta L_{30})$	(L)
15°E	$(L+3\Delta L_{15})$	$(L+2\Delta L_{15})$	$(L+\Delta L_{15})$	(L)
0°	(L)	(L)	(L)	(L)
15°W	(L)	$(L+\Delta L_{15})$	$(L+2\Delta L_{15})$	$(L+3\Delta L_{15})$
30°W	(L)	$(L+\Delta L_{30})$	$(L+2\Delta L_{30})$	$(L+3\Delta L_{30})$
49°W	(L)+(L)	$(L+\Delta L_{15})+(L+\Delta L_{30})$	$(L+2\Delta L_{15})+(L+2\Delta L_{30})$	$(L+3\Delta L_{15})+(L-3\Delta L_{30})$

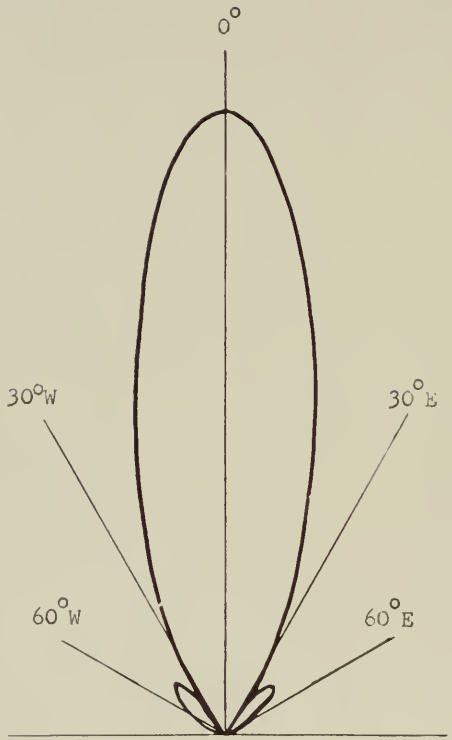

Fig. 18.--Measured east-west pattern of the 22.2 Mc/s corner reflector array.

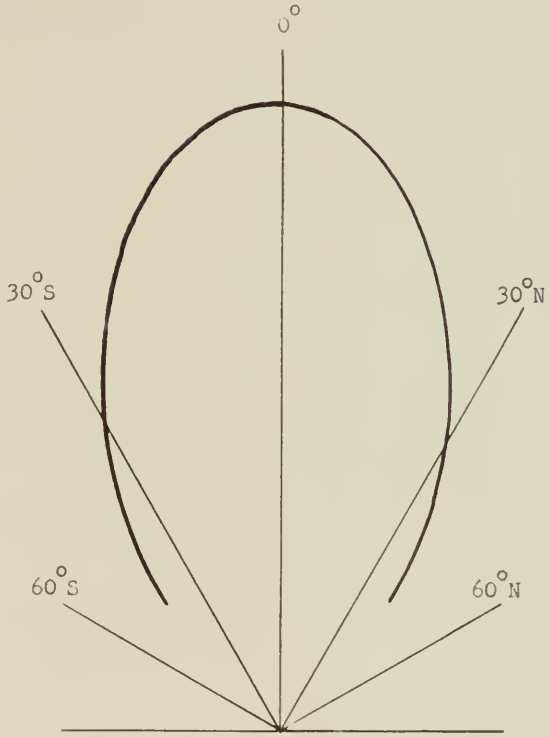

Fig. 19.--Measured north-south pattern of the 22.2 Mc/s corner reflector array.

The gain of the array was measured at the same time that the pattern was determined. The gain can also be estimated from empirical data. In reference (24) it is stated that a gain of about 10 db can be obtained from a single-dipole corner reflector antenna with sides one wavelength from vertex to edge. A factor of 4.3 db is given as the gain of 4 collinear half wave dipoles end to end. Thus the gain to be expected from the 22.2 Mc/s corner reflector array is 14.3 db. However, the measured gain was about 11 db, or a bit more than 3 db too low. Despite many changes in the array in an attempt to improve it, many tests, and consultation with Professor Kraus at Ohio State University, the cause of this discrepancy has not been determined. Professor Kraus stated that a possible cause of the trouble lies in dissipative or re-radiation losses in the reflectors. He stated that 60° corner reflector antennas are much more susceptible to such difficulties than are the 90° type, and he strongly recommended changing to the latter. However, this was not feasible at the time. There is a possibility that as a result of more recent changes the gain is now greater than 11 db. Unfortunately, there has not been time to make the new series of tests which would be necessary to determine this.

A Method for the Measurement of the Pattern and Gain of Large Antennas

In connection with the testing of the corner reflector array, a technique was developed for measuring directional patterns and gains of large antenna arrays. In this method an airplane carrying a

transmitter flies at approximately constant altitude (about 5,000 feet) along either an east-west or a north-south course passing through the beam of the array under test. The signal received by the array is compared with that received at the same time by a simple array of known characteristics. This is accomplished by using a single receiver-recorder channel, which is switched alternately between the array under test and the standard array at a switching period of about two seconds. The standard array consists of a horizontal east-west half wave dipole suspended a quarter wavelength above a large horizontal plane made of parallel wires. By drawing smooth curves through the two sets of segments of the commutated record, relative signal strengths from the two arrays are obtained as a function of time. The direction of the airplane from the arrays is periodically indicated at 15° intervals on the same record by an observer. These directions are obtained from the alignment of pairs of sighting wires with the passing airplane, the pairs of wires being oriented at 15° intervals. A typical commutated record is shown in Figure 20. The sighting structure is shown in Figure 21.

In order to obtain the directional pattern of the array under test from a commutated record such as that in Figure 20 it is necessary to make use of the known pattern of the standard array. The latter (i.e., the pattern of a horizontal half-wave dipole a quarter wavelength above a perfectly reflecting horizontal plane) can be found in reference (24). The unknown pattern is computed point by point by multiplying the standard pattern by the ratio of the signal from the array under

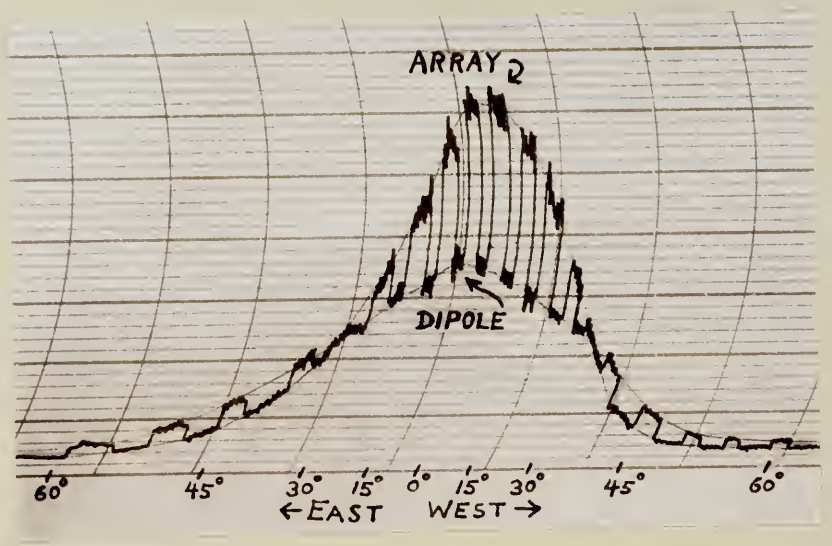

Fig. 20.--Commutated record comparing a single-dipole corner reflector array with a standard array. Segments labelled "Array" are deflections from the array under test; those labelled "Dipole" are deflections from the standard array. Indicated angles are directions of the airplane from the vertical.

Fig. 21.--Sighting structure for determining direction of the airplane. Observer notes times at which the airplane is aligned with the lower wire (nearest his eye) and one of the upper wires.

test to that from the standard array as measured from the record at corresponding angles.

The gain of the standard array is about 6 db relative to a free space dipole. The gain of the array under test is therefore equal to 6 db plus the ratio in db of the beam-center signal from this array to that from the standard array. It is, of course, necessary that each of the arrays be properly matched to the transmission line.

The transmitter used in the airplane is a spark transmitter, designed for maximum simplicity of construction and operation. It consists essentially of an automobile ignition coil, a spark plug, and an automobile radio vibrator. The primary current, supplied from a 6-volt storage battery, is interrupted by means of the vibrator, causing rapidly repeated sparking of the spark plug. The airplane antenna is coupled to the two sides of the spark gap. The transmitted signal is very broad in frequency. The radiated power, although quite low, is adequate for the purpose.

Two antennas are required in the airplane, one of which is polarized for north-south flights and the other for east-west flights. These antennas are dipoles, somewhat shorter than a half wavelength, suspended beneath the craft.

The corner reflector array patterns shown in Figures 18 and 19 were obtained by the method just described. As an example of the use of the method for the measurement of gain, the case represented by Figure 20 will be considered. Here the ratio of maximum deflection

for the single-dipole 60° corner reflector array to that for the standard array is 5.2 db, and the gain of the latter is 6 db. Therefore the gain of the single dipole corner antenna must be 5.2 db + 6 db = 11.2 db. This is in agreement with the generally accepted gain for a single-dipole 60° corner reflector antenna with sides one wavelength from vertex to outer edge (24).

Since the method outlined above involves comparison with a standard antenna, it is relatively free from possible errors caused by varying distance to the airplane, anisotropy of the airplane antenna pattern, and fluctuations in transmitter power and receiver gain.

The 18 Mc/s Yagi Array

Since the 18 Mc/s broadside array can effectively receive radiation from a planet only while it is within about 20° of the meridian, corresponding to about 3 hours of observing time, it was decided to supplement this array with an 18 Mc/s Yagi array which could easily be steered in azimuth, so as to keep the planet within its beam for a longer time. Accordingly, a 5-element Yagi array was purchased from Telrex, of Asbury Park, New Jersey. A mast providing azimuth steering was constructed, and the array was erected with the aid of a motor crane. The antenna is shown in Figure 22. The height of the array above ground is 28 feet, or about a half wavelength.

The mast consists of an outer frame of aluminum television tower sections resting on a steel table set on a concrete base, with

Fig. 22.--The antenna field. The 18 and 27.6 Mc/s Yagi arrays are at the center and far left, respectively. The polarimeter array is just left of center, and the corner reflector array is to the right.

a $2\frac{1}{4}$" pipe inside the tower. The pipe rests on a thrust bearing beneath the table, passes through a hole in the table, through the entire height of the tower, and projects 10 feet above a bearing in the top of the tower. The antenna boom is clamped at its center to the projecting part of the pipe. An azimuth steering lever is attached to the pipe beneath the steel table at the base, the table being so constructed that the lever is unobstructed by the table supports for a swing of 180°. The antenna can quickly be locked to any of a series of azimuths 15° apart by means of a pin which can be dropped through the steering lever into properly spaced holes in an underlying stationary plank. The aluminum tower is guyed with three wires which are broken up into non-resonant lengths by insulators. Adjustment of the elevation angle of the antenna is made by loosening the clamp holding the antenna boom to the vertical pipe, tilting the boom to the desired elevation angle, and clamping again. The boom is of such length (36 feet) that it sags if not given additional support near the ends. This is accomplished by means of two nylon ropes, which are attached to the ends of the boom, passed through pulleys at the top of the 8-foot length of pipe extending above the antenna, and tied. Whenever the elevation angle is changed, these ropes must be adjusted.

Included with the purchased antenna were a matching loop and a J-type balun, which match the antenna to 50-ohm coaxial cable. About 300 feet of RG-8/U cable is used to connect the antenna with its receiver.

The gain of the 18 Mc/s Yagi array, as specified by the manufacturer, is 12.5 db relative to a free space dipole.

The 27.6 Mc/s Yagi Array

In order that observations could be made at another frequency besides 18 and 22.2 Mc/s, a 27.6 Mc/s, 7-element Yagi array was also purchased from Telrex. A simpler and more satisfactory mast than the previous one was constructed, and the array was erected. The array is 20 feet, a bit over a half wavelength, above ground. It can be seen in Figures 22 and 23.

The mast consists of a 25-foot telephone pole and a 27-foot length of $2\frac{1}{2}$" galvanized water pipe. The telephone pole was set in a 6-foot hole by the Gainesville Electric Department. The pipe is fastened alongside the pole in such a way that it can rotate, and it projects $8\frac{1}{2}$ feet above the top of the pole. A steel plug in the base of the pipe rests on a single large ball bearing embedded in a steel plate which is bolted to the pole, forming the thrust bearing on which the pipe rotates. At the top of the pole, the pipe passes through a hole in a right-angled bracket bolted to the pole to serve as the upper bearing. The antenna boom is clamped at its center to the pipe about two feet above the top of the pole. Nylon ropes, to prevent the 36-foot long antenna from sagging, pass from its ends through pulleys at the top of the pipe, and down to the level of the antenna, where they are tied. These ropes and pulleys were also used to hoist the antenna from the ground to its final position.

Fig. 23.--The 27.6 Mc/s Yagi array (left), and the polarimeter array (right center). The observatory, with its roof open, and the west end of the corner reflector array can also be seen.

The azimuth of the array is controlled by means of a steering lever fastened to the base of the pipe, just above the bearing. The antenna can quickly be locked to any of a series of azimuths 15° apart by passing a pin through a hole in the end of the steering lever into an appropriate matching hole in an underlying stationary plank. To change the elevation angle of the array, the clamp holding it to the pipe must be loosened, the boom of the array tilted to the desired angle, the nylon ropes readjusted, and the clamp tightened again.

The antenna was supplied with a matching loop and J-type balun, which match it to the 50-ohm RG-8/U coaxial cable leading into the observatory building.

The gain of the 27.6 Mc/s Yagi array, as specified by the manufacturer, is "13 db plus" relative to a free space dipole.

The 22.2 Mc/s Polarimeter

In order to determine the degree and sense of the polarization of radiation from Jupiter, a 22.2 Mc/s polarimeter was built. This array and its associated switching circuits were constructed by Mr. R. J. Pepple, and are described in detail by him in reference (31). The antenna was designed by Mr. Pepple, and the switching circuitry by the writer. The polarimeter antenna is shown in Figures 22 and 23.

The polarimeter antenna consists of a pair of identical 4-element Yagi arrays mounted along the same axis but with their polarization planes at right angles to each other (both planes being

inclined at 45° with respect to the horizontal). The common axis of the pair of arrays can be steered along the celestial equator by adjusting the guy ropes; however, for all the measurements made to date, the axis lay approximately within the meridian plane.

Separate 75-ohm coaxial cables lead from gamma-matched outputs of the two Yagi arrays to switching circuit SC1 (Figure 25) inside the observatory, the two transmission lines up to this point being of exactly the same electrical length. Switching circuit SC1 periodically introduces an extra quarter wavelength of line first into one transmission line and then into the other, the period of the complete switching cycle being one second. The two lines then merge into a single line which passes out of SC1 to M at the receiver input.

The rectified audio output of the receiver is switched periodically by circuit SC2 (Figure 25) between one channel and the other of a dual channel, quick-response Brush pen recorder in synchronism with the switching of the extra quarter wavelength of line alternately into the two transmission lines by SC1. Thus, pen number 1 can show a deflection only when the path length from antenna A is a quarter wavelength greater than that from antenna B, and pen number 2 can show a deflection only when the path length from antenna B is a quarter wavelength greater than that from antenna A. The deflection sensitivities of the two pens are made equal by adjustment of their associated d-c amplifiers.

The switching in SC1 and SC2 is accomplished by relays which are actuated by a motor-operated switch in SC3. The switching in the

antenna circuits causes apparently unavoidable transients due to contact potential effects. The usefulness of the polarimeter was at first seriously impaired by these brief but relatively intense transients. However, the difficulty was solved by adding another switch, also in SC3 (and actuated by the same motor as the previously described switch), which momentarily short-circuits the audio output of the receiver during the brief intervals that the transients are being produced. This effectively prevents them from appearing at the recorder. The transient-suppression feature is not described in reference (31).

If an incident signal causes the two pens, in their respective halves of the switching cycle, to deflect the same amount, the incident radiation must be plane polarized. If pen 1 deflects and pen 2 does not, the polarization is circular, and it is in the right-handed sense. If pen 2 deflects and pen 1 does not, the polarization is again circular, but in the left-handed sense. If both pens deflect, but one deflects more than the other, the polarization is elliptical. The sense of elliptical polarization is right-handed if pen 1 deflects more than pen 2, and left-handed if pen 2 deflects more than pen 1. The ratio of major to minor axis lengths of the polarization ellipse can be determined from the relative deflections of the pens. The formula relating the axial ratio to the deflections will now be derived.

The contribution of the galactic noise to the resultant deflection of the pens is not negligible, and so must be taken into account. Since the galactic radiation is randomly polarized, the

deflections of the two pens will be equal when caused by galactic radiation alone. Let

G = deflection of either pen by galactic noise alone;

D_1 = deflection of pen 1 by simultaneous presence of Jupiter noise and galactic noise;

D_2 = same for pen 2;

J_1 = deflection which pen 1 would experience if galactic noise were somehow removed, leaving only Jupiter noise;

J_2 = same for pen 2.

Since the noise from the two sources is random and uncorrelated,

$$J_1^2 + G^2 = D_1^2 ; \qquad J_2^2 + G^2 = D_2^2 .$$

$$J_1 = (D_1^2 - G^2)^{\frac{1}{2}} ; \qquad J_2 = (D_2^2 - G^2)^{\frac{1}{2}}. \qquad (21)$$

Assume that the crossed Yagi arrays are directed toward Jupiter, and neglect any reflection from the ground. A 90° clockwise rotation of Yagi A, as viewed from Jupiter, will bring it into exact coincidence with Yagi B. A right-handed coordinate system is now defined in which the x axis is in the direction of propagation from Jupiter, the y axis is parallel to the dipole element of Yagi A and positive toward the end which feeds the central conductor of the coaxial line, and the z axis is parallel to the dipole of Yagi B, with the positive direction specified in the same way. Let the component of the electric vector inducing current in Yagi A be E_y, and in Yagi B, E_z. With E_y and E_z expressed in complex vector notation to account for their relative phases, the axial ratio of the polarization ellipse can be specified as

$$R = E_z/E_y. \qquad (22)$$

Thus if the wave is plane polarized, R will be 0, ∞, or some real number, depending upon whether the polarization plane is parallel respectively to the y axis, the z axis, or to neither.

For waves which are circularly polarized, R is -j for the right-handed sense and +j for the left-handed sense. If R is any other negative or positive imaginary number, the polarization is elliptical and the sense is right-handed or left-handed, respectively. This interpretation is consistent with that of Eq. (5).

Before proceding further, it should be demonstrated how the interpretations thus far given come about. Suppose that a right-handed circularly polarized wave is incident at the antenna. This means that as the electric vector propagates forward it rotates in the same sense as a right-handed screw. Thus, the peak of the sinusoidal current cycle induced in Yagi A will be reached a quarter period before that in Yagi B; in other words, the current in A leads that in B by a quarter cycle. Now, when the switching circuit has added an extra quarter wavelength to the line from A, the signal from A, after travelling the extra distance, finds itself exactly in phase with that from B at the point where they merge. As a result, pen 1 deflects. On the other hand, when the extra quarter wavelength is added to the line from B, the signal arriving from B at the junction is retarded a quarter cycle, and now finds itself a half cycle behind that from A, or 180° out of phase. Consequently, the signals cancel, and no deflection is produced on pen 2 during its period of sensitivity. This is in agreement with the earlier statement that deflection on pen

1 and none on pen 2 signifies right-handed circular polarization. Now, any function $f(\omega t)$ leads the function $f(\omega t - \delta)$, δ being positive. Thus, if the induced current in A (for right-handed circular polarization) is proportional to $\cos \omega t$, that in B will be proportional to $\cos (\omega t - \frac{1}{2}\pi)$. In complex vector notation, the current in A can, for this case, be designated $I e^{j(0)} = I$, and that in B as $I e^{-j(\frac{1}{2}\pi)} = -j I$, I being the amplitude and 0 and $\frac{1}{2}\pi$ the phase angles. Therefore R, which is the ratio of E_z to E_y, and also the ratio of the current in B to that in A, is -j. This agrees with the earlier statements that R = -j signifies right-handed circular polarization.

It will now be shown how the axial ratio R can be determined by means of the polarimeter deflections for the special case when the major and minor axes of the polarization ellipse are parallel to the E_y and E_z axes, respectively, which in turn are parallel to the elements of antennas A and B, respectively.

Parametric equations of the circle in Figure 24 are

$$E_y = a \cos \omega t, \tag{23}$$

$$E_z = a \sin \omega t, \tag{24}$$

where ω is the angular rotational frequency of a generating point rotating clockwise about the circle, and t is the time.

Let the heavy vertical line be the locus of another generating point moving according to the equation

$$E_y = (b - a) \cos \omega t, \tag{25}$$

If the components of the two generating points are added linearly, the resulting figure can be expressed parametrically by

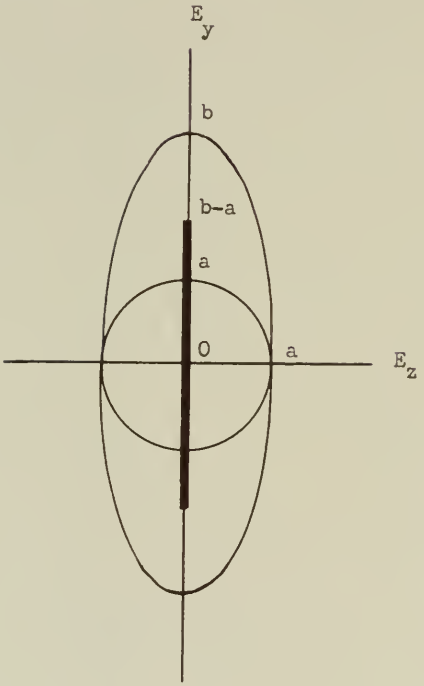

Fig. 24.--Polarization diagram.

Eq. (24) and the sum of the right-hand sides of Eqs. (23) and (25). Thus

$$E_y = b \cos \omega t, \tag{26}$$

$$E_z = a \sin \omega t. \tag{24}$$

Squaring and adding these equations, we get

$$E_y^2/b^2 + E_z^2/a^2 = 1,$$

which is a standard form for an ellipse such as that in Figure 24. Thus the addition of the linearly and circularly moving points results in an elliptically moving point.

Applying the converse of what has just been proven, we can say that if the axes of the polarization ellipse are parallel to antennas A and B, the induced currents can be considered as due to the linear superposition of currents from a circularly polarized wave and a linearly polarized one, the relationships between the three polarization figures being as indicated in Figure 24.

Expressing Eqs. (26) and (24), respectively, in complex vector notation,

$$E_y = b\, e^{j(0)} = b \tag{27}$$

$$E_z = a\, e^{-j(\frac{1}{2}\pi)} = -ja \tag{28}$$

The complex axial ratio of the polarization ellipse is thus given by

$$R = E_z/E_y = -ja/b. \tag{29}$$

At the inputs to the switching circuit the currents from antennas A and B are proportional to b and -ja respectively, in complex vector notation. When one of these currents is made to traverse a

quarter wavelength more line than the other, its phase is retarded by $\frac{1}{2}\pi$, and consequently the expression for the current must be multiplied by $e^{-j(\frac{1}{2}\pi)}$, or -j. We are now in a position to derive the expression for R in terms of the polarimeter deflections.

Assume first that the polarimeter is at the half of the switching cycle for which pen 1 is sensitive and the extra quarter wavelength is added to the line from A. At the junction of the lines the resultant current is proportional to (-j)(b) + (-ja), or -j(a + b). The deflection of pen 1 is proportional to the amplitude of the complex current, so

$$J_1 = k(b + a) \tag{30}$$

where k is the constant of proportionality.

Now assume that the polarimeter is at the half of the switching cycle for which pen 2 is sensitive and the extra quarter wavelength is added to the line from B. At the junction the resultant current will be proportional to (b) + (-j)(-ja), or b - a. Thus

$$J_2 = k(b - a). \tag{31}$$

After succesively adding and subtracting Eqs. (30) and (31), and using Eq. (29), it follows that

$$R = -j(J_1 - J_2)/(J_1 + J_2), \tag{32}$$

or in terms of the deflections including the galactic component, one obtains by the use of Eqs. (21),

$$R = -j\,\frac{(D_1^2 - G^2)^{\frac{1}{2}} - (D_2^2 - G^2)^{\frac{1}{2}}}{(D_1^2 - G^2)^{\frac{1}{2}} + (D_2^2 - G^2)^{\frac{1}{2}}}\,. \tag{33}$$

Finally, it is necessary to investigate the general case in which the axes of the polarization ellipse are inclined with respect to the planes of the polarimeter arrays. The angle of inclination cannot be determined without supplementary measurements which cannot be made with present equipment. However, it will be shown that Eq. (33) still applies in this general case.

First, the problem will be examined intuitively. For plane polarized waves, the polarimeter deflections are independent of the inclination of the polarization plane. The circularly polarized wave is, of course, radially symmetrical about the antenna axis. Thus, for an elliptically polarized wave, which is considered to be compounded from a plane polarized one and a circularly polarized one, changes in the inclination of the major axis of the ellipse with respect to the antenna elements will likewise not result in any change in deflection. Therefore Eq. (33) applies to the general case of any inclination.

Now, the same result will be proven more rigorously. Establish two right-handed coordinate systems x, y, z, and x, y', z', the common x axis of the two being in the direction of propagation and collinear with the axis of the antennas. Let y' be inclined at an acute angle φ with respect to y, and of course, z' at angle φ with respect to z. Let the major axis of the polarization ellipse lie along the y' axis, and the planes of Yagi arrays A and B along the y axis and z axis, respectively. The standard formulas for transformation of coordinates in such a case are

$$y = z' \sin\varphi + y' \cos\varphi$$

$$z = z' \cos\varphi - y' \sin\varphi \,. \qquad (34)$$

The components of the electric field vector along the major and minor axes of the ellipse are $E_{y'}$ and $E_{z'}$, respectively. Thus the components in the planes of antennas A and B are, respectively,

$$E_y = E_{z'} \sin\varphi + E_{y'} \cos\varphi$$

$$E_z = E_{z'} \cos\varphi - E_{y'} \sin\varphi \,. \qquad (35)$$

But from Eqs. (26) and (24) (remembering that the coordinate axes for which the ellipse is symmetrical have now been relabelled),

$$E_{y'} = b \cos\omega t$$

$$E_{z'} = a \sin\omega t. \qquad (36)$$

Substituting Eqs. (36) into Eqs. (35), one obtains

$$E_y = a \sin\varphi \sin\omega t + b \cos\varphi \cos\omega t$$

$$E_z = a \cos\varphi \sin\omega t - b \sin\varphi \cos\omega t. \qquad (37)$$

In complex vector notation, Eqs. (37) become

$$E_y = -j\, a \sin\varphi + b \cos\varphi$$

$$E_z = -j\, a \cos\varphi - b \sin\varphi \,. \qquad (38)$$

When pen 1 is sensitive, the resultant current at the transmission line junction is proportional to

$$(-a \sin\varphi - jb \cos\varphi) + (-ja \cos\varphi - b \sin\varphi)$$

$$= (b + a)(-\sin\varphi - j \cos\varphi).$$

Since the amplitude of this expression is $(a + b)$, it follows that

$$J_1 = k(b + a). \qquad (39)$$

When pen 2 is sensitive, the resultant current is proportional to

$$(-ja \sin \varphi + b \cos \varphi) + (-a \cos \varphi + jb \sin \varphi)$$
$$= (b - a)(\cos \varphi + j \sin \varphi),$$

from which it follows that

$$J_2 = k(b - a). \qquad (40)$$

Eqs. (39) and (40) are identical with Eqs. (30) and (31); therefore it has been proven that Eq. (33) applies for the general case of an inclined polarization ellipse.

The polarimeter is an extremely valuable adjunct to instrumentation for the study of the planetary noise bursts, for by using polarimeter measurements in Eqs. (33) and (5), and correcting for the effect of the terrestrial magnetic field, one can determine whether or not a planet has a magnetic field. The result obtained from Eq. (5) will be in the form of a relation between the magnitude of the field and its direction with respect to the burst propagation direction; if one of these parameters is known, the other is thus determined.

Receiving and Recording Equipment used During the Second Apparition

A block diagram of the receivers, recorders, and associated electronic equipment used during the second apparition, from December, 1957 until late in the spring of 1958, is shown in Figure 25. Five antennas were used; they were the 18 Mc/s Yagi array (18Y), the 22.2 Mc/s corner reflector array (22C), the 18 Mc/s broadside array (18B), the 27.6 Mc/s Yagi array (27Y), and the 22.2 Mc/s crossed-Yagi polarimeter array (22Y). Signals from all these arrays were brought into the observatory via coaxial cable; the types and impedances of the

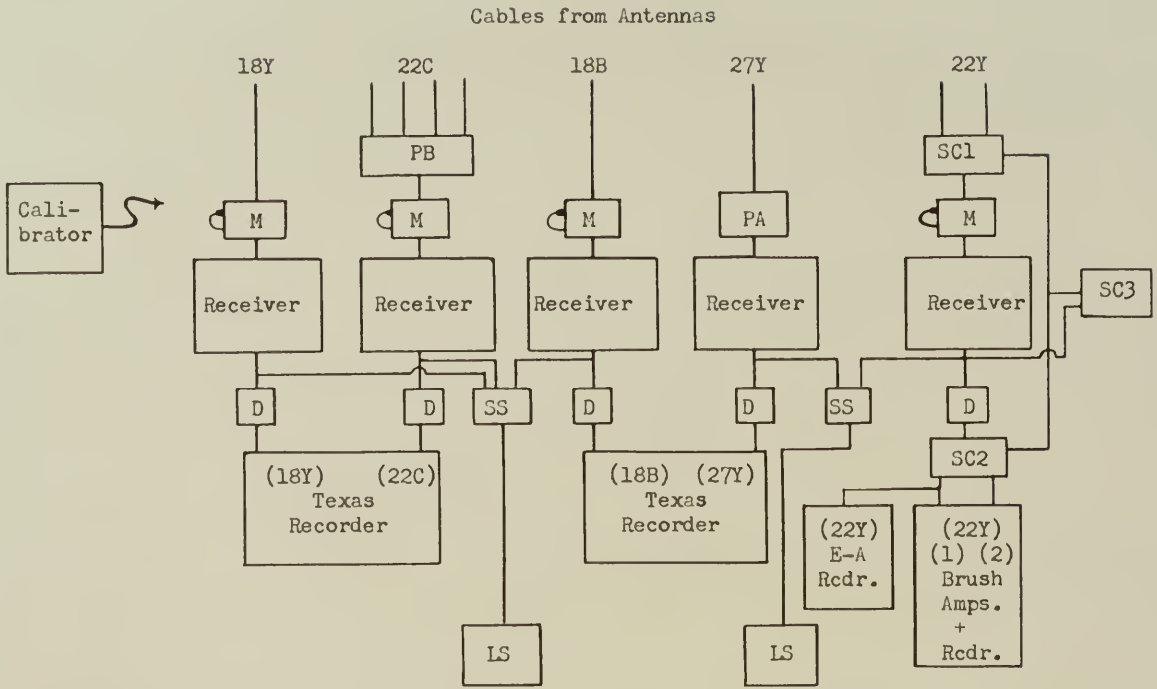

Fig. 25.—Block diagram of receiving and recording equipment used during the second apparition. Abbreviations: 18Y = 18 Mc/s Yagi; 22C = 22 Mc/s corner reflector array; 18B = 18 Mc/s broadside array; 27Y = 27.6 Mc/s Yagi; 22Y = 22.2 Mc/s polarimeter; PB = phasing box; M = matching network and calibration input; PA = preamplifier; D = diode rectifier; E-A Rcdr. = Esterline-Angus recorder; SC1, SC2, and SC3 = switching circuits; SS = speaker switching circuit; LS = loudspeaker.

respective transmission cables are 18Y, RG-8/U, 50-ohm; 22C (4 cables), RG-11/U, 75-ohm; 18B, RG-11/U, 75-ohm; 27Y, RG-8/U, 50-ohm; 22Y (2 cables), RG-11/U, 75-ohm. The 18Y and 18B transmission lines pass directly into the matching and calibration input circuits, M in Figure 25. The four transmission lines from the dipoles in array 22C pass first into phasing and mixing box PB (shown in detail in Figure 17), and then into the matching and calibration input circuit M. The two lines from 22Y enter into the phase-switching and mixing circuit SC1 (already described in the section on the polarimeter), from which a single line connects with the matching and calibration input circuit, M.

The schematic diagram for the four boxes labelled M is shown in Figure 26. This circuit performs two functions; it first transforms the impedance of the coaxial transmission line from the antenna (either 50 or 75 ohms) to that of the calibrator (300 ohms), and then transforms the latter impedance to that of the receiver (different impedances for different receivers). Each of these two impedance transformations is accomplished with an L-section network. Approximate values for the inductances and capacitances were first determined by calculation, and final adjustments were made while the apparent resistance of each L-section, properly terminated, was actually measured with the antenna bridge. When the antenna is being used for reception the link of flexible cable in Figure 26 is left connected; the 50- or 75-ohm antenna output is thus properly matched to the receiver input. However, when it is desired to connect the calibrator instead of the antenna,

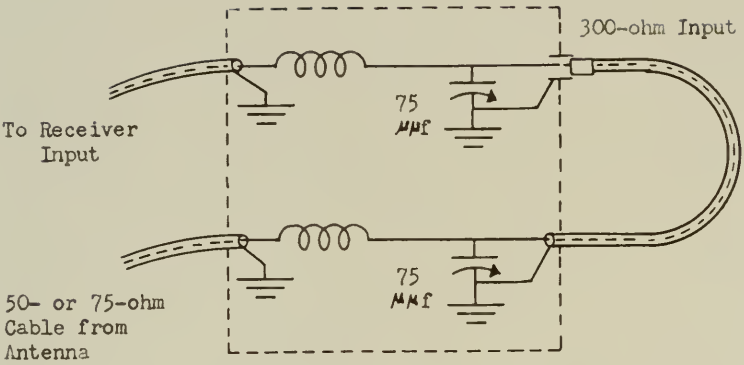

Fig. 26.--Antenna matching and calibration input circuit.

the plug at the upper end of this link is removed, and the calibrator is connected in its place. Now the 300-ohm calibrator output is matched to the receiver. The calibrator is used with just one receiver at a time.

The line from antenna 27Y is connected to an RF preamplifier, PA in Figure 25, the output of which goes to the receiver. An adjustable input impedance matching network is contained in PA. Receiver noise is greater at the higher frequencies, and at 27.6 Mc/s the receiver noise was excessive without the preamplifier. However, with the preamplifier the instrumental noise level was sufficiently reduced relative to the signal level for satisfactory operation. This is due to the fact that the design of the preamplifier is superior to that of the RF section of the receiver. The preamplifier used is the RME Model DB23; it has about 25 db gain. Since channel 27Y has no 300-ohm calibrator input, special measures had to be taken to calibrate it. It was necessary to reduce the calibrator output impedance temporarily to 50 ohms and to connect it to the output of PA in place of the antenna. This inconvenience was not serious, because the infrequent planetary noise at this frequency made it unnecessary to calibrate very often.

The receivers used in channels 18Y, 22C, and 18B were the Hammarlund HQ-150; those in channels 27Y and 22Y were the Hallicrafters SX-62A and SX-62, respectively. The crystal selectivity knobs of the Hammarlund receivers were set at "1", giving a frequency bandwidth between half voltage points of about 2 Kc/s, according to the

instruction book. These receivers were used with the noise limiter off, the Q-multiplier off, manual rather than automatic volume control, beat frequency oscillator off, the RF gain control on maximum, and the audio frequency gain adjusted to give the desired deflection. The crystal selectivity knobs of the Hallicrafters receivers were set at "Sharp-Normal" (no crystal), giving an estimated bandwidth of 3 to 5 Kc/s between half voltage points. Noise limiters of the Hallicrafters receivers were off, tone controls on "Hi-Fi", and beat frequency oscillators off. The SX-62 receiver RF gain control was set at maximum, and deflection level adjusted by means of the audio gain control. The SX-62A receiver (the one with which the RF preamplifier was used) was operated with the audio gain control on maximum and the RF gain control adjusted to give the desired deflection.

Since the audio frequencies at the outputs of the receivers are too high to deflect the recorder pens, it is necessary to rectify them; the deflections thus are proportional to the envelopes of the output audio frequencies smoothed by the inertia of the pens. This rectification is accomplished with 1N34 crystal diodes, D in Figure 25. In the case of the Brush recorder channel (22Y) it was found adviseable to provide additional smoothing by means of a simple resistance-capacitance filter, contained (in addition to the diode) in the box D. This filter had a time constant of about 0.1 second.

One dual-channel Texas pen recorder was used in channels 18Y and 22C, and another such dual recorder in channels 18B and 27Y. When the polarimeter was not in operation, channel 22Y was connected

directly to an Esterline-Angus pen recorder, without switching and without the Brush recorder. In this case, the 22C antenna was receptive to right-handed circularly polarized signals and, with 3 db less gain, to plane-polarized signals. The Texas and Esterline-Angus recorders were operated at a paper speed of 12 inches per second. The time constant of these recorders is about one second.

When the polarimeter is in operation, switching circuit SC2 connects the receiver output alternately to pens 1 and 2 of the Brush recorder, as already described in the section on the polarimeter. Each of the two Brush pens is driven from a separate d-c amplifier, these amplifiers being considered as part of the recorder. The time constant of the Brush pens is about 1/30 second, but this is increased to about 0.1 second by the filter in D. The Brush Recorder, when used with the polarimeter, was usually operated at a paper speed of 5 mm/second.

A very important part of the system is the loudspeakers used for aural monitoring. Two speakers, LS in Figure 25, were used simultaneously, since it had been found that more than this number resulted in a confusion of sound. One speaker can be switched to any one of the channels 18Y, 22C, or 18B, and the other to 27Y or 22Y. Each channel which is not connected to a speaker at a given time must be connected to a dummy load resistor equivalent to the speaker. Otherwise, the change in loading caused by switching a speaker into or out of a receiver output would result in a change in audio gain, altering the recorder deflection. The circuits containing the speaker selector switches and dummy load resistors are represented by SS in Figure 25.

The calibrator has already been described. The circuit is the same as that in Figure 6, with the exception that an inductance was added in parallel to R to neutralize in part the shunt diode capacitance. Although R is 300 ohms, the output impedance was measured to be about 350 ohms at 18 Mc/s and 250 ohms at 22.2 Mc/s, both impedances were resistive.

A photograph of the electronic equipment is shown in Figure 27.

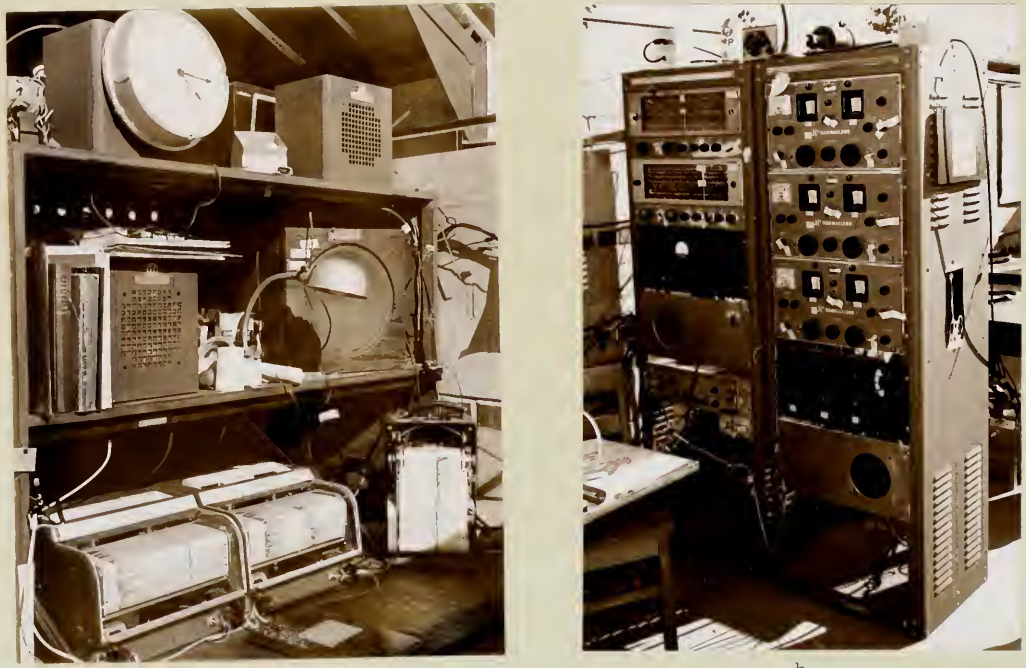

a b

Fig. 27.--Electronic equipment used during the second apparition.
a.--Recorders and loudspeakers.
b.--Racks containing receivers, calibrator, and matching networks.

CHAPTER V

OBSERVATIONAL PROCEDURES

Shortly after the first array was completed it was discovered that reliable reception of planetary radiation at a frequency as low as 18 Mc/s would be possible only between about 2 AM and 6 AM. At other times, interference from atmospheric noise and radio stations is usually excessive, and absorption of the planetary signal in the terrestrial ionosphere may greatly reduce its intensity. The optimum observing season for planets outside the orbit of the earth is that for which transit of the planet occurs between approximately 2 AM and 6 AM. Since transit occurs about 4 minutes earlier each day, the optimum season for a single planet is limited to about 60 days, although if the antenna is steerable, observations can be made for longer periods.

This limitation is related to the diurnal fluctuation of ion density in the terrestrial ionosphere. The ionization results principally from solar ultraviolet radiation, which is of course most intense at noon and is completely absent at night. As would be expected, the ionization is greatest at noon or shortly after, but due to relatively low recombination rates in the F layer, appreciable ionization persists for several hours after sunset (refer to the earlier discussion of the terrestrial atmosphere). As soon as the rays of the rising sun strike the upper atmosphere, the ion densities rapidly increase. Thus the ionization drops to a low value after

midnight and remains low until sunrise.

Except during summer, most of the atmospheric noise interference originates in the tropics, perhaps 500 to 2,500 miles from Gainesville. It will not be received at 18 Mc/s or above unless the ionosphere is sufficiently dense to reflect the disturbances at the required angles. The ion density is always sufficient for this during daylight and early evening. However, sometime after midnight the ion density usually drops below the critical value for reflection, and the rays from the atmospheric noise sources which would at other times arrive at Gainesville pass into space instead. The same is true for rays from distant radio stations at the same frequency. It is only by utilizing the quiet period occurring between 2 AM and 6 AM that satisfactory observations of planetary noise on frequencies as low as 18 Mc/s can consistently be made.

It was found necessary to have an observer on duty during every recording period to monitor the received signals. This was the only way in which it could be ascertained with any degree of reliability which disturbances were from the planet and which were terrestrial interference. The observer maintained a close watch on all the recording pens, and at the same time listened to loudspeakers connected to one or two of the channels. As soon as any one of the pens began to show signs of activity, the observer switched one of the speakers to that channel, and attempted immediately to decide whether the disturbance was from the planet or was terrestrial interference. The principal sources of terrestrial interference are listed in the order

of their severity as follows:

a) Atmospheric noise

b) Radio stations

c) Automobile ignition noise

d) Power line leakage and switching transients

Atmospheric noise has a characteristic crashing sound, each burst beginning very abruptly. Automobile ignition noise has an unmistakeable stacatto sound. The sound from power line leakage is a hum or buzz, and that from a switching transient is an isolated "pop". A faint radio station can at times sound almost exactly like weak Jupiter noise--a series of rising and falling hisses. The distinction can fortunately be made by the simple expedient of rocking the receiver tuning knob back and forth over a range of about 0.1 Mc/s. If this has no noticeable effect on the received noise, it is not a station, since station bandwidths seldom exceed a few kilocycles. On the other hand, the noise from Jupiter covers at least half a megacycle, and slight retuning would not affect it. If an observed disturbance does not appear to be any of the above types of interference, but has the characteristic "swishing" sound of Jupiter and covers a frequency range of at least 0.1 Mc/s, and if the planet is within the antenna beam, then the observer can conclude with reasonable certainty that the noise is of planetary origin.

Another form of interference which is always present is the galactic noise. This is a steady noise having a Gaussian (random) distribution of instantaneous amplitudes. It produces a deflection

which appears constant but which actually varies by a factor of about 2 or 3 during a sidereal day, the maximum occurring when the antenna beam is directed nearest the galactic center. The galactic noise produces a steady hiss in the loudspeaker, having the same quality as receiver noise and shot-effect noise from the calibrator. When terrestrial interference is low it is galactic noise (rather than receiver noise) which sets the minimum detectability limit for planetary noise.

During the first apparition, the recorder in the 18 Mc/s channel was regularly allowed to run all night, and the observer was present during the three hours that the planet was in the broadside array beam. Jupiter was the sole object of study during the first three months; then Saturn was also studied for about a month. As a check on the condition of the terrestrial ionosphere, it was one of the duties of the observer to determine periodically by means of an auxiliary receiver the maximum frequency at which distance stations could be received. During the early part of the season this frequency fell as low as 10 Mc/s (so that 18 Mc/s was completely free of interference from stations and atmospheric noise), but later in the year, with transit occurring about midnight, the maximum station frequency seldom fell below 22 Mc/s. Another of the observer's duties was to operate the higher speed Brush recorder during periods of especial interest.

During the second apparition Jupiter, Uranus, Saturn, and Venus were studied on frequencies of 18, 22.2, and 27.6 Mc/s.

Polarimeter records of Jupiter radiation were also made. During much of the season an observer was on duty for as long as 6 hours a night -- from 1 AM to 7 AM. The maximum station frequency checks were discontinued because of a shortage of receivers. Before each watch, the 18B and 22C arrays were set at the approximate declination of the planet to be observed. The 18Y and 27Y arrays were left at an elevation angle of about 40°. Once an hour during the watch the 22C beam was shifted an additional 15° westward by phasing adjustments, and the 18Y and 27Y Yagi arrays were shifted an additional 15° in azimuth. At the end of every watch, the receiver inputs were shorted to establish the zero deflection level. All channels on which planetary noise had been received were also calibrated at the end of a successful watch.

CHAPTER VI

JUPITER DURING THE FIRST APPARITION

Observational Data

Recordings during the passage of Jupiter through the beam of the 18 Mc/s broadside array were made nightly from December 31, 1956 until the latter part of April, 1957. Only the data collected through March 6, 1957 were used in the following analysis, since increasing terrestrial interference made subsequent observations less reliable. It seems almost certain, however, that there was very little major activity from Jupiter during the period from March 6 to the end of the observing season in April. The first-season Jupiter results are presented in substantially the same form in which they were published by the writer and his co-workers in reference (22).

A typical low-speed recording made during a period of moderate Jupiter activity is shown in Figure 28a. A common duration for such a period of activity was about an hour, although some lasted but a few seconds and others persisted for as long as three hours. The disturbances consisted of a succession of bursts of near-Gaussian noise. Burst amplitudes were random, with one burst often appearing to interrupt a preceding one. Other characteristics of the noise, discernible in recordings made at higher speeds, will be discussed later. The deflections caused by Jupiter noise must always rise above the steady

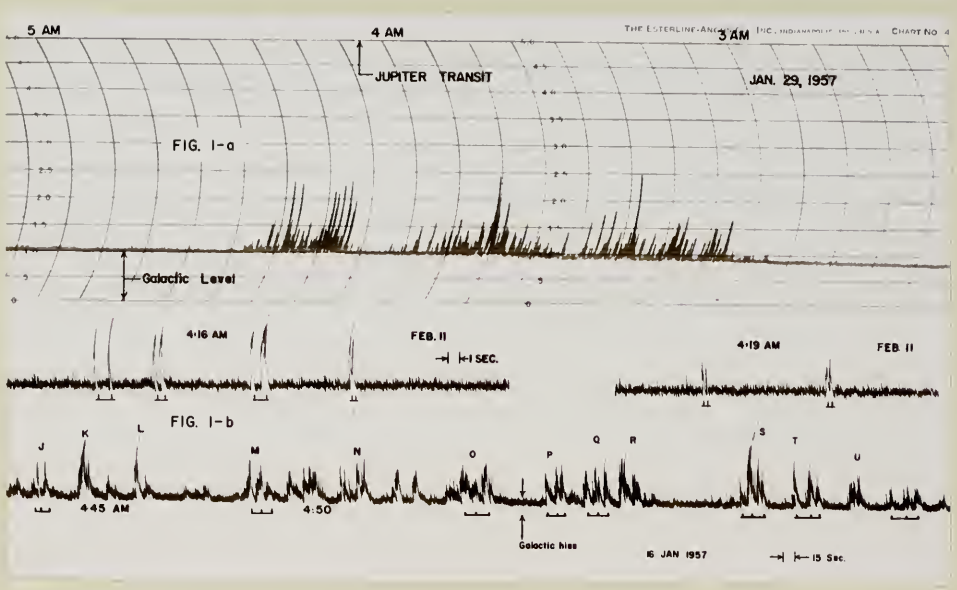

Fig. 28.--Typical recordings of Jupiter noise made at 18 Mc/s.
a.--Low speed Esterline-Angus recording.
b.--Higher speed Brush recording.

deflection resulting from galactic noise, which is also indicated in Figure 28.

The data were plotted in the form illustrated in Figure 29, as a first step in the analysis, to bring to light periodicities corresponding to possible rotational periods. The System II longitude of the central meridian of Jupiter is plotted horizontally, and the dates of the observations are plotted vertically. On each date a single horizontal line denotes the range of central meridian longitudes for which Jupiter was outside the antenna beam, or the receiving system was for some other reason incapable of detecting the presence of Jupiter radiation (e.g., during periods of station interference). Thus the gap in each line indicates the longitudes for which the apparatus could have detected Jupiter noise. The broad horizontal bars within the gaps indicate longitudes for which Jupiter noise actually was received. The solid black bars indicate that the deflection on the record exceeded 0.5 inch at least once every 5 degrees of longitude. Cross-hatched bars indicate deflections between 0.2 and 0.5 inch, and white bars indicate deflections less than 0.2 inch.

When the recorded signal was small, there was sometimes uncertainty as to its origin. It is believed that there is practically no contamination of the Jupiter data represented by black bars, and but slight contamination of that represented by cross-hatched bars. In cases of considerable uncertainty, the horizontal line indicating non-receptivity of the system was extended through the uncertain region.

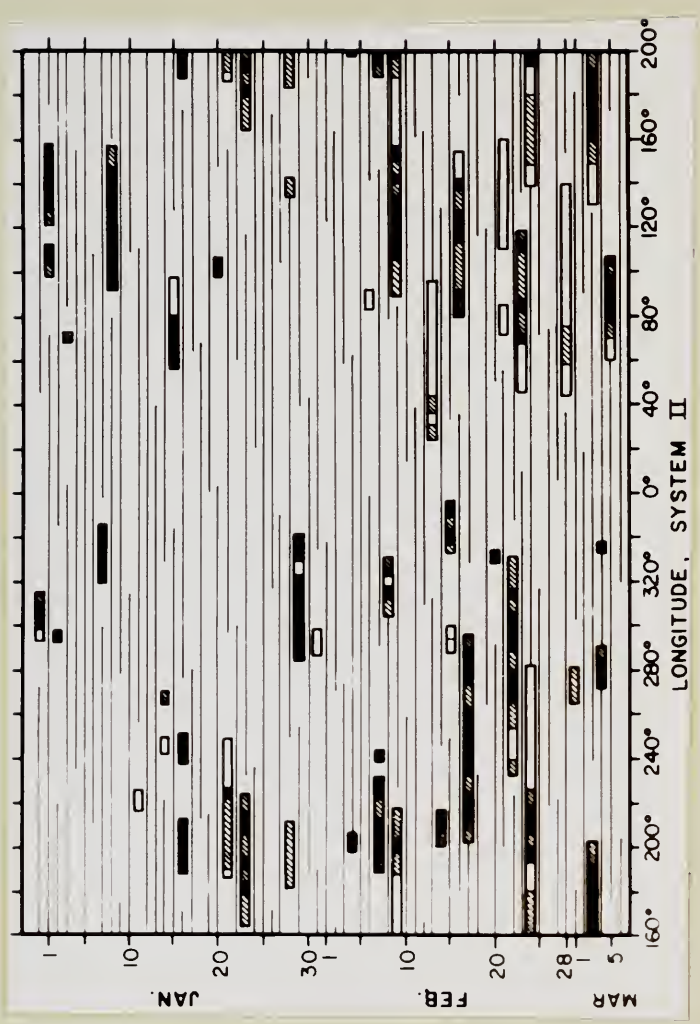

Fig. 29.—Periods of occurrence of 18 Mc/s radiation from Jupiter (first apparition) plotted against System II longitude of the central meridian at the time of observation.

Rotational Periods

A histogram of the probability of occurrence of Jupiter noise as a function of System II longitude of the central meridian, plotted from the data of Figure 29, is shown in Figure 30. The black, cross-hatched, and white areas represent the same deflection ranges as in Figure 29. The probability of occurrence for a particular 5° longitude interval was considered to be the number of occurrences of Jupiter noise within that interval, divided by the number of days the receiving system was in a receptive condition for noise during the same interval. It can be seen that this histogram displays some rather striking features--a main peak reaching 0.48 probability, two lower and broader peaks, and a zone of zero probability 30° wide. The positions of the principal features of this historgram are listed in Table 2, with comparable positions from similar histograms plotted from the data of Shain (Figure 1) and from that of Burke and Franklin (Figure 2). The numbers in parentheses are the estimated maximum errors in the locations of the peaks or minimum.

A histogram of occurrence probability as a function of System I longitude was also plotted. Unlike the System II histogram, that for System I displayed no significant peaks or minima, the ordinate heights being distributed randomly. This is in agreement with Shain's findings.

When the System II positions of the main peak from the three sets of data are plotted as a function of date, they are found to lie very nearly in a straight line, as shown in Figure 31. Moreover, when the positions of the secondary peak found in Shain's data and in the

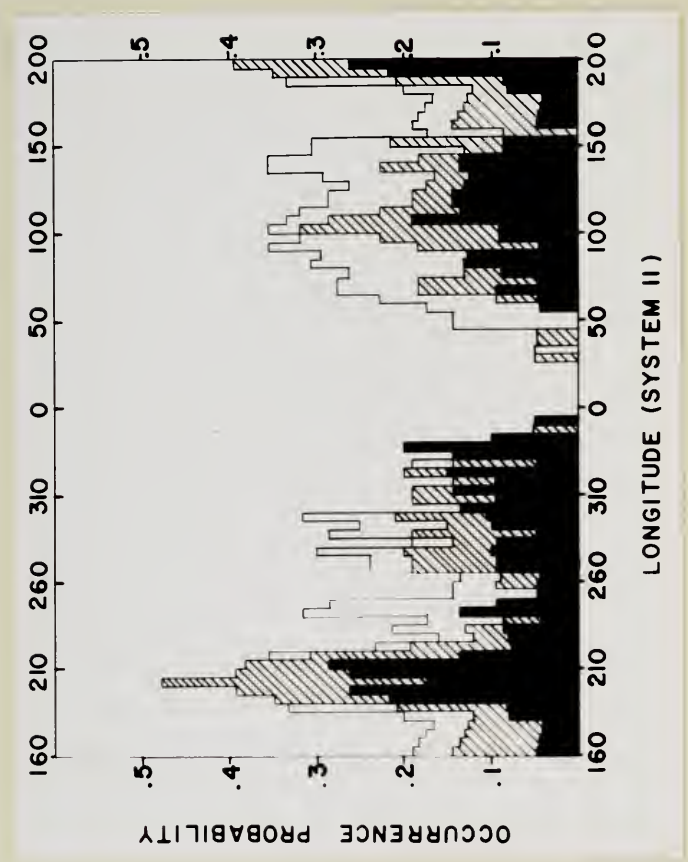

Fig. 30.—Probability of occurrence of 18 Mc/s radiation from Jupiter (first apparition) plotted for 5° intervals of System II longitude.

TABLE 2

SYSTEM II LONGITUDES OF RADIO SOURCES

Observer	Median Date	Freq. Mc/s	Main Peak	Tertiary Peak	Principal Minimum	Secondary Peak
Shain	Sept. 8, 1951	18.3	$57^{\circ}(\pm 10^{\circ})$		$225^{\circ}(\pm 10^{\circ})$	$310^{\circ}(\pm 10^{\circ})$
Burke & Franklin	Nov. 26, 1955	22.2	$317^{\circ}(\pm 5^{\circ})$			
Carr, Smith, Pepple, & Barrow	Feb. 2, 1957	18.0	$203^{\circ}(\pm 5^{\circ})$	$300^{\circ}(\pm 15^{\circ})$	$12^{\circ}(\pm 10^{\circ})$	$110^{\circ}(\pm 10^{\circ})$

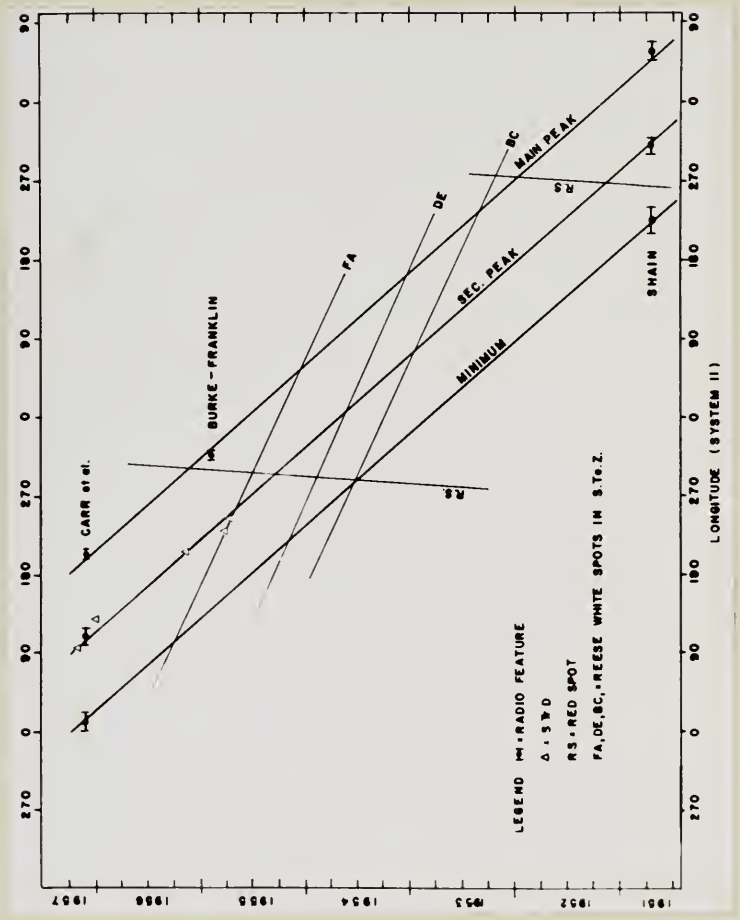

Fig. 31.—Long-term drift lines for radio and visual features of Jupiter.

data from this observatory are plotted, the straight line connecting the two points is parallel to the main peak line. The same is true of the line representing the principal minimum. These three parallel lines pass through the seven points within the error limits given in Table 2. Although the observations of Burke and Franklin plotted in Figure 2 cover a period of only 47 days, a drift in this data is also readily apparent. The slope of the drift is in the same direction and of the same approximate magnitude as that of the radio drift lines in Figure 31. This is further evidence that the latter have been drawn correctly.

The fact that the three features of the histograms which can be compared seem to exhibit linear and parallel drifts over a period of 5½ years is particularly noteworthy. It suggests that the centers of activity on Jupiter are rotating with a constant period slightly less than the period of System II, and that the centers are fixed with respect to each other. If such is actually the case, the only reasonable explanation is that the radio centers are related to the solid surface of Jupiter. The observed rotational period would then be that of the planet itself, rather than of some feature drifting in the atmosphere. (Since the solid surface is perpetually obscured by clouds, it has of course not been possible to determine the rotational period of the surface by optical means.)

The rotational period corresponding to the rate of drift, with respect to System II, of the radio drift lines in Figure 31 is easily calculated. Each of the radio features drifts backward relative to

System II longitude at the rate of 0.28845°/day, as determined from the slope of the lines. This corresponds to a rotational period for the radio centers which is 11.8 seconds shorter than that of System II. The System II period is $9^{h}\ 55^{m}\ 40^{s}.6$, so that the radio rotation period must be $9^{h}\ 55^{m}\ 28^{s}.8$. An error of 10° in locating the center of a peak (or a minimum) in the histograms will result in an error in the radio rotational period of only about 0.2 second.

If, as appears likely, the radio rotational period corresponds to that of the surface of Jupiter, it would not be inappropriate to define a new longitude system based on this rotational period and designated "System III". Accordingly, the new system is defined as follows:

a) System III coincided with System II at 0^{h} UT on January 1, 1957.

b) The rotational period for System III longitude is $9^{h}\ 55^{m}\ 28^{s}.8$ (present best value).

The System III longitude of the central meridian of Jupiter can be found for 0^{h} UT on any date by means of the formula

$$\lambda_{III} = \lambda_{II} + 0.28845\ D, \qquad (41)$$

where λ_{III} = System III longitude;

λ_{II} = System II longitude, as found from tables in reference (32);

D = Number of days having elapsed since 0^{h} UT on January 1, 1957.

The quantity D can most easily be found from the formula

$$D = J-2435839.5, \qquad (42)$$

where J is the Julian Day Number at 0^h UT on the date in question, as found in reference (32).

The System III longitude having been found for 0^h UT on Julian Day J, it can be found for any other time on that date from the formula

$$\Delta\lambda_{III} = 36.27\ H + 0.605\ M, \qquad (43)$$

where $\Delta\lambda_{III}$ is the increase in System III longitude since 0^h UT, and H and M are the elapsed hours and minutes since 0^h UT.

The data from this observatory were replotted in the form of a histogram of occurrence probability as a function of the System III longitude of the central meridian, as shown in Figure 32. As before, black areas represent deflections over 0.5 inch, cross-hatched areas represent deflections between 0.2 and 0.5 inch, and white areas represent deflections less than 0.2 inch. The use of System III rather than System II resulted in a slight but definite sharpening of the peaks. Histograms of the Shain data and of the Burke and Franklin data were also plotted as a function of System III longitude, and are shown in Figure 33. Here again, there was a slight improvement in the definition of the peaks when System III was used instead of System II. The three sets of data (Figures 32 and 33) show an unmistakable correspondence when plotted as a function of System III longitude, which they did not possess when plotted in System II longitudes.

There have been various attempts to identify the radio centers on Jupiter with the few persistent optical features. Figure 31 shows the approximate drift with respect to System II of the average centers

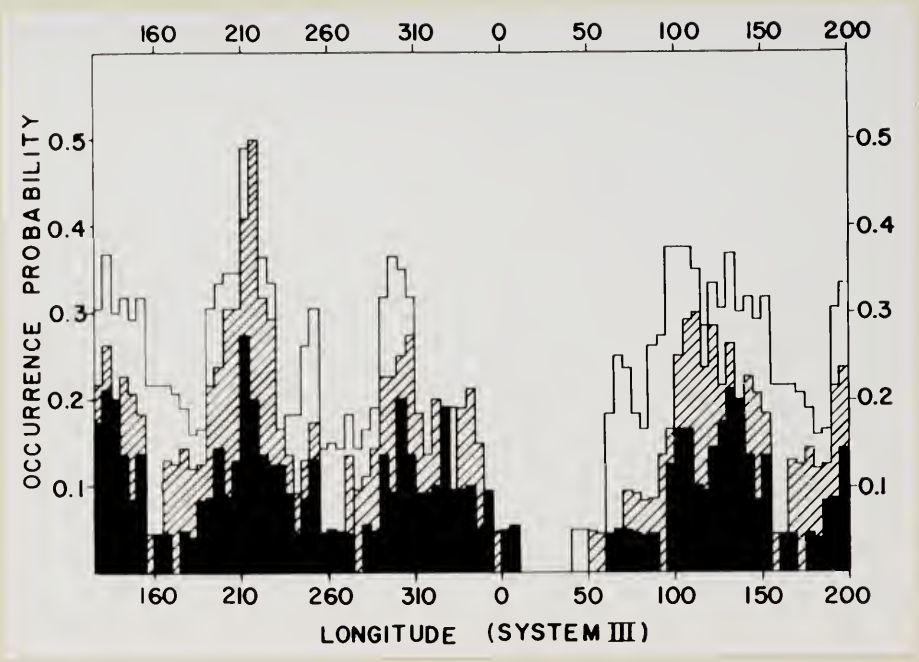

Fig. 32.—System III histogram of observations of Jupiter made between December 31, 1956 and March 6, 1957.

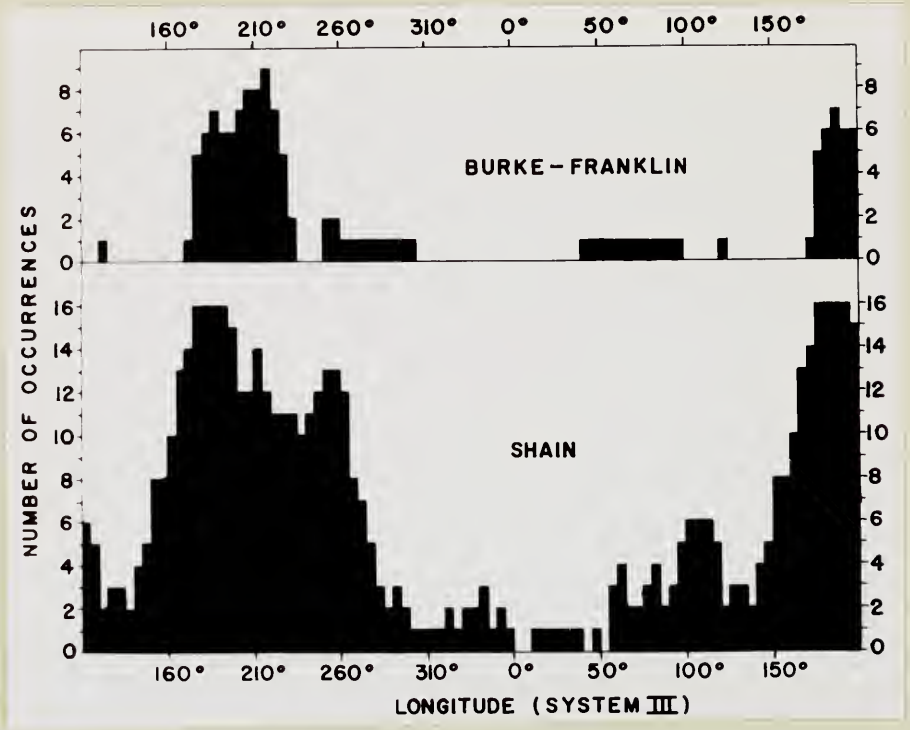

Fig. 33.—Histogram of the observations of Shain and of Burke and Franklin plotted in System III longitudes.

of those optical features which have been followed during recent years. The Red Spot actually drifts in the opposite direction from that of the radio centers. The fact that the Red Spot was similar in longitude to the main radio center in 1955, when the measurements of Burke and Franklin were made, appears to have been a coincidence. The white spots in the South Temperate Zone which have been followed since 1940 by Reese (33, 34, 35, 36, 37) also show a drift which is incompatible with the assumption that they are associated with the radio sources. However, the South Tropical Disturbance, which reappeared in 1955 after being lost since 1940, seems to be maintaining approximately the same longitude as the secondary radio peak. Five positions of the South Tropical Disturbance reported by Reese (37) and Peek (38) are shown as triangular points on Figure 31, all being close to the secondary peak drift line. Whether or not this proximity is a coincidence must be established by continued comparison of optical and radio observations.

The Jovian Ionosphere

It is almost certain that Jupiter is surrounded by some medium which makes possible resolution of the peaks of radio noise activity, as was originally pointed out by Shain (5). If there were no such medium, then a point radio source would be observable for about 180° of rotation of the planet, and a distributed source would be observable over a greater angle. The peaks in Figures 32 and 33, on the other hand, are much narrower than 180°. That this restriction is caused by an ionosphere seems plausible, resolution of the peaks being brought

about by the fact that radiation incident on the ionosphere from below at an angle greater than the critical angle cannot escape.

Qualitatively, a comparison of the width of the main peak of the data of Figure 32 with that of Shain in Figure 33 supports the argument for an ionosphere. The two sets of data were taken at virtually the same frequency, but at times of greatly different sunspot activity. The narrower peak in Figure 32 is consistent with the greater sunspot activity prevailing in 1957. However, the peak width in the data of Burke and Franklin does not seem to be consistent with the above argument, since it is too narrow for the higher frequency used and the relatively low sunspot activity existing at the time of measurement. This discrepancy can be illustrated numerically by comparing the critical frequencies calculated from the three sets of data. The critical frequency can be defined as the lowest frequency capable of penetration at normal incidence. For the ionosphere of Jupiter, let

θ_c = the critical angle (with respect to the normal) at frequency f;

f_o = the critical frequency.

Approximating the curved ionospheric boundary by a plane and applying Snell's Law, we have

$$f_o = f \cos \theta_c . \qquad (44)$$

If it is assumed that the principal radio noise source on Jupiter is near the equator, then the angular width near the base of the main peak in Figures 32 and 33 should be roughly equal to $2\theta_c$,

Substituting the value of θ_c so determined into Eq. (44), one thus obtains the approximate value of f_o. The calculated values of f_o are tabulated with corresponding 12-month running average sunspot numbers in Table 3. If the radio source was actually a considerable distance north or south of the equator, then the true critical frequencies must all have been smaller than indicated in Table 3.

TABLE 3

COMPARISON OF RADIO PEAK WIDTHS WITH SUNSPOT NUMBERS

Observer	f Mc/s	$2\theta_c$	f_o Mc/s	Sunspot Number
Shain	18.3	125°	8.5	62
Burke and Franklin	22.2	55°	19.7	78
Carr, Smith, Pepple, and Barrow	18.0	40°	16.9	172

In Table 3, the calculated value of the critical frequency is higher for a sunspot number of 78 than for 172, which is contrary to what one would expect. Additional measurements will be necessary before this seeming contradiction can be resolved.

Jupiter receives from the sun less than 4 percent of the ultraviolet flux that falls on the earth. Nevertheless, the indications are that the critical frequencies for the two planets are comparable. If this is so, conditions in the outer atmosphere of Jupiter must be such that a much lower intensity of ultraviolet radiation can maintain a given ion density.

The 8-Day Cycle

A strong tendency was noted for Jupiter disturbances to occur in cycles of four successive nights of activity followed by four nights of silence. An arbitrary measure of nightly activity, based upon both the maximum burst amplitude and the duration of the active period, was established, and is shown as a function of the date in Figure 34. The existence of a periodicity cannot be denied. The average period of the 9 cycles observed is 8.0 days.

It was at first believed that the phenomenon is a stroboscopic effect resulting from a fixed relationship between the rotation of the earth and that of Jupiter. However, it was found impossible to account for the 8-day period on this basis.

A detailed investigation further showed that a given cycle of Figure 34 may be due to radiation from any one, any two, or all three of the sources in Figure 32, which are of course widely spaced around the planet. This strongly suggests that all of the sources radiate together or are silent together. A study has been made of possible correlations with sunspot number, with geomagnetic indices, and with the transparency of the terrestrial ionosphere as indicated by the recorded galactic noise levels and limiting station frequencies. All of the results were negative.

It will be noted from Figure 34 that there is also a suggestion of a 32-day cycle, with maxima occurring around January 16 and February 17. Observations were continued for about a month after March 8, but very little Jupiter radiation was recorded during this period. Since

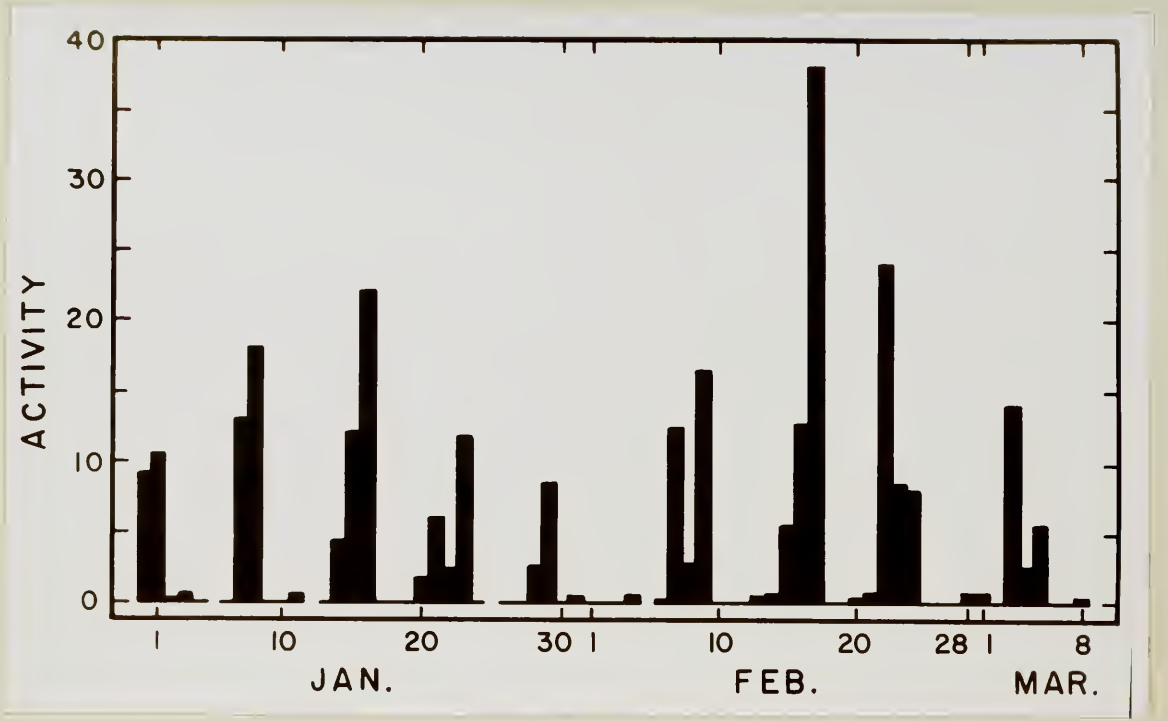

Fig. 34.—Jupiter activity (in arbitrary units) plotted as a function of date, showing 8-day cyclic behavior.

there was apparently no corresponding increase in the opacity of the terrestrial ionosphere, it must be concluded that for some reason Jupiter had lapsed into a state of relative inactivity.

A possible explanation of these phenomena is that they result from variations in the transparancy of the ionosphere of Jupiter. If the ionospheric cut-off frequency happened to remain for a time near the observing frequency (18 Mc/s), then it is conceivable that a relatively slight external influence could cause the ionosphere to become either transparent or opaque. The 7.15-day orbital period of Jupiter's largest satellite, J III, suggests that the tidal effect of this satellite upon the Jovian ionosphere might account for the observed 8-day periodicity. Although the theoretical tide-raising force of J III is less than that of the inner moons, it is possible that some atmospheric resonance might enhance its effect, as in the case of solar tides in certain regions of the Pacific Ocean.

The marked reduction in noise activity after March 6, 1957 could be due to the reduction of the cut-off frequency well below 18 Mc/s with the general increase in sunspot activity. If this explanation is correct, then the cut-off frequency would not be expected to rise again to 18 Mc/s until some time after the maximum of the 11-year sunspot cycle had passed. The present sunspot cycle is expected to pass its maximum sometime in late 1958 (personal communication from Dr. Seth B. Nicholson of Mt. Wilson Observatory). It is therefore unlikely that Jupiter will resume its original activity at 18 Mc/s during the second apparition, if the above theory is correct.

Radiation Intensity Distribution

Conditions for the reception of radio noise from Jupiter on 18 Mc/s were favorable on 62 of the observing nights between December 31, 1956 and March 6, 1957, for a total time of 115 hours. The average favorable reception period was thus 1.9 hours per night. Although the observer was on duty for an average of almost 3 hours per night, about one-third of the time was wasted because of excessive interference.

By using the noise diode calibrator and applying Eqs. (11a) and (18), it was possible to estimate the power flux per unit bandwidth for the radiation received from Jupiter. Values occured as follows:

a) On 42 percent of the nights the flux exceeded 3 pfu, which corresponded on the average to 0.5 inch deflection. (We have invented the "pfu", or planetary flux unit, for the sake of brevity; 1 pfu = 10^{-21} watts $m^{-2}(c/s)^{-1}$.)

b) On 11 percent of the nights the flux exceeded 50 pfu, which corresponded on the average to full scale deflection.

The above figures are based on plane polarized radiation. If it is assumed that the polarization is circular, as seems from later polarimeter measurements to be more nearly correct, the above flux values must be doubled.

Waveform Studies

The sound of a burst of Jupiter noise is a rising and falling hiss, the build-up of a typical burst lasting a second or so, and the decay a like period. However, when the noise is recorded with a quick-response pen recorder, as in Figure 28b, a certain amount of fine

structure becomes apparent. Individual rather sharp pulses may be present, superimposed upon erratically varying slower components. In some cases there are intermittent, widely-spaced single pulses, and in others complex overlapping bursts of dozens of pulses. The single pulses seem to vary in length from less than 0.1 to 1 second, while sustained bursts lasting 10 or 15 seconds are not uncommon.

The tendency of pulses to occur in pairs or triplets, first reported by Kraus (9), is apparent in Figure 28b. This phenomenon can be detected best when the pulses are rather sporadic, since the confusion of pulses in a major burst tends to obscure it. As an example of the occurrence of pulses in pairs, in a 17-minute period of activity on January 23, 1957, 22 out of a total of 45 pulses occurred in pairs, with spacings ranging from 0.7 second to 1.0 second. In another case, a 22-minute record made on February 19, 1957, 28 out of a total of 49 pulses occurred in pairs, with spacings from 0.15 to 0.30 second. Triplets of pulses occur less frequently than pairs. The amplitudes of the pulses in the doublets or triplets are usually similar, the weaker preceding the stronger as often as the converse. Thus the pulse multiplicity does not seem to be due to echoes, for in such a case succeeding pulses would always grow weaker. It is possible that the multiplicity is due to some sort or relaxation oscillation of the source (whatever the source may be), as in the case of multiple lightning strokes.

CHAPTER VII

JUPITER DURING THE SECOND APPARITION

Flux Intensity Distributions

Of the radio observations of Jupiter made simultaneously at 18 Mc/s and 22.2 Mc/s between December 19, 1957 and March 31, 1958, conditions were considered favorable on 73 nights, for a total time of 216 hours. The average favorable reception period was thus about 2.95 hours/night. Observations were also made on 27.6 Mc/s during a considerable part of the season, but due to excessive man-made interference from local sources at this frequency, the results were considered a good deal less reliable than those on the lower frequencies.

On 18 Mc/s Jupiter noise deflections greater than 0.5 inch occurred on 34 percent of the nights (25 nights), and full scale deflections occurred on 3 percent of the nights (2 nights). The data reduction necessary to express these results in terms of absolute power flux has not yet been completed; however, flux values accurate to within a factor or two can be obtained by assuming that the average deflection sensitivity was the same during this period as it was during the first apparition. It will be assumed that a deflection of 0.5 inch corresponded to 3 pfu, and full scale to 50 pfu. It can further be assumed that the probability of occurrence of a given flux is proportional to the time of observation. The 18 Mc/s data from

the second apparition can thus be adjusted for comparison with that from the first apparition by multiplying occurrence percentages of the former by 1.9/2.95, the ratio of the mean watch durations for the two seasons. The distribution of flux values for 18 Mc/s Jupiter data obtained during the second apparition, adjusted for equivalent 1.9-hour watches, is as follows:

a) On 22 percent of the nights the flux would have exceeded 3 pfu.

b) On 2 percent of the nights the flux would have exceeded 50 pfu.

It is seen that flux values exceeding 3 pfu were just ½ as probable during the second apparition as during the first, and those exceeding 50 pfu were only 1/5 as probable. The sunspot number on the median date during the first apparition observations was 172; that for the second apparition must have been about 200 (since these sunspot numbers are 12-month running average values, accurate values are not available until at least 6 months after the date of interest). If the increasing sunspot activity was actually the cause of the decrease in Jupiter noise activity, then the latter must be very responsive to slight changes in the former. It is entirely possible, however, that observed variations in Jupiter noise activity are due, at least in part, to other factors than sunspot activity.

On 22.2 Mc/s, Jupiter noise deflections greater than 0.5 inch occurred on 26 percent of the nights (19 nights), and no deflections reached full scale. There were occasions when activity occurred on both 22.2 Mc/s and 18 Mc/s at about the same times, and other occasions

when only one of the frequencies was active. Activity occurred on 18 Mc/s alone on 12 nights, on 22.2 Mc/s alone on 10 nights, and on both frequencies at more or less the same times on 16 nights. With one notable exception to be discussed later, the individual bursts on the two frequencies were never correlated, even when the general periods of activity coincided.

From the above observations, and the fact that very little Jupiter activity was observed on 27.6 Mc/s, the following deductions can be made:

a) The average spectrum of Jupiter noise increases in intensity with a decrease in frequency from 27.6 Mc/s to 18 Mc/s. The activity on 22.2 Mc/s is perhaps $\frac{1}{2}$ or 2/3 that on 18 Mc/s.

b) The spectrum of an individual burst of Jupiter noise is concentrated in a band less than 4 Mc/s wide. On the other hand, it has been observed many times by varying the receiver tuning while a burst is in progress that the single-burst spectrum is at least 0.5 Mc/s wide. Therefore it is estimated that the frequency bandwidth of a single burst is about 2 Mc/s between half voltage points, on the average.

Correlation with System III Longitude

In order to test the earlier conclusion that the Jupiter noise source concentrations remain fixed with respect to the newly defined System III longitude coordinates, a histogram was plotted showing the number of noise occurrences during the second apparition as a function of System III longitude (see Figure 35). This is a preliminary presentation of the data, subject to a certain amount of revision. The histogram includes occurrences on both 18 Mc/s and 22.2 Mc/s, although

whenever both frequencies were active it was counted as a single occurrence. Figure 35 should be compared with Figures 32 and 33. It is seen that the main peak has maintained its identity and approximate position, occurring in Figure 35 at about 230° as compared with about 215° in Figure 32. Peaks in the vicinity of 315° and 130° have also persisted. However, a new peak has appeared at about 75°. It may be significant that this new peak is made up mostly of relatively small deflections.

Although the number of occurrences of Jupiter radiation during the second apparition was rather small for statistical accuracy, it can be said that this most recent evidence substantiates the earlier conclusion that the noise sources are fixed relative to the System III coordinates.

Polarimeter Measurements

A typical polarimeter record of a Jupiter burst on 22.2 Mc/s is shown in Figure 36. Polarimeter records of the radiation from Jupiter were obtained on 7 nights, and 5 of these have been analyzed in detail. On 6 of the 7 records, every burst exhibited right-handed elliptical or circular polarization. On the one exceptional record the polarization was left-handed; this and other unusual characteristics indicated that the activity in this particular case was certainly not typical Jupiter noise. The polarimeter measurements are summarized in Table 4.

In Table 4, the first three columns after the date are the numbers of left-handed polarized, plane polarized, and right-handed

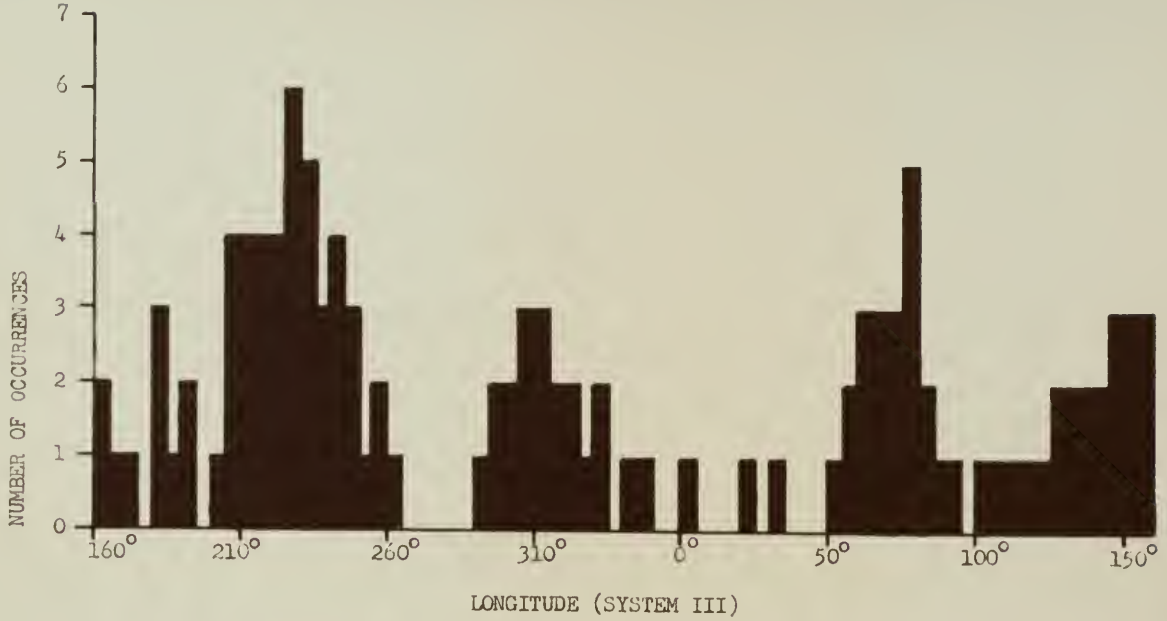

Fig. 35.—System III histogram of observations of Jupiter radiation on 18 and 22.2 Mc/s between December 19, 1957 and March 31, 1958.

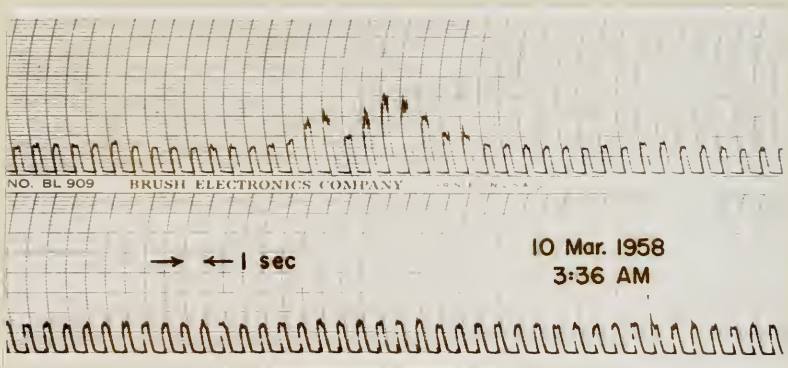

Fig. 36.--Polarimeter record of a Jupiter burst on 22.2 Mc/s. The upper trace was produced by pen 1; the lower by pen 2. The record indicates that the polarization of the received radiation was right-handed circular.

polarized bursts, respectively, on each record. R is the mean axial ratio of the polarization ellipse, σ the standard deviation of R, and φ the approximate angle of Jupiter east or west of the antenna axis at the time of the measurements (the antenna was directed approximately toward 0° declination and 0° hour angle).

TABLE 4

POLARIMETER DATA

Date (1958)	No. LH	No. PP	No. RH	R	σ	φ
Feb. 24	0	0	14	-0.58j	0.06	5° E
Mar. 6	0	0	4	-0.91j	0.15	14° W
Mar. 8	5[a]	0	0	+0.20j	0.02	11° E
Mar. 10	0	0	6	-0.25j	0.17	2° E
Mar. 18	0	0	6	-0.44j	0.09	22° E

[a] Measurements in this case were made at five points on the single abnormally long burst.

All of the typical Jupiter polarimeter bursts were of about 1 to 4 seconds duration, exhibited right-handed elliptical or circular polarization, and were not simultaneously accompanied by a burst on 18 Mc/s or 27.6 Mc/s. On the other hand, the activity on March 8 consisted of a single slowly undulating burst of about 120 seconds duration, which exhibited left-handed elliptical polarization and

appeared simultaneously on all three frequencies. This was obviously not a typical Jupiter burst, but sounded in the loudspeaker just like a solar burst. However, the sun was about $3\frac{1}{2}$ hours below the eastern horizon (the time was 0236 EST). It is perhaps conceivable that the disturbance was a solar burst reflected off of the moon, which was in the beam at the time, one of the lunar craters possibly being so situated that it concentrated the radiation in the direction of the earth. In any event, it is believed that the disturbance was of extraterrestrial origin. Whether it originated on Jupiter or the sun, its occurrence was most unusual and is of great interest.

Evidence must now be presented that the consistently right-handed sense of polarization of typical Jupiter bursts is a real Jovian effect and is not due to the action of the terrestrial magnetic field. Three arguments that the effect is not of terrestrial origin are as follows:

a) There does not seem to be any dependence of R upon φ in Table 4, which would be expected if the polarization is caused by the terrestrial magnetic field.

b) The occurrence of left-handed polarization in the disturbance of March 6 indicates that the terrestrial magnetic field is not polarizing all radiation of extraterrestrial origin in the right-handed sense.

c) Calculations indicate that the change in R produced by the terrestrial ionosphere is small.

For the calculation of the effect of the terrestrial magnetic field upon the polarization of a signal of extraterrestrial origin, Eq. (2) is used. The average critical frequency during Jupiter watches was about 6 Mc/s, as determined from the ionospheric data bulletins

issued monthly by the National Bureau of Standards. The gyrofrequency of the electron in the ionosphere above Gainesville is 1.3 Mc/s, corresponding to a magnetic field strength of 0.51 gauss. Since the magnetic dip is 58° and the declination of Jupiter is -11°, θ is 9° at the transit of Jupiter. The values of R calculated from these data are -1.001j (right-handed) for the extraordinary mode, and +0.999j (left-handed) for the ordinary. If θ is assumed to be 30° (i.e., when Jupiter is about 2 hours from transit), the values of R for the extraordinary and ordinary modes are -1.01j and +0.99j, respectively. It is thus seen that the effect of the terrestrial field is to split a plane polarized wave into two components which are very nearly circularly polarized, but in opposite senses. If neither of these components is reflected or appreciably absorbed in the ionosphere, their combined effect at the antenna will be the same as that of a plane polarized wave. However, the plane of polarization will in general have become rotated from its original orientation due to slight differences in phase velocity and path of the two components. It is now necessary to show that there was no reflection or appreciable absorption of either of the components.

The refractive index for the ordinary ray, being independent of the magnetic field, is given by Eq. (4) (neglecting collisions). Its value is 0.962. The critical angle for a ray with this refractive index is found from Eq. (2) to be 74°. Reflection of the ordinary ray was therefore impossible for rays from the direction of Jupiter.

The condition for reflection of a normally incident extraordinary

ray is $f_o^2/f^2 = 1 \pm (f_H/f)$, instead of $f_o^2/f^2 = 1$, as in the case of the ordinary ray. For the purpose of the present argument, an equivalent extraordinary ray refractive index, n', can be defined by analogy with Eq. (4) as

$$n'^2 = 1 - f_o^2/f'^2,$$

where

$$f'^2 = \left[1 \pm (f_H/f)\right] f^2.$$

This is a double-valued function. For the Jupiter observations the two values of n' were 0.965 and 0.960, neither of which is significantly different from the value for the ordinary ray. Since the ordinary ray is far from the condition for reflection, it follows that the extraordinary ray must also be unreflected.

The possibility of the observed right-handed sense of the Jupiter radiation being due to selective absorption of the left-handed (ordinary) component can quickly be disposed of. It is apparent from graphs presented in reference (19) that for the present case, in which the wave frequency is well above both the critical frequency and the gyrofrequency and the collision frequency is well below the critical collision frequency, absorption is greater for the extraordinary ray than for the ordinary ray. Therefore, selective absorption could not account for the observed right-handed polarization sense.

From the various arguments which have been given, it seems relatively certain that the observed polarization effects were not of terrestrial origin.

Finally, it will be shown how a value of the Jovian magnetic

field intensity can be calculated from the polarimeter measurements and Eqs. (5) and (33), if the latitude of the noise sources and the orinentation of the magnetic axis are assumed. The assumptions are made that the magnetic and rotational axes of Jupiter coincide; that the north magnetic pole coincides with the north geographic pole; that the noise sources are at latitude 20° S[1]; and that the magnetic vector at this latitude is inclined 25° above the horizontal. Thus θ in Eq. (5) is 45°. It is also assumed that f_o is 17 Mc/s, which is more or less consistent with Table 3. The average value of R (excluding the March 8 data) is about -0.5j. It should be noted at this point that the absolute value of R as determined from polarimeter measurements and Eq. (33) represents the minor to major axis ratio, while Eq. (5) can yield either this or its reciprocal. Thus, in the present case, it must be assumed that R can be either -0.5j or -2.0j, but only the latter value gives a solution to Eq. (5). The resulting value of H turns out to be 7 gauss. If the foregoing analysis is correct, the magnetic field intensity at the surface of Jupiter is an order of magnitude higher than it is for the earth.

The Sunrise Effect

It is believed that an interesting new ionospheric effect has been discovered from the observations made during the second apparition. It was noticed on many occasions that at about the time of sunrise, Jupiter noise would be distinctly heard for just a minute or so,

---

[1] A partial justification of this assumption lies in the fact that optical observations show this zone to be the most active region of the planet.

sometimes at relatively high intensity. This phenomenon often occurred at the end of an otherwise unproductive watch. It occurred entirely too often to be due to chance. The phenomenon is believed to have resulted from a transitory focussing effect upon rays from Jupiter by the terrestrial ionosphere, which is always unstable at sunrise, permitting the detection of Jupiter flux intensities so low as to be ordinarily inaudible. The times at which the sunrise effect was observed are listed in Table 5, along with the reception frequency, the mean System III longitude (λ_{III}) of Jupiter, and the mean altitude of the sun (α) for each occurrence.

TABLE 5

OCCURRENCES OF THE SUNRISE EFFECT

Date (1958)	Time (EST)	Freq. Mc/s	λ_{III} Deg.	α Deg.
Jan. 4	0613	18, 22.2	91	-15
Jan. 5	0613, 0622-0628	18	248	-13
Jan. 11	0633, 0643	18	80	-10
Jan. 25	0628-0630	18	22	-12
Jan. 26	0647-0650	22.2	183	- 9
Jan. 31	0645-0648	18	215	- 8
Feb. 10	0610	18, 22.2	260	-14
Feb. 16	0623-0628	18	343	-11
Feb. 26	0620	22.2	73	-10

The ionospheric electron density slowly decreases throughout the night, falling to its diurnal minimum just before sunrise. However, as soon as the rays from the rising sun strike the atmosphere at ionospheric altitudes, the electron density begins increasing rapidly. Thus at sunrise there is a strong horizontal positive gradient of ionospheric electron density overhead from west to east. Since the phase velocity of radio wave propagation increases with an increase in electron density (so long as the frequency is below the critical frequency), the horizontal gradient will refract the rays from Jupiter toward the west. If the velocity gradient is constant, the refraction will merely cause a change in direction of all the rays by a fixed amount, as in the case of a prism (neglecting the curvature of the ionosphere). However, if the velocity gradient increases from west to east, which is actually the case for a short time after sunrise, there will be a focussing effect upon the rays. Although the rays are probably not focussed to a point, there is at least a good probability that they will be concentrated at the receiving antenna briefly. It is believed that this concentration permitted the observation of extremely low Jupiter flux intensities on the occasions listed in Table 5.

The average value of α for the 9 occurrences listed in Table 5 is -11°, the negative sign indicating that the sun was below the horizon for an observer at sea-level. However, from heights greater than about 70 miles the sun would be visible. Since most of the ionosphere lies above 70 miles, the indicated values of α are not

inconsistent with the theory.

If the sunrise effect is indeed due to focussing by a great ionospheric lens (a cylindrical lens), and if it is assumed that the lens is rotating with the earth, the order of magnitude of its effective beamwidth can be estimated (considering it to be an antenna). A common duration of the Jupiter noise during occurrences of the sunrise effect was about two minutes, corresponding to about 0.4° of rotation of the earth. It seems reasonable to assume that the lens beamwidth is equal to this. The 18 Mc/s broadside array would have to be increased in its east-west dimension to two miles or so in order to have such a beamwidth.

CHAPTER VIII

SATURN, URANUS, AND VENUS

Saturn During the First Apparition

Of the radio observations of Saturn made at 18 Mc/s between April 7, 1957 and May 8, 1958, conditions were considered favorable on 21 nights, for a total time of 41 hours. The average favorable reception period was thus about 1.95 hours per night. Disturbances of possible Saturnian origin were actually observed on three nights, i.e., on about 14 percent of the nights. Although these disturbances were very weak and were of short duration, it was determined that they were not due to any of the usual forms of interference. Since Saturn was the only object recognized as a possible emitter of sporadic radiation which was within the main lobe of the antenna beam at the time, there seems to be a fair degree of probability that the disturbances were from Saturn. However, the possibility has not been entirely ruled out that they resulted from the reception of powerful Jupiter bursts by minor side lobes of the antenna. Therefore, the possible presence of radiation from Saturn on 14 percent of the nights should be considered as an upper limit for Saturn activity rather than conclusive proof of its existence.

The average minimum detectable power flux for the 21 nights of Saturn observation during the first apparition was 4.2 pfu (where, as

before, 1 pfu = 10^{-21} watts m^{-2} $(c/s)^{-1}$). The dates and maximum flux values for the three nights of possible Saturn activity were as follows:

2.7 pfu on April 16 (0315 to 0330 EST).

4.6 pfu on April 18 (0330 to 0420 EST).

5.6 pfu on April 26 (0406 to 0408 EST).

It is of interest to compare the observations of Saturn with those of Jupiter, after taking into account the greater distance of Saturn from the earth. It is first necessary to calculate the received flux which would be expected if Jupiter had been at the same distance from the earth as was Saturn. On the median dates of the respective observation periods Jupiter was 4.7 AU (astronomical units) from the earth, and Saturn was at a distance of 9.3 AU. To correct for the difference in inverse square attenuation in the two cases, it is necessary to multiply the Jupiter flux intensities by the factor $(4.7/9.3)^2$, or 0.256. Thus, if Jupiter had been at the same distance as Saturn, the following flux values would have been expected from Jupiter:

a) On 42 percent of the nights the flux would have exceeded 0.8 pfu.

b) On 11 percent of the nights the flux would have exceeded 13 pfu.

Actually, in the case of Saturn, the flux exceeded 2.6 pfu on 14 percent of the nights (if it is conceded that the three disturbances were really from Saturn). Although this is a somewhat lower level of activity than the equivalent Jupiter case in (b) above, it is at least of the same order of magnitude. Thus the conclusion is that if the

three Saturn disturbances were valid, Saturn activity was somewhat less, but probably not a great deal less, than that of Jupiter. On the other hand, if the validity of none of the three disturbances is admitted, then Saturn must have been much less active than was Jupiter.

Uranus During the Second Apparition

Of the radio observations of Uranus made at 18 Mc/s and at 22.2 Mc/s between January 17, 1958 and March 4, 1958, conditions were considered favorable on 35 nights, for a total time of about 65 hours. The average favorable reception period was thus about 1.85 hours per night. No trace of any possible disturbance from Uranus was ever received during this period.

The average minimum detectable flux for the 35 nights was 0.35 pfu at 18 Mc/s and 0.45 pfu at 22.2 Mc/s.

It is now necessary to calculate the received flux which would have been expected from Jupiter during the first apparition of Jupiter had been the same distance from the earth as was Uranus during the second apparition. The distances of Jupiter and Uranus were 4.7 AU and 17.5 AU, respectively, and the factor by which to multiply the Jupiter flux to equalize the inverse square attenuations is $(4.7/17.5)^2$, or 0.072. Thus, if Jupiter had been at the same distance as Uranus, one would have expected the following flux values at 18 Mc/s from Jupiter during the first apparition:

a) On 42 percent of the nights (i.e., on 15 nights) the flux would have exceeded 0.22 pfu.

b) On 11 percent of the nights (i.e., on 4 nights) the flux would have exceeded 3.6 pfu.

Since actually no radiation was detected from Uranus, even though the minimum detectable level was an order of magnitude lower than the 3.6 pfu in (b) above, it must be concluded that if Uranus is a radio emitter at all, it is very much less active than Jupiter.

Saturn During the Second Apparition

Observations of Saturn on 18 and 22.2 Mc/s during the second apparition were begun on February 10, 1958, and are still in progress at the time of writing. Occasions upon which disturbances from Saturn are believed to have occurred thus far are listed in Table 6. Corresponding maximum flux values have not yet been calculated.

TABLE 6

OCCURRENCES OF SATURN NOISE (SECOND APPARITION)

Date (1958)	Time (EST)	Freq. Mc/s
Mar. 17	0237-0245	18
Apr. 9	0508-0509	22.2
Apr. 12	0515-0516	22.2
Apr. 25	0504-0507	18
May 7	0443-0444	22.2

Venus During the Second Apparition

Observations of Venus on 27.6 Mc/s during the second apparition were begun on February 9, 1958, and are still in progress at the time

of writing. None of the data have yet been reduced. Since even under the best observing conditions Venus rises only two or three hours before the sun, observing periods are limited to an hour or two before sunrise. A great deal of difficulty has been experienced with interference from automobile traffic during this period. Nevertheless, an appreciable amount of relatively interference-free Venus observing time has been logged. There has yet been no instance of noise which could reasonably be attributed to Venus. The equipment sensitivity is believed to be adequate for detecting a flux intensity of the order of magnitude of that which Kraus (11, 12, 13) claimed to have received from Venus.

CHAPTER IX

SUMMARY

Sporadic radio noise from the planets has been studied during the winter and spring of 1956-1957 and of 1957-1958. The primary objectives of the study were: (a) to learn from measurements of the radio radiation from Jupiter as much as possible about the characteristics and origin of the radiation, and about the rotation, the atmosphere, and the magnetic field of the planet; and (b) to ascertain whether or not Saturn, Uranus, and Venus are also variable radio emitters. In order to make possible the achieving of these objectives, an antenna development and construction program of considerable magnitude was carried out. A secondary objective was to acquire experience with several types of antenna arrays and to determine which are the most suitable for future studies of planetary radiation.

Gratifying results were obtained, and great progress was made toward the achievement of the stated objectives.

The concentration of the noise sources on Jupiter within certain zones of longitude was verified. It was shown that the noise centers remain fixed relative to each other, and that they rotate with a fixed period which is different from the recognized periods of the visible clouds on Jupiter. The evidence is strong that this period, which was determined to an accuracy of a few tenths of a second, is the period of rotation of the unseen solid surface of Jupiter.

Additional proof for the existence of a Jovian ionosphere was obtained. It was found the electron density of this ionosphere is of the same order of magnitude as that of the earth. The ionization seems to vary with sunspot activity, as does that of the terrestrial ionosphere.

The occurrence of pairs and larger groups of correlated pulses in the radiation from Jupiter was verified. Data were also obtained regarding both the average spectrum of the Jupiter noise and the spectrum of the individual bursts. This information will be of value in future studies of the origin of the radiation.

It was ascertained that the radiation from Jupiter is elliptically polarized in the right-handed sense. This is believed to be conclusive proof of the existence of a magnetic field on Jupiter. After making some seemingly reasonable assumptions about the location of the magnetic poles relative to the noise source locations, it was possible to calculate the Jovian magnetic field intensity from the polarization measurements. The calculated value for Jupiter is about ten times greater than the terrestrial magnetic field intensity.

A well-defined periodicity of eight days was observed in the noise from Jupiter, which is assumed to be due to a tidal effect in its ionosphere, excited by one of its satellites which has approximately the same period. This effect can apparently be observed only on relatively infrequent occasions when the transmission characteristics of the Jovian ionosphere at the radio frequency employed are abnormally sensitive to external influences.

Observations of Saturn indicated that this planet probably emits radio noise also, but less frequently than does Jupiter. However, additional observations with improved equipment (or from a location in the southern hemisphere) will be necessary to establish this fact conclusively.

No radiation was received from Uranus during a long series of observations of this planet. The data indicate that if Uranus emits at all, it cannot be more than 1/10 as active as was Jupiter during the first months of 1957.

No radiation has been received from Venus, although the observations have not yet been terminated. Previous reports by Kraus of variable radiation from Venus are not substantiated by observations made to date.

An interesting effect in the terrestrial ionosphere is believed to have been discovered. It was found that a horizontal ionization gradient existing at sunrise can occasionally cause for a short time a focussing of radiation from Jupiter at the receiving apparatus. Upon such occasions the effective detection sensitivity is increased by a factor of perhaps 100 or more, briefly permitting the observation of much lower Jupiter noise levels than usually is possible.

The future extension of the investigation of planetary radio noise offers great promise. By means of continued research over a period of years with present types of equipment the effects already discovered can be verified and studied in more detail. However, by using improved equipment, or by making observations from a more

advantageous geographic location (preferably both), important new discoveries can undoubtedly be made.

Recommended directions for future research are as follows:

a) Continued monitoring of planetary noise on several fixed frequencies to obtain further information on rotational and other periodicities, planetary ionospheric effects, average noise spectrum, and other phenomena.

b) Development and operation of a swept-frequency system for the determination of the spectrum of the individual noise bursts.

c) Development and operation of a phase switching or swept-lobe interferometer which will permit the observation of lower planetary noise intensities.

d) Continued development and operation of the polarimeter as a device for the detection of very low planetary noise levels as well as for the determination of wave polarization.

e) Development of a receiving and telemetering system for use in artificial earth satellites for the study of planetary noise at frequencies below the cut-off frequency of the terrestrial ionosphere.

f) Establishment of a field station of the University of Florida Radio Observatory in the southern hemisphere (perhaps near Santiago, Chile). Since Jupiter and Saturn will remain near the southern extreme of declination for a number of years, such a field station would permit the study of these planets with high-angle antenna beams capable of rejecting atmospheric noise and other serious forms of interference, all of which arrive at low angles. It would then be possible to detect much lower planetary noise levels and to make observations over a considerably longer period of the year than can now be done.

LIST OF REFERENCES

1. Jansky, K. G. "Electrical Disturbances apparently of Extra-terrestrial Origin", Proceedings of the Institute for Electrical Engineers 21, 1387 (1933).

2. Burke, B. F. and Franklin, K. L. "Observations of a Variable Radio Source Associated with the Planet Jupiter", Journal of Geophysical Research 60, 213 (1955).

3. Editor. "Radio Emission from Jupiter", Nature 175, 1074 (1955).

4. Shain, C. A. "Location on Jupiter of a Source of Radio Noise", Nature 176, 836 (1955).

5. Shain, C. A. "18.3 Mc/sec Radiation from Jupiter", Australian Journal of Physics 9, 61 (1956).

6. Smith, F. G. "A Search for Radiation from Jupiter at 38 Mc/s and at 81.5 Mc/s", Observatory 75, 252 (1955).

7. Brookes, R. G. "Jupiter in 1955-56; Special Report on Radio Radiation", Journal of the Association of Lunar and Planetary Observers 10, 13 (1956).

8. Franklin, D. L. and Burke, B. F. "Radio Observations of Jupiter", Astronomical Journal 61, 177 (1956). Abstract.

9. Kraus, J. D. "Some Observations of the Impulsive Radio Signals from Jupiter", Astronomical Journal 61, 182, (1956). Abstract.

10. Editor. "American Astronomers Report: Radio Noise from Jupiter", Sky and Telescope XV, 358 (1956).

11. Kraus, J. D. "Impulsive Radio Signals from the Planet Venus", Nature 178, 33 (1956).

12. Kraus, J. D. "Radio Observations of the Planet Venus at a Wavelength of 11 Meters", Nature 178, 103 (1956).

13. Kraus, J. D. "Class II Radio Signals at a Wavelength of 11 Meters", Nature 178, 159 (1956).

14. Gallet, R. M. "The Results of the Observations of Jupiter's Radio Emissions on 18 and 20 Mc/sec in 1956 and 1957", Program for U.R.S.I.-I.R.E. Spring Meeting, May 1957. Unpublished Abstract.

15. Smith, H. J. and Douglas, J. N. "First Results of a Planetary Radio Astronomy Program at the Yale Observatory", Astronomical Journal 62, 247 (1957). Abstract.

16. Jones, H. S. Life on Other Worlds, 1st ed., (The New American Library, New York, 1956), pp. 80-130.

17. Kuiper, G. P. The Atmospheres of the Earth and Planets, 1st ed., (The University of Chicago Press, Chicago, 1949), pp. 304-345.

18. Chalmers, J. A. Atmospheric Electricity, 1st ed., (Oxford University Press, Oxford, 1949), pp. 154-163.

19. Mitra, S. K. The Upper Atmosphere, 2nd ed., (The Asiatic Society, Calcutta, 1952), pp. 176-291.

20. Pawsey, J. L. and Bracewell, R. N. Radio Astronomy, 1st ed., (Oxford University Press, Oxford, 1954), pp. 78-93.

21. Jaeger, J. C., and Westfold, K. C. "Transients in an Ionized Medium with Applications to Bursts of Solar Noise". Australian Journal of Scientific Research A, 2, 322 (1949).

22. Carr, T. D., Smith, A. G., Pepple, R., and Barrow, C. H. "18-Megacycle Observations of Jupiter in 1957". Astrophysical Journal 127, 274 (1958).

23. The Radio Amateur's Handbook, American Radio Relay League, 30th ed., (Rumford Press, Concord, N. H., 1953), pp. 307-360, 412-420.

24. The American Radio Relay League Antenna Book, 7th ed., (Rumford Press, Concord, N. H., 1955), pp. 26-56, 81-87, 133-150, 232-233.

25. Terman, F. E. Radio Engineer's Handbook, 1st ed., (McGraw-Hill Book Co., New York, 1943), pp. 209-210.

26. Barrow, C. H. An 18 Mc/s Array for the Investigation of Planetary Radiation, (M.S. Thesis, University of Florida, 1958).

27. Barrow, C. H. A Radio Investigation of Planetary Radiation, (M. Sc. Thesis, University of London, 1958).

28. Starr, A. T. Radio and Radar Technique, 1st ed., (Pitman & Sons, London, 1953), pp. 213-217, 621-636.

29. Laport, E. A. Radio Antenna Engineering, 1st ed., (McGraw-Hill Book Co., New York, 1952).

30. Kraus, J. D. "The Corner Reflector Antenna". Proceedings of the Institute for Radio Engineers 28, 513 (1940).

31. Pepple, R. J. Design and Construction of a Radio Frequency Polarimeter for Planetary Studies, (M. S. Thesis, University of Florida, 1958).

32. The American Ephemeris and Nautical Almanac, (U. S. Government Printing Office, Washington, D. C., issued yearly).

33. Reese, E. J. Journal of the Association of Lunar and Planetary Observers 6, 33 (1952).

34. _____. Ibid., 6, 53 (1952).

35. _____. Ibid., 8, 133 (1954).

36. _____. Ibid., 9, 126 (1955).

37. _____. Ibid., 11, 29 (1957).

38. Peek, B. M. Private communication (1957).

BIOGRAPHICAL SKETCH

Thomas Deaderick Carr was born January 2, 1917 in Fort Worth, Texas. His early education was pursued in the secondary schools of Savannah, Georgia and Umatilla, Florida. He received the degrees Bachelor of Science, with Honors, and Master of Science, respectively, in 1937 and 1939 from the University of Florida, his major field being physics. He was later engaged in graduate study in physics at Duke University for 1½ years and at The University of Chicago for 1 year, performing research in cosmic radiation at both institutions. In February, 1956 he again entered the University of Florida, following a course of study and research leading to the degree Doctor of Philosophy in June, 1958. His employment has been as follows: Physicist at the Ballistic Research Laboratories, Aberdeen Proving Ground, Maryland, from 1940 to 1945; Civilian Scientist for the U. S. Navy Bureau of Ordnance at the Bikini atomic bomb tests in 1946; Physicist at the Air Force Missile Test Center, Patrick Air Force Base, Florida, from 1950 to 1956. He is a member of Phi Eta Sigma and Phi Kappa Phi homorary fraternities and an associate member of the Society of Sigma Xi. He was awarded the Citation for Exceptional Civilian Service by the Secretary of War in 1945.

This dissertation was prepared under the direction of the chairman of the candidate's supervisory committee and has been approved by all members of the committee. It was submitted to the Dean of the College of Arts and Sciences and to the Graduate Council and was approved as partial fulfillment of the requirements for the degree of Doctor of Philosophy.

June 9, 1958

C. I. Byers

Dean, College of Arts and Sciences

Dean, Graduate School

SUPERVISORY COMMITTEE

Chairman